



FACULTE DE BIOLOGIE ET MEDECINE

Département de Biologie Moléculaire Végétale



**ORGANISATION AND ROLE OF ACTIN MICROFILAMENTS DURING
CELLULAR GROWTH AND MORPHOGENESIS IN THE MOSS
*PHYSCOMITRELLA PATENS***

Thèse de doctorat ès sciences de la vie

présentée à la

**Faculté de Biologie et Médecine de
L'Université de Lausanne**

par

ANDRIJA FINKA

Diplômé en biologie moléculaire de
L'Université de Zagreb

Jury

Prof. Jean-Pierre Zryd, Directeur de thèse

Dr. Didier G. Schaefer

Prof. Jean-Marc Neuhaus

Dr. Laurent Blanchoin

to my family

ACKNOWLEDGMENTS

I would like to thank Professor Jean-Pierre Zryd for giving me the opportunity to undertake this fascinating project in his laboratory and for its critical contribution to the *in-vivo* labelling and analysis of F-actin cytoskeleton in moss *Physcomitrella patens*.

My sincere thanks go to Dr. Didier Schaefer for his generous support and helpful advices concerning transformation, molecular biology and phenotypic analysis of *Physcomitrella patens* transformants. I strongly appreciated the freedom and the confidence he granted me during the last six years.

Also I would like to use the opportunity to thank Prof. Pierre Goloubinoff and Younousse Saidi for their helpful advices and support.

I would like to thank Prof. Rose-Marie Hofer and Jean MacDonald-Petetot for the useful advices and help in microscopical techniques.

My particular thanks go to Professor Jean-Marc Neuhaus and Dr. Laurent Blanchoin for accepting to be experts on the thesis committee and their important suggestions concerning the writing of this manuscript.

I would like to thank all members of the DBMV for their technical help, suggestions and the pleasant atmosphere.

Finally, my thoughts go to my family for their essential logistical help, and especially to my wife Caroline for her support in my work and her love.

ABSTRACT

The network of actin cytoskeleton is composed of actin filaments (F-actin) that are made by polymerisation of actin monomers and actin binding proteins. It is required for growth and morphogenesis of eukaryotic cells. The labelling of F-actin with constitutively expressed GFP-Talin (Kost et al., 1998) reveals the organisation of cellular actin networks in plants. Due to the lack of information on actin cytoskeleton through gametophytic development of the model moss plant *Physcomitrella patens*, stable transgenic lines overexpressing GFP-Talin were generated to detect F-actin structures.

It is shown that the 35S promoter driven expression is not suitable for F-actin labelling in all cells. When it is replaced by the inducible heat-shock promoter *Gmhsp17.3* from soybean, one hour mild heat stress at 37°C followed by recovery at 25°C is enough to induce efficient and transient labelling in all tissues without altering cellular morphology. The optimal observations of F-actin structures at different stages of moss development can be done between 12-18 hours after the induction. By using confocal microscopy, we demonstrate that stellated actin arrays were densely accumulated at the growing tip in regenerating protoplasts, apical protonemal cells and rhizoids and connected with a fine dispersed F-actin mesh. Following three-dimensional growth, the cortical star-like structures are widespread in the meristematic cells of developing bud and young gametophores. On the contrary, undulating networks of actin cables are found at the final stage of cell differentiation. During redifferentiation of mature leaf cells into protonemal filaments the rather stagnant web of actin cables is replaced by diffuse actin meshwork.

In eukaryotes, nucleation of the actin monomers prior to their polymerization is driven by the seven-subunit ARP2/3 complex and formins. We cloned the gene encoding the ARP3 subunit of *P. patens* and generated *arp3* mutants of the moss through gene disruption. The knockout of *ARP3* affects the elongation of chloronemal cells and blocks further differentiation of caulonemal cells and rhizoids, and the gametophores are slightly stunted compared to wild-type. The *arp* mutants were created in the heat-shock inducible GFP-Talin strains allowing us to visualise a disorganised actin network and a lack of star-like actin cytoskeleton arrays. We conclude that ARP2/3 dependent nucleation of actin filaments is critical for the growth of filamentous cells, which in turn influences moss colonization. In complementation assays, the overexpression of *Physcomitrella* and *Arabidopsis* *ARP3* genes in the moss *arp3* mutant results in full recovery of wild type phenotype. In contrast the ARP3 subunit of fission yeast is not able to complement the moss *arp3* mutant of moss indicating that regulation of the ARP2/3 dependent actin nucleation diverged in different kingdoms.

RESUME

Le réseau d'actine est composé de filaments de F-actine et d'un ensemble de protéines s'y attachant (Actin binding proteins). Le réseau d'actine est nécessaire à la croissance et à la morphogenèse de toutes les cellules eucaryotes. Chez les plantes, le marquage ainsi que l'étude de l'organisation du réseau d'actine ont été réalisés en utilisant une fusion GFP-Talin (Kost et al., 1998) exprimée sous le control d'un promoteur constitutif. Afin d'étudier les structures F-actine dans les cellules de *Physcomitrella Patens* et pour combler le manque d'information sur le développement des gamétophores, des lignées transgéniques stables surexprimant GFP-Talin ont été créées.

Nous avons démontré que l'utilisation du promoteur 35S est inadéquate pour le marquage complet et homogène des filaments d'actine dans toutes les cellules de *P. patens*. Par contre, l'utilisation du promoteur inductible *Gmhsp17.3* nous a permis de réaliser un marquage transitoire et général dans tous les tissus de la mousse. Une heure de choc thermique à 37°C suivis d'un temps de récupération de 12-18h à 25°C sont les conditions optimales (sans dommages cellulaires) pour l'observation des structures F-actine à différentes étapes de développement de la mousse. En utilisant la microscopie confocale, nous avons observé l'existence de structures F-actine accumulées en forme d'étoiles. Ces structures, qui sont liées au réseau de microfilaments d'actine, ont été observées dans les protoplastes en régénération, les cellules des protonema apicales ainsi que dans les rhizoïdes. En suivant la croissance tridimensionnelle, ces structures en étoiles ont été observées dans les cellules meristématiques des bourgeons et des jeunes gamétophores. Par contre, dans les cellules différenciées ces structures laissent place à des réseaux de câbles épais. Nous avons également remarqué que durant la redifférenciation des cellules foliaires le réseau de câbles de F-actine est remplacé par un réseau de F-actine diffus.

Dans les cellules eucaryotes, la nucléation des filaments d'actine précédant leur polymérisation est contrôlé par sept sous unités du complexe ARP2/3 et par des formines. Nous avons isolé le gène codant pour la sous unité ARP3 de *P. patens* et nous avons créé des mutants *arp3* par intégration ciblée (Knockout). L'élongation des cellules chloronema est clairement affectée dans les mutants *arp3*. La différenciation des caulonemata et des rhizoïdes est bloquée et les gamétophores sont légèrement plus courts comparé au type sauvage. A fin d'étudier l'organisation des filaments d'actines dans les mutants *arp3*, nous avons aussi réalisé un *arp3*-knockout dans la lignée Hsp-GFP-Talin. La nouvelle lignée générée nous a permis de visualiser une désorganisation du réseau d'actine et une absence complète de structures de F-actine accumulée en forme d'étoiles. Les résultats obtenus nous amènent à conclure que la nucléation (ARP2/3 dépendante) des filaments d'actine est indispensable à la croissance des cellules filamenteuses. Par conséquent, les filaments d'actine semblent avoir un rôle dans la colonisation des milieux par les mousses. Nous avons également procédé à des essais de complémentation du mutant *arp3*. La surexpression des gènes *ARP3* de *Physcomitrella* et d'*Arabidopsis* dans les cellules du mutant *arp3* rétabli complètement le phénotype WT. Par contre, le gène *ARP3* des levures n'est pas suffisant pour complémenter la même mutation dans les cellules de mousses. Ce résultat démontre que les mécanismes de régulation de la nucléation des filaments d'actine (ARP2/3 dépendante) sont différents entre les différents groupes d'eucaryotes.

TABLE OF CONTENTS

I. GENERAL INTRODUCTION.....	1
1. ROLE OF CYTOSKELETON IN PLANT CELL GROWTH	1
2. THE PLANT ACTINS AND ARP2/3 COMPLEX	2
3. VISUALIZATION OF ACTIN CYTOSKELETON IN PLANTS	6
4. THE ORGANIZATION OF F-ACTIN IN PLANT CELLS	7
5. DEVELOPMENTAL STAGES OF <i>PHYSCOMITRELLA PATENS</i>	9
6. THE AIM OF THE PRESENT WORK.....	10
II. RESULTS AND DISCUSSION.....	12
CHAPTER I: THERMAL INDUCTION OF GFP-TALIN DRIVEN BY SOYBEAN HEAT SHOCK PROMOTER EFFICIENTLY LABELS ACTIN NETWORK IN MOSS <i>PHYSCOMITRELLA PATENS</i>	12
ABSTRACT	12
1. INTRODUCTION	13
2. RESULTS	15
3. DISCUSSION	25
4. MATERIALS AND METHODS.....	27
CHAPTER II: DISTINCT SPATIO-TEMPORAL F-ACTIN ASSEMBLIES ARE PRESENT AT DIFFERENT DEVELOPMENTAL STAGES IN THE MOSS <i>PHYSCOMITRELLA PATENS</i>	30
ABSTRACT	30
1. INTRODUCTION	31
2. RESULTS	33
3. DISCUSSION	41
4. MATERIALS AND METHODS.....	43
CHAPTER III: THE <i>ARP3</i> GENE IS REQUIRED FOR PROPER ORGANISATION OF F-ACTIN AND FOR NORMAL CELLULAR ELONGATION AND DIFFERENTIATION IN THE MOSS <i>PHYSCOMITRELLA PATENS</i>	45
ABSTRACT	45
1. INTRODUCTION	46
2. RESULTS	48
3. DISCUSSION	61
4. MATERIALS AND METHODS.....	65
CHAPTER IV: GENERAL DISCUSSION.....	69
ANNEX 1.....	73
ANNEX 2.....	75
ANNEX 3.....	79
REFERENCES	83

I. GENERAL INTRODUCTION

1. Role of cytoskeleton in plant cell growth

Cell polarity is defined by asymmetry in cell shape, organelle distributions and cell functions. Compared to animal cells, the plant cell is surrounded by a wall consisting of a network of cellulose microfibrils embedded in a matrix of polysaccharides and proteins. Cell expansion is driven by the spatial and temporal control of cell wall deposition. In most plant cells, growth is restricted to the walls longitudinal to the plant organ and driven by turgor pressure. This type of growth is referred to as diffuse or intercalary growth. Another type of growth is found in cylindrical plant cell types that exhibit apical elongation like pollen tubes, root hairs, hyphae of fungi, moss and fern protonemata, algal and moss rhizoids. In these cells, the site of expansion is focused to the dome-shaped apex (Kropf et al., 1998). This type of growth represents polar growth *in sensu stricto* and such cells are denoted as the tip-growing cells.

Eukaryotic cells differ in their shape and function, but despite this variety, they all possess a basic set of evolutionarily-conserved mechanisms that are responsible for maintaining their polarized organization (Nelson, 2003). These mechanisms include signaling complexes, cytoskeleton assembly and recruitment, mobilization of proteins from intracellular pools, and targeted vesicle delivery to the sites of membrane growth for example. The hierarchical pathway generating polarity is initiated by environmental cues and defines a point on the cell surface, which orients cellular assemblies and trafficking. This point is recognized and reinforced by the localized assembly of a signaling complex made of small GTPases, which in turn activates other protein complexes that regulate the assembly and orientation of the cytoskeleton, and mediates the delivery of vesicles to the plasma membrane.

The cytoskeleton is composed of three types of linear proteinaceous polymers: actin filaments (F-actin or microfilaments), microtubules, and intermediate filaments. A single 7 nm wide helix of actin filament is made of two protofilaments of polymerized actin. A microtubule is a hollow cylinder with a diameter of 25 nm, formed from 13 parallel protofilaments. Each protofilament is built from dimers of α - and β -tubulin where the α -tubulin of one dimer binds to the β -tubulin of the next. The numerous microtubule-associated proteins and actin-binding proteins polymerize, anchor, crosslink or regulate the cytoskeletal

networks thus modulating their organisation and dynamics. Hence, the dynamic activity of the cytoskeleton is essential to cell cycle completion in plants. In the G2 phase of the cell cycle, interphase cortical microtubules disassemble and are reorganized into a cortical ring called the preprophase band. This unique plant structure defines the later position of the new cross wall. Microtubules of the preprophase band are then recruited to form the mitotic spindle, which segregates chromosomes during anaphase. At the transition between anaphase and telophase, the formation of the phragmoplast takes place, a structure composed of two rings of interconnected microtubules and actin filaments. It first appears as a bundle of microtubules between the daughter nuclei which expands outwards to assist formation of the new cell plate. After mitosis, interphase cortical microtubules are reassembled and the cytoskeleton contributes to the identification of the sites where cell wall expansion occurs, defining cell shape and morphogenesis. Although this process is poorly understood, the general principles of cell polarity indicate that microtubules help to determine the sites of growth while the actin microfilaments have a prominent role in directing secretory vesicles with new cell wall material, docking them at the selected sites (Mathur and Hulskamp, 2002).

2. The plant actins and Arp2/3 complex

Actins are a family of highly conserved proteins that are ubiquitously found among eukaryotes. In *Arabidopsis thaliana* eight functional genes (out of ten) can be classified according to sequence homology or expression pattern in a vegetative class and a reproductive class (McDowell et al., 1996). The vegetative class is composed of *ACT2*, *ACT7* and *ACT8* while the reproductive class is composed of the *ACT1*, *ACT3*, *ACT4*, *ACT11* and *ACT12* paralogs. The two non-functional pseudogenes are *ACT5* and *ACT9*. Expression within subclasses often overlaps, and at least one actin isovariant is present in every tissue at every stage of development (Meagher et al., 1999). T-DNA insertional mutagenesis did not induce any obvious phenotype in *act2*, *act4* and *act7* mutants (Gilliland et al., 1998; McKinney et al., 1995), but the progeny obtained by natural fertilization has lower frequency of mutant alleles indicating some deleterious effect of the mutation (Gilliland et al., 1998). In addition, the *act7* mutant is also affected in callus formation (Kandasamy et al., 2001). Analysis of a chemically generated mutation in *deformed root hairs 1 (der1)* where the phenotype is

restricted to root hairs, revealed mutations in the *ACT2* gene (Ringli et al., 2002). Ectopic expression of a reproductive actin (*ACT1*) under the control of a vegetative actin gene (*ACT2*) promoter generated severe developmental perturbations including reduced organ size, altered branching patterns of trichomes and inflorescence stems and delayed flowering (Kandasamy et al., 2002).

The globular, monomeric 42 kDa protein G-actin can catalyse the hydrolysis of ATP by binding the nucleotide deep in the cleft near the centre of subunit. *In vitro* at physiological salt concentration, actin monomers can readily polymerise into F-actin (Straub, 1942) without ATP. In living cell, ATP bound to F-actin signifies nascent microfilament. In eukaryotes, dynamic remodelling of the actin network depends on the coordinated activity of actin-binding proteins, which are represented by more than 70 families (Pollard, 2001). They can be grouped into several categories based on their biochemical activities. Thus, monomer-binding proteins such as profilins regulate polymerisation by binding and sequestering G-actin (Kang et al., 1999; Pantaloni and Carlier, 1993). The F-actin depolymerization factors and cofilins play a crucial role in the disassembly of actin microfilaments (Bamburg, 1999; Chen et al., 2002). The cross-linking of actin microfilaments is dependent on the side binding proteins fimbrin and villin, which also have the obvious function to generate robust microfilament bundles (Hepler et al., 2001; Wasteneys and Galway, 2003). The myosins are a large superfamily of molecular motors that create movement and mechanical force by ATP-dependent interactions along actin filaments (Thompson and Langford, 2002).

Nucleation of actin leads to the formation of short filaments composed of two or three actin monomers. This is the rate limiting step due to the poor ability of actin monomers to initiate new filament formation. Nucleation factors, such as formins and the Arp2/3 complex, overcome this rate limiting step of filament assembly by creating “seeds” for actin polymerization (Fig. 1). In interphasic animal cells, microtubule nucleation takes place near the nucleus, whereas actin filament nucleation most frequently occurs at the plasma membrane. Formins are large multidomain proteins that regulate the assembly of straight actin microfilaments (Pruyne et al., 2002; Sagot et al., 2002), whereas the seven-subunit Arp2/3 complex nucleates new filaments at a 70° angle to an already existing filament, thus creating a branched network (Mullins et al., 1998).

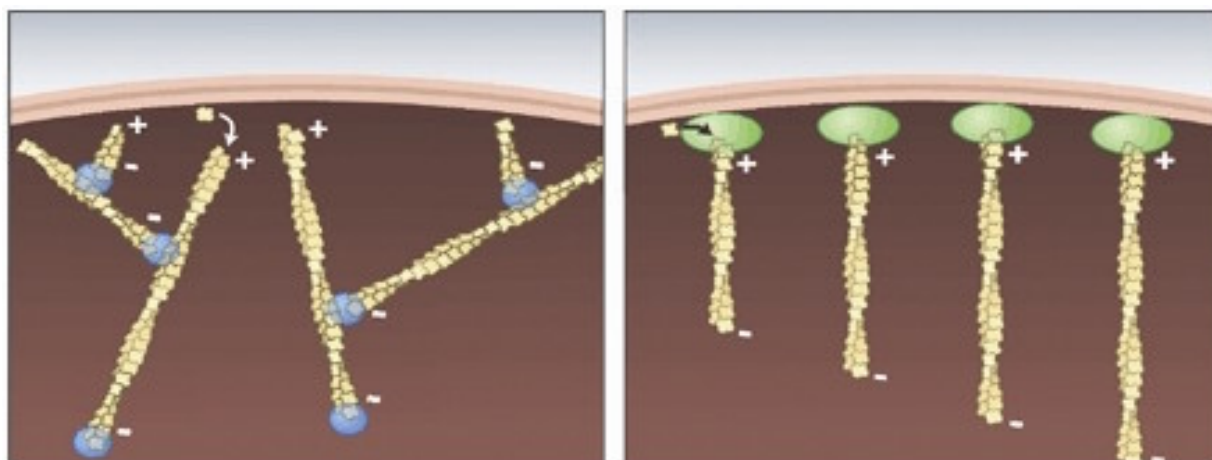


Figure1. The Arp2/3 complex and formins organize different actin structures (Chang and Peter, 2002). (Left) The Arp2/3 complex (blue) tends to nucleate new actin filaments at the sides of existing actin filaments, resulting in a branching filament network. (Right) In contrast, formins (green) nucleate the assembly of straight filaments.

This protein complex is named after the two actin- related proteins Arp2 and Arp3 which share about 45% identity with actin, and includes five other polypeptides called ARPC1-5 (a comparison between different species is given in Table 1). It has been purified from the mold *Acanthamoeba castellanii* (Kelleher et al., 1995), the yeast *Saccharomyces cerevisiae* (Winter et al., 1997) and human cells (Welch et al., 1997). The crystal structure of the Arp2/3 complex at a resolution of 2.0 Ångström (Robinson et al., 2001) reveals that Arp2 and Arp3 are folded like actin, ARPC1 is a seven-blade β -propeller, ARPC2 and ARPC4 are in the core of the complex and ARPC3 and ARPC5 are globular α -helical subunits with large basic patches on their exposed surfaces. Genetic and biochemical experiments have provided additional information on both the structure of the complex and the functional significance of the individual subunits. In yeast cells, the Arp2/3 complex is localized in the actin patches (Pelham and Chang, 2001). The Arp2, Arp3, and ArpC1 are essential for viability in *Schyzosaccharomyces pombe* (McCollum et al., 1996), (Balasubramanian et al., 1996), (Morrell et al., 1999). In *S. cerevisiae* ArpC1 is essential, whereas strains lacking Arp2, Arp3, ArpC2, or ArpC5 grow very poorly (Winter et al., 1999). The Arp3 mutants of *Drosophila* die in the embryonic stage due to the absence of pseudocleavage furrows that are required for

further developmental processes (Hudson and Cooley, 2002). In migrating animal cells, it is concentrated in lamellipodia and actin-rich regions (Higgs and Pollard, 2001).

Subunit	<i>Arabidopsis</i> Gene Acc. No. MATDB	% amino-acid identity/similarity					
		Dd	Sp	Sc	Ce	Dm	Hu
ARP2	At3g27000	63/80	53/73	57/73	60/79	61/80	62/80
ARP3	At1g13180	59/75	55/72	53/66	56/73	57/71	59/74
ARPC1p41	At2g30910	43/59	34/51	34/51	39/58	37/54	41/60
ARPC1p41	At2g31300	43/58	34/51	34/51	38/57	24/41	42/61
ARPC2p34	At1g30825	33/54	26/46	28/46	n.a.	26/48	26/46
ARPC3p20	At1g60430	41/58	43/59	39/58	41/60	40/62	47/66
ARPC4p20	At4g14150	n.a.	49/72	n.a.	48/69	n.a.	57/72
ARPC5p16	At4g01710	31/51	25/44	23/45	32/50	35/55	32/53

Table 1. ARP2/3 complex subunits in *Arabidopsis* and their amino acid similarity to other organisms (Mathur et al., 2003a). Dd, *Dictyostelium discoideum*; Sp, *Schizosaccharomyces pombe*; Sc, *Saccharomyces cerevisiae*; Ce, *Caenorhabditis elegans*; Dm, *Drosophila melanogaster*; Hu, human; n.a., not applicable.

However, efficient nucleation of actin polymerization by the Arp2/3 complex depends on the presence of an Arp2/3 activator. Although many Arp2/3 activators have been identified in animal cells, the most intensively studied are the Wiskott-Aldrich Syndrome protein (WASP) and members of suppressor of cAMP receptor (Scar) family (Weaver et al., 2003). The human pathogenic bacterium *Listeria monocytogenes*, has the ActA protein at its surface that binds to the Arp2/3 complex and promotes actin polymerization (Welch et al., 1998). This in turn propels the bacteria through the cytoplasm of the host cell. In plants, the genes encoding all homologues of the ARP2/3 subunits in *Arabidopsis* have been identified and cloned (McKinney et al., 2001). All these characterised genes are unique except the ARPC2 subunit, which has two paralogs (El-Assall et al., 2004). Several reports revealed that *Arabidopsis* mutational phenotypes *WURM*, *DISTORTED1*, *DISTORTED2* and *CROOKED* are encoded by mutations in *ARP 2*, *ARP 3* (Le et al., 2003; Li et al., 2003; Mathur et al.,

2003a), *ARPC2* (El-Assall et al., 2004) and *ARPC5* genes (Mathur et al., 2003b), respectively. In general, mutations of *ARP2* and *ARP3* in *Arabidopsis* lead to misdirected expansion in various cell types (Mathur et al., 2003a). Hypocotyls of the mutants are up to three times shorter than those of wild-type plants, mutant root hairs are wavy, pavement cells do not produce lobes and trichome expansion is randomised. Mutations in the *ARPC5* subunit cause the absence of stomatal complexes. At the subcellular level these morphological changes are linked to disorganised actin assembly.

3. Visualization of actin cytoskeleton in plants

Depending on research requirements F-actin can be visualized in fixated tissue following formaldehyde and/or glutaraldehyde chemical fixation, or in living plant tissue using *in vivo* reporters. In contrast to microtubules, actin filaments are extremely sensitive to aldehyde fixation procedures and results obtained by these techniques have to be interpreted cautiously. The protein cross-linking agent m-maleimidobenzoyl-N-hydroxysuccinimide ester (MBS) greatly improves the stability of F-actin prior to aldehyde fixation (Sonobe and Shibaoka, 1989). Several protocols employing different concentrations and components of the fixative followed by techniques to improve its permeability have been tried in order to obtain more reliable figures of F-actin organization (Traas et al., 1987); (Doris and Steer, 1996); (Olyslaegers and Verbelen, 1998); (Wasteneys et al., 1997). Labeling of microfilaments in fixated material is achieved either indirectly with antiactin antibodies or directly by employing fluorescent derivatives of phalloidin (fungal metabolite with a high affinity for F-actin). Although phalloidin gives a better resolution of F-actin than the antibodies, this technique is not free of problems. Various actin-binding proteins might mask phalloidin binding sites.

In vivo, microinjection of phalloidin conjugates facilitates the visualization of the F-actin organization in living plant cells, but this procedure is technically demanding and time-consuming and is restricted to certain types of plant cells. The 238 amino-acids green fluorescent protein (GFP) of the jellyfish *Aequorea victoria* is an ideal expression marker in living cell due to its strong fluorescence (Chalfie et al., 1994). The fluorophore is formed by cyclation and oxidation of three amino-acids Ser65, Tyr66 and Gly67 (Cubitt et al., 1995).

The wild type *GFP* cDNA has been mutagenized extensively in order to enhance the fluorescence quantum yield (Cubitt et al., 1995; Miyawaki et al., 2003) as well as to eliminate cryptic splicing sites (Haseloff et al., 1997). The real breakthrough for *in vivo* studies of protein cellular localization was achieved by transformation of cells with GFP linked to polypeptides (Tsien, 1998). In most cases, chimeric genes that encode either N- or C-terminal fusions to GFP retain the normal biological activity of the fused protein, as well as maintaining fluorescent properties similar to native GFP. Among the fluorescently tagged proteins that were targeted to different cell organelles, GFP-based markers were developed for the labelling of microtubules (Marc et al., 1998) and microfilaments (Kost et al., 1998). Attempts to express GFP-actin in living animal cells resulted in labelling not only actin filaments but also monomeric subpopulations (Westphal et al., 1997; Yumura and Fukui, 1998). In *Dictyostelium*, GFP-actin interferes with cellular morphology and functions (Aizawa et al., 1997). Fortunately, efficient labelling of plant actin filaments has been achieved *in vivo* by linking GFP to the F-actin binding domain I/LWEQ of mouse talin (GFP-Tn) (Kost et al., 1998) and to the *Arabidopsis* actin-bundling protein, fimbrin (Kovar et al., 2001).

4. The organization of F-actin in plant cells

In angiosperms, studies of F-actin organisation in diffusely growing interphasic cells revealed that cortical microfilaments are co-aligned with microtubules perpendicularly to the major axis of cell expansion while cytoplasmic F-actin bundles are oriented longitudinally (Baluska et al., 1997); (Blancaflor, 2000). In the early stages of *Arabidopsis* trichome development, GFP decorated microfilaments are diffusely distributed and become organised into characteristic strands in the later stages (Mathur et al., 1999). It is also known that F-actin structures form a network around the nucleus, which extends into the cytoplasm of *Arabidopsis* (Kost et al., 1998). In tip-growing root cells and pollen tubes, F-actin bundles are longitudinally oriented, whereas a mesh of fine actin filaments is found in the sub-apical region (Baluska et al., 2000); (Hepler et al., 2001). At the very tip, the dome is filled with secretory vesicles representing region of dynamic actin organization orchestrated by numerous actin-interacting proteins.

Studies of actin cytoskeleton in mosses have been limited on analysis of rhodamine-phalloidin stained protonemata. Longitudinally-oriented actin cables have been detected in the caulonemata from *Physcomitrella patens* (Doonan et al., 1988) as well in the protonemata of both *Ceratodon purpureus* (Walker and Sack, 1995); (Meske and Hartmann, 1995) and *Funaria hygrometrica* (Quader and Schnepf, 1989). In other moss cell types, the description of the actin structures is incomplete. Actin strands have not been visualized in the very tip of caulonemata of *Ceratodon* (Meske and Hartmann, 1995). In *Funaria*, particular F-actin arrays have been detected at the prospective outgrowing sites during side branch initiation, which could represent actin organizing centres at the plasma membrane (Quader and Schnepf, 1989).

Important tools to study the function of cytoskeletal elements are chemical inhibitors that specifically interfere with their function. Treatments with microtubule drugs such as oryzalin or taxol cause swelling of diffusely growing cells in the leaf epidermis, hypocotyl and root (Baskin et al., 1994). In tip-growing cells, a similar treatment results in multiple root hairs in *Arabidopsis* (Bibikova et al., 1999), while a microtubule disrupting drug cremart causes lateral branching in moss *Physcomitrella patens* (Doonan et al., 1988). All this implies that the selection of the sites for polar growth may depend upon microtubules (Mathur and Hulskamp, 2002). Actin depolymerising drugs like cytochalasins and latrunculin drastically reduce cell expansion. Cytochalasins are fungal metabolites, which bind to the ends of actin filaments, thus preventing polymerisation and causing depolymerization. Generally, cytochalasins induce disappearance and fragmentation of actin filaments (Geitmann and Emons, 2000). Cytochalasin B caused dispersion of microtubule bands colocalized with F-actin in wheat mesophyll cells (Wernicke and Jung, 1992). Latrunculins, isolated from sponges, bind tightly to monomeric actin in an equimolar ratio (Coue et al., 1987), decreasing the amount of the filamentous form. Latrunculin B inhibits pollen germination and tube growth in *Arabidopsis* (Gibbon et al., 1999) in addition to causing severe dwarfism in seedlings (Baluska et al., 2001). Although, drug-treatment experiments have shown the importance of the cytoskeleton in the elongation and shaping of the plant cells, another way to characterize the function of the cytoskeletal elements is through molecular genetics and the analysis of mutants.

5. Developmental stages of *Physcomitrella patens*

In the moss *Physcomitrella patens* (Hedw) B.S.G. (Funariales) after spore germination (Fig. 2A), the initial filament is made up of a chloronemal apical cell (Fig 2B) and a linear array of subapical chloronemal cells (Fig. 2C) that are produced by successive divisions of the tip cell (Schumaker and Dietrich, 1997). These cells are about 120 μm long and 20 μm in diameter, have large round chloroplasts, contain walls that are perpendicular to the filament axis and their division that occurs once every 24 hours is strictly light dependant. The chloronemal filament grows by apical cell division and subapical chloronemal cells undergo cell division giving rise to side branches. In response to increases in light and to auxin, some apical chloronemal cells undergo a developmental change to generate a second cell type called caulonemal cells (Fig. 2D). The caulonemata have lengths between 130-180 μm and oblique cell walls to the filament axis. They divide more often than chloronemal cells (every 5 to 6 hr) in a light independent manner and contain fewer, smaller, and more elliptical chloroplasts. The second subapical caulonemal cell branches to form a caulonemal side branch initial (Fig. 2D, arrowhead). Under standard conditions, about 3% of these cell initials undergo a developmental switch from unidirectional to three-dimensional growth by producing simple three-faced cell (Cove, 1992), whereas the rest of them give raise to new side branch filaments (Fig. 2E, arrow). This meristem initial is termed a bud. Following further caulinary growth, they develop into leafy shoots called gametophores (Fig. 2F). The epidermal cells of the gametophore stem produce a third type of multicellular filaments named rhizoids. The rhizoids support the gametophore and are involved in water and nutrient absorption. The basal and mid-stem rhizoids have distinct developmental patterns but the same morphology (Sakakibara et al., 2003). Finally, both male and female sex organs named antheridia and archegonia appear in the same gametophore. Gametogenesis occurs at a temperature below 19°C. Both the antheridium and archegonium have a sterile jacket of cells, which protects the gametes against desiccation in the terrestrial environment. The antheridium sterile jacket has a cap cell, which disintegrates when the gametophyte is wetted with hypotonic rain water due to increased turgor pressure. The released antherozoids are chemotactic and swim up a concentration gradient of the chemotactic agent to find the egg cell in an open archegonium. After fertilization the sporophyte develops with a short stalk carrying about 5000 spores (Fig. 2G) (Reski, 1998).

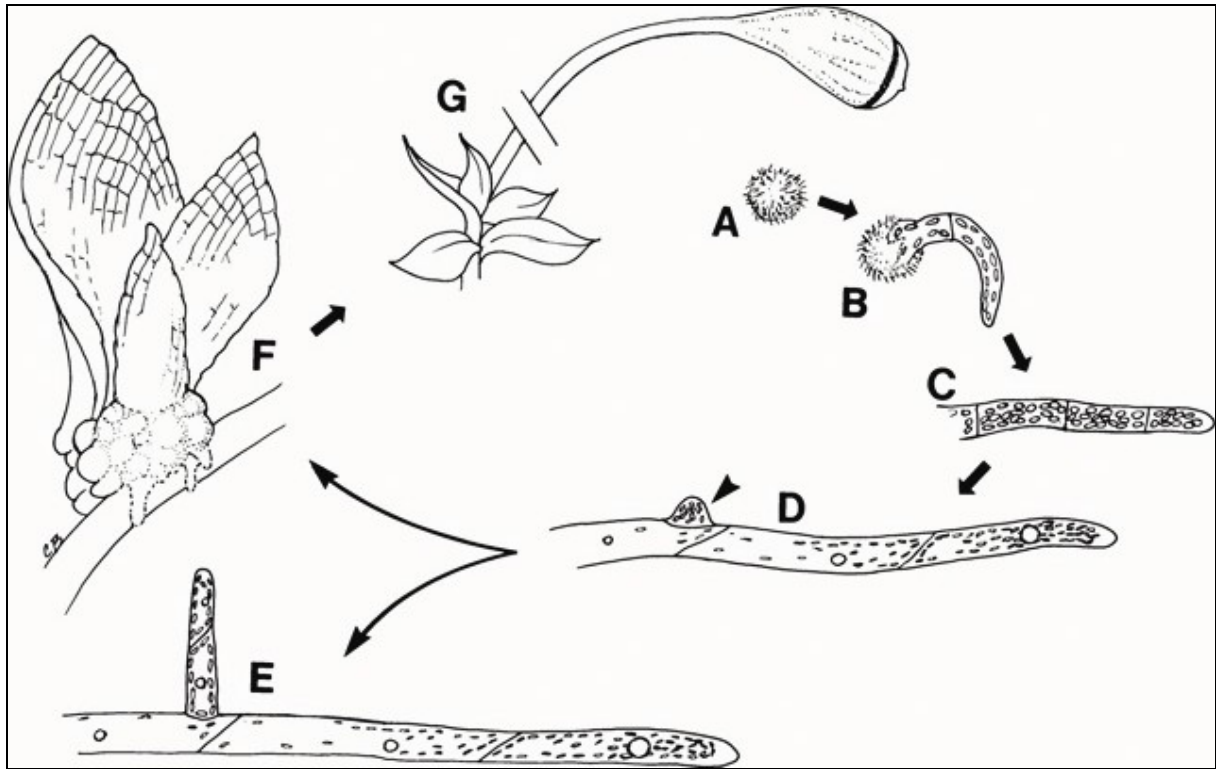


Figure 2. Stages of moss development (Schumaker and Dietrich, 1997). Haploid spores (A) germinate to form a filament consisting of chloronema cells (B and C). Subsequently, light and auxin induce changes in the tip cell to give rise to caulonema cells (D). A single-celled initial (D, arrowhead) forms on the second subapical cell of the caulonema filament. This initial cell has two potential fates. In the absence of cytokinin, the initial cell will continue to grow by tip growth to form a new lateral filament (E). In the presence of cytokinin, the initial cell takes on the morphology associated with the assembly of a bud to form the leafy shoot (F and G) that eventually bears the gametangia (not shown). Following fertilization, a diploid capsule (G) forms on the leafy shoot. Ultimately, meiosis occurs within the capsule to produce haploid spores.

6. The aim of the present work

This study has been initiated with the intention to answer two crucial questions: how are actin microfilaments organized during the different stages of moss development and how regulating elements such as the Arp2/3 complex contribute to these processes. In this regard, the moss *Physcomitrella patens* seemed to be an ideal model for two reasons. First, cytoskeletal organisation in moss can be examined in a complete cell lineage at the single cell level (Schnepf, 1986). Second, this is the only plant in which foreign DNA integrates in the

genome by homologous recombination at targeted locations with a very high efficiency (Schaefer, 2001; Schaefer, 2002).

In order to achieve a complete description of actin filaments related to the moss developmental cycle, we have created stable transformants containing GFP-Talin under the control of a heat-shock inducible promoter. Upon heat stress, GFP-Talin efficiently labeled F-actin structures in all moss tissues. Confocal imaging revealed fluorescent stellated structures at the apex of tip growing cells and juvenile cells of buds and gametophores, whereas differentiated cells were engaged in a network of actin bundles. This study was planned to gain full benefit in a long-term perspective to focus on analysis of different cytoskeletal proteins by gene disruption (Schaefer and Zryd, 1997). In our example we have chosen a gene encoding the Arp3 subunit of Arp2/3 complex. The mutations in this gene resulted in a developmental phenotype displaying shortened chloronemal cells and gametophores followed by the notable absence of caulonemal cells and rhizoids. At the subcellular level this mutation abolished the GFP-labeled actin arrays confirming that the Arp2/3 complex is responsible for proper organization of actin microfilaments, which influence cellular morphogenesis.

II. RESULTS AND DISCUSSION

Chapter I: Thermal induction of GFP-talin driven by soybean heat shock promoter efficiently labels actin network in moss *Physcomitrella patens*

ABSTRACT

The dynamic organisation of actin cytoskeletal structures plays a central role in cell polarity, differentiation and morphogenesis. Non-invasive labelling of plant F-actin can be achieved with GFP-Talin (GT) fusion protein. Here, we compare in stable *Physcomitrella patens* transformants the efficiency of F-actin labelling with GT driven either by a constitutive 35S CaMV promoter or by the soybean heat shock inducible promoter from *Hsp17.3* gene. In 35S-GT strains, labelling of F-actin was accumulative and strongly depended on the stage of development being completely absent in juvenile cells. In Hsp-GT strains, actin structures were not detected under non-induced conditions, but were clearly visible in every cell types up to 24 hours following heat-shock induction. Optimal parameters for transient labelling of the F-actin have been established, enabling the precise description of actin structures in each individual moss cell.

1. Introduction

The actin cytoskeleton and its associated proteins are directly involved in cellular polarization, growth and morphogenesis. To study the *in vivo* organisation of the F-actin network a non-invasive labeled marker is needed, which can interact with actins. *In planta*, the fluorescent labelling of the F-actin network has been achieved by the overexpression of GFP-Talin (GT) under the control of a 35S promoter (Kost et al., 1998). Yet, F-actin labelling was restricted to few cell types in these transgenic plants. The examination of the 35S activity in the whole plant often reveals variable expression profiles of the reporter genes in different tissues (Yang and Christou, 1990), (Ponappa et al., 1999), (Sunilkumar et al., 2002), (Zhou et al., 2004). This suggests that the 35 S promoter may not be the best one for strong and uniform labelling of F-actin in whole plants.

Fine quantitative tuning of the temporal expression of reporter genes can be accomplished by using inducible promoters. Ideal inducible expression systems should have a high level of expression under the action of mild physical factors or of non-toxic level of chemical inducers (Gatz, 1997). Heat-inducible gene expression systems are properly regulated in plants (Ainley and Key, 1990); (Holtorf et al., 1995). Earlier studies of the heat-shock inducible promoter of the soybean small heat-shock protein *GmHsp17.3* have demonstrated its value in transgenic plants (Schoffl et al., 1989), (Prandl and Schoffl, 1996). The heat-shock has the advantage of being easy to apply and to control.

In plants, labelling of plant actin filaments by constitutive expression of GT (Kost et al., 1998) showed two main drawbacks: it was impossible to successfully label the F-actin structures in early stages of trichome development of *Arabidopsis* (El-Assall et al., 2004) and the overproduction specifically blocked growth of pollen tubes in tobacco (Kost et al., 1998). To explore alternatives for GFP tagging of the plant actin cytoskeleton, it is shown that fusion protein between GFP and the second actin-binding domain (fABD2) of *Arabidopsis* fimbrin, AtFIM1 labels highly dynamic and dense actin networks in diverse plant species and cell types (Sheahan et al., 2004).

Mosses (bryophytes) are suitable plant models for studying the modification of the cytoskeletal organisation during development as the complete cell lineage can be followed at

the single cell level (Schnepf, 1986). In the course of our work, we investigated the possibility to use GFP-Talin to label actin structures in the moss *P. patens* where the techniques for gene disruption and allele replacement have been well established (Schaefer, 2002; Schaefer and Zryd, 1997). For this purpose, we compared transgenic moss plants expressing the GT marker constitutively (*i.e.* driven by the 35S promoter) or in a heat inducible way (*i.e.* driven by the heat-shock promoter *Gmhsp17.3* from soybean).

Here, we demonstrate that an optimal thermal induction of *Gmhsp17.3* GT leads to a complete and transient labelling of F-actin in transgenic moss tissue that could not be achieved by a 35S driven overexpression. In addition, we report valuable information concerning the nature of the heat treatments required for optimal induction while not impairing cytoskeletal structure and cell morphology.

2. Results

2.1 Generation of transgenic plants carrying GFP-mTn expression cassettes

The highly efficient gene targeting system of *P. patens* allows the integration of a transgene at a specific location of the genome minimizing possible positions effects common in transformed plants. In order to integrate heat-shock inducible GT at the already known genomic locus 108 of *P. patens*, we employed the vector pGmHGT-AH108 (Fig. 3). In parallel, protoplasts were co-transformed with the vector pYSC14 containing 35S GT (Kost et al., 1998) and the vector pGL108 bearing a cassette for hygromycin resistance and the 108 locus (Schaefer and Zryd, 1997). After standard selection, fifteen hygromycin resistant colonies transformed by pGmHGT-AH108 (HGT strains) and four strains transformed by pGL108-pYSC14 (35SGT strains) were selected. All of the Hsp-GT strains as well as 35SGT6 and 35SGT8 lines were phenotypically indistinguishable from wild type and showed a stable integration of the plasmid constructs into locus 108 (data not shown).

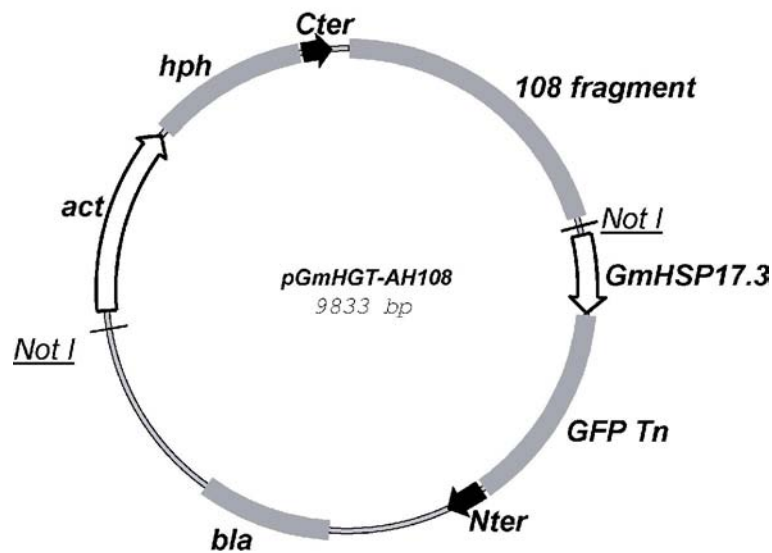


Figure 3. The plasmid vector used for the stable transformation of moss. pHsp-GT-AH108 contains the GT cassette under the soybean Hsp promoter, a plant hygromycin resistance cassette driven by an actin promoter from rice and a 2 kb fragment of genomic DNA corresponding to locus 108 (Schaefer and Zryd, 1997). *GmHSP17.3*; soybean Hsp promoter, *GFP-mTn*; GFP-Talin, Cter; *CaMV* terminating sequence, *bla*; beta-lactamase, *Act*; rice actin 1 promoter, *hph*; hygromycin phosphotransferase, *Nter*; nopaline synthase polyadenylation signal.

2.2 The 35S promoter allowed only poor expression of GT labelling of F-actin in rapidly growing protonemal cells and in dark grown tissue

In 35S-GT strains, the fluorescent signal accumulates only in three-four days old cells of rapidly growing protonemal cell tissue (Fig. 4) as well as in the adult leaves of the gametophore (not shown). In twenty protoplast-derived colonies having each over 300 cells, we quantified the number of labeled cells in protonemal filaments. We found a strong correlation between the GFP labelling of microfilaments and the age of the cells (Fig. 4b). We could not detect any labelling in apical and adjacent subapical cells (first and second cells, respectively). The number of labeled cells increased steadily away from the tip cells and reached a maximum at the cell number six along the main filament and cell number three along lateral branches. This indicates that successful labelling of F-actin results from sufficient accumulation of GT over time. It is interesting to note that about thirty percent of apical cells in the lateral filament originated from the sixth strongly labeled cell of the primary filament were labeled. This suggests that the large amount of GT in the sixth cell of the primary filament enables labelling of some lateral apical cells.

We analysed GT labelling of actin in dark grown tissue and surprisingly could not detect any fluorescent caulonemata. To investigate the activity of the 35S promoter in darkness we compared the level of hygromycin resistance in 35S-GT and HGT strains that carry the resistance cassette driven by the 35S or the stronger rice *act-1* gene promoter, respectively. Stuningly, the growth of HGT line in darkness was not affected by the presence of the antibiotic whereas growth of the 35S-GT strains was seriously inhibited (Fig. 4c). In addition, when independent lines with integrated 35S-neomycin phosphotransferase were tested on medium containing G418, caulonemal growth similarly ceased (not shown). These data suggested that the 35S promoter had only a weak activity in moss under standard growth conditions that is down-regulated in dark-growth conditions, whereas the actin-1 promoter does not appear to be down-regulated in darkness.

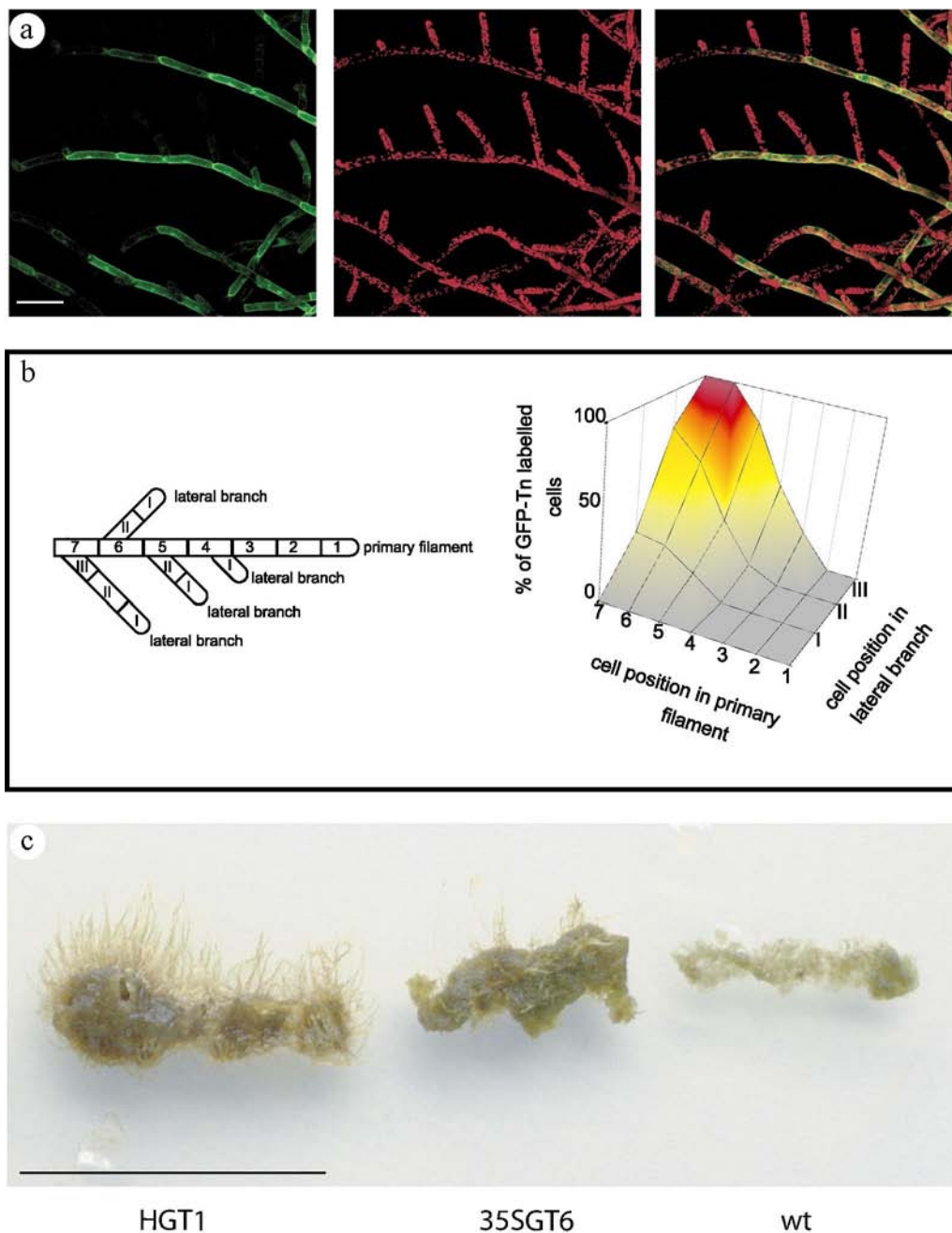


Figure 4. (a) Confocal images displaying fluorescence signal of either GFP (left) or of chloroplasts (middle) or merged (right). (b) Graph showing the distribution of labeled cells in the primary protonemal filaments and the lateral outgrowing branches. (c) Dark grown tissue. In HGT1 lines, hygromycin phosphotransferase was driven by rice *act1* promoter and caulonemata were produced, whereas 35S GT6 clone has 35S hygromycin resistance cassette with no visible caulonemal filaments.

Bar: (A)100 μ m; (C) 10 mm

2.3 Initial heat shock induction

At normal (25°C) temperature the HGT strains did not show any visible fluorescence. To find the optimal temperature conditions for the induction of GT labelling we submitted an aliquot containing about 200 000 freshly isolated protoplasts of lines HGT1 and 35S GT6 strains to a 20 minutes treatment at 25°C, 35°C or 37°C. After 16 hours, we examined the fluorescence of more than two hundred cells for each treatment (Fig. 5). We found that 50% of HGT1 cells induced at 37°C over 20 minutes were labeled. In addition, prolonged exposure of one hour yielded 91 % fluorescent cells (data not shown). The number of 35S GT labeled protoplasts remained below 30% independently of the temperature. In this strain, we could not observe any fluorescent cell in regenerated protonemal colony until it reached the 10-15 cells stage and then it was displaying the same previously described pattern.

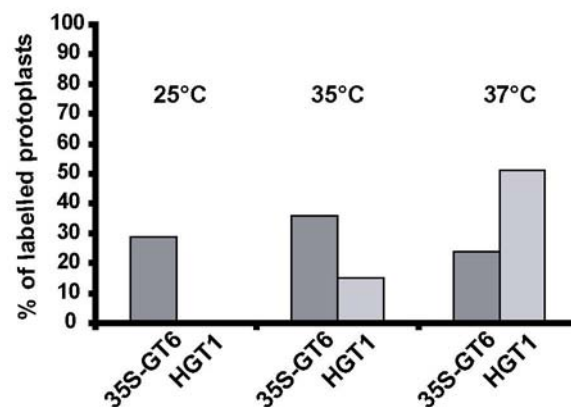


Figure 5. Graph displays amount of labeled HGT1 and 35S-GT6 protoplasts that are observed 16 hours upon induction at 25°C (control), 35°C and 37°C for 20 minutes.

2.4 Optimization of the duration of heat treatment at 37°C

Six day old moss protonemal tissue of HGT1 strain was submitted to heat stress at 37°C for 15, 30, 60 and 120 minutes and fluorescence was monitored 16 hours later (Fig. 6a). A slight induction of fluorescence could be observed in protonemal cells following a 15 minutes exposure. The GFP expression and fluorescence generally increased with prolonged time exposure. A period of one hour at 37°C enabled a complete labelling of protonemal cells. The saturation level of GFP fluorescence was reached after two hours of heat shock induction. The immunoblot confirmed the drastic increase in the levels of GT protein relative to the steady

state of the actin pool (Fig. 6b). At this stage we could not observe any effect on moss viability or morphology that could have been caused either by heat shock or by GT overproduction.

The heat-shock driven GT gene efficiently marks F-actin after a thermal induction of one hour at 37°C. Suboptimal heat treatments resulted mostly in labelling apical cells suggesting higher sensitivity of these cells to heat stress.

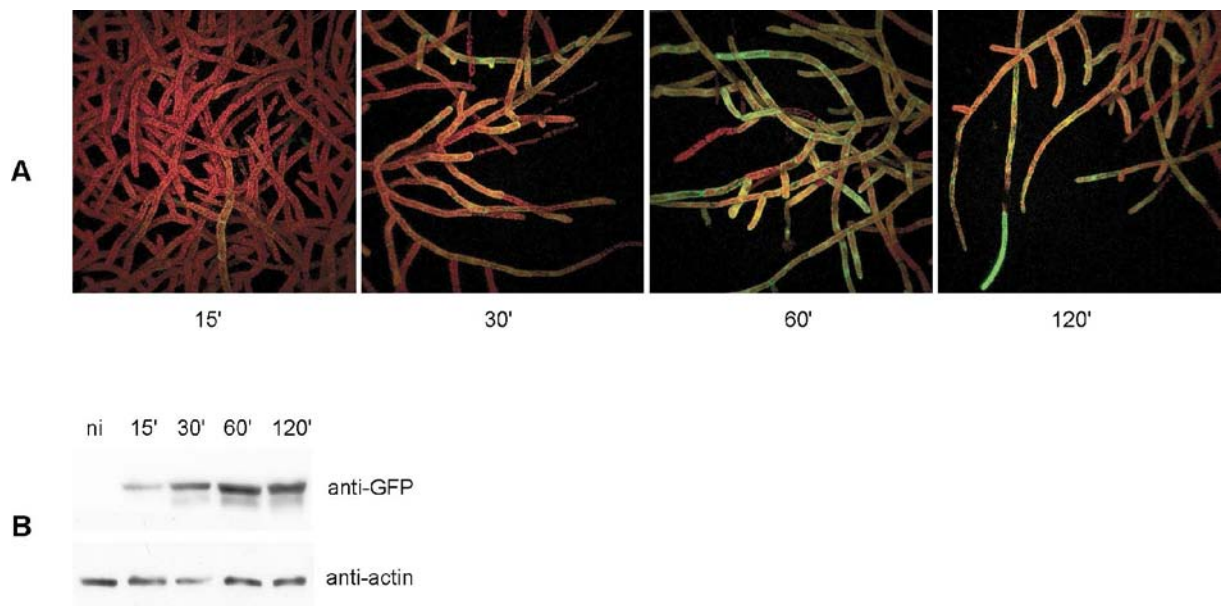


Figure 6. GT expression is differentially induced at various periods of heat shock. (A) 6 days old protonemal tissue is submitted to heat treatment for the indicated times and imaged 16 hours later by CLSM. (B) A corresponding immunoblot confirms that different amounts of GFP are produced.

Bar: 100 μ m

2.5 Up- and down- regulation of GT fluorescence

Southern analysis showed that the HGT13 line has a higher number of transgene copies compared with the two sister strains HGT1 and HGT10 (Fig. 7a). To determine whether the induction level was dependent of the transgene copy number and to determine the stability of the labelling over time we induced two HGT strains, HGT1 and HGT13, for one hour at 37°C. A time course observation of the colonies by confocal microscopy indicated that F-actin labeling by GT could be detected as early as two hours in the HGT13 strain and six hours in the HGT1 strain (Fig. 7b). After heat-shock, GFP fluorescence in all lines appeared to reach a maximum at 12 hours and remained stable for the following six hours in HGT1

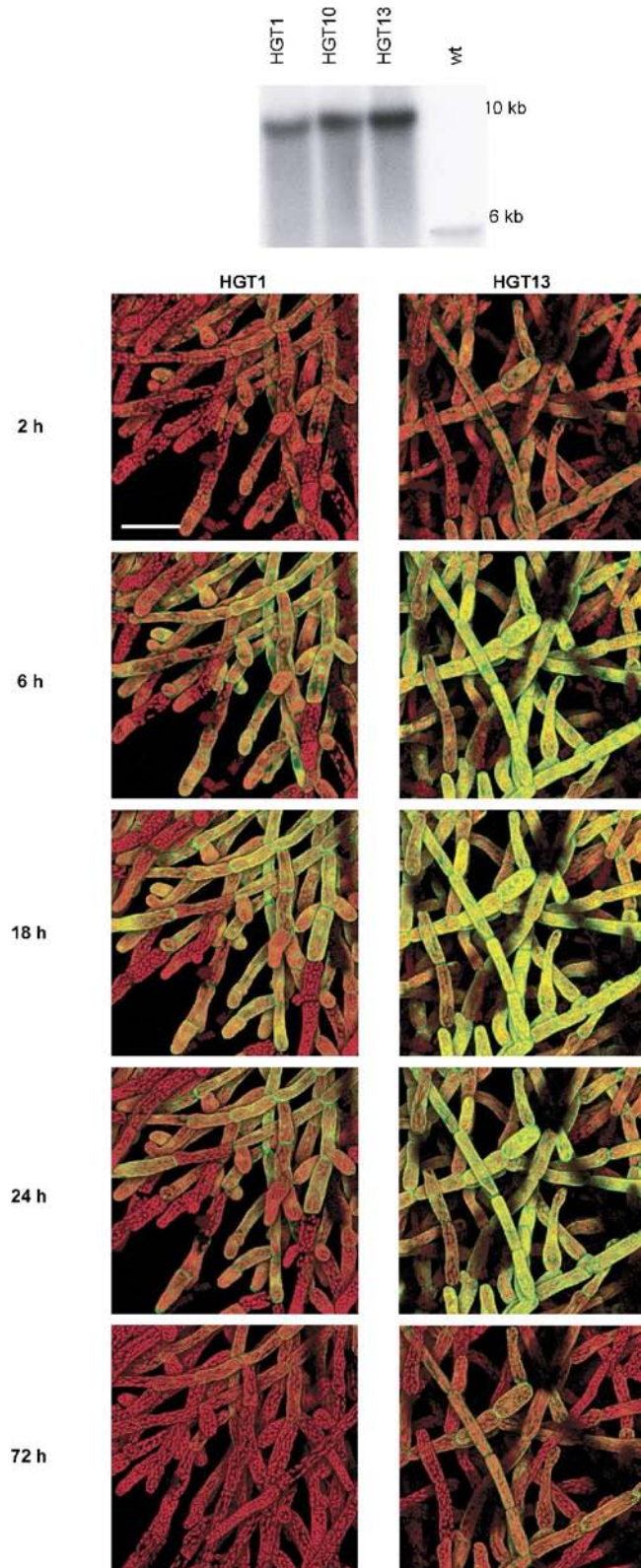


Figure 7. Time course of GT induction and decay after optimal heat stress in different clones is related to the number of copies of integrated pGmHGT-AH108. (A) Southern analysis of HGT1, HGT10 and HGT13. 2 kb of 108 locus was used as a probe (B) Protonemal colonies of strains HGT1 and HGT13 were grown for six days and then submitted to heat shock for one hour at 37°C and observed in given time period.

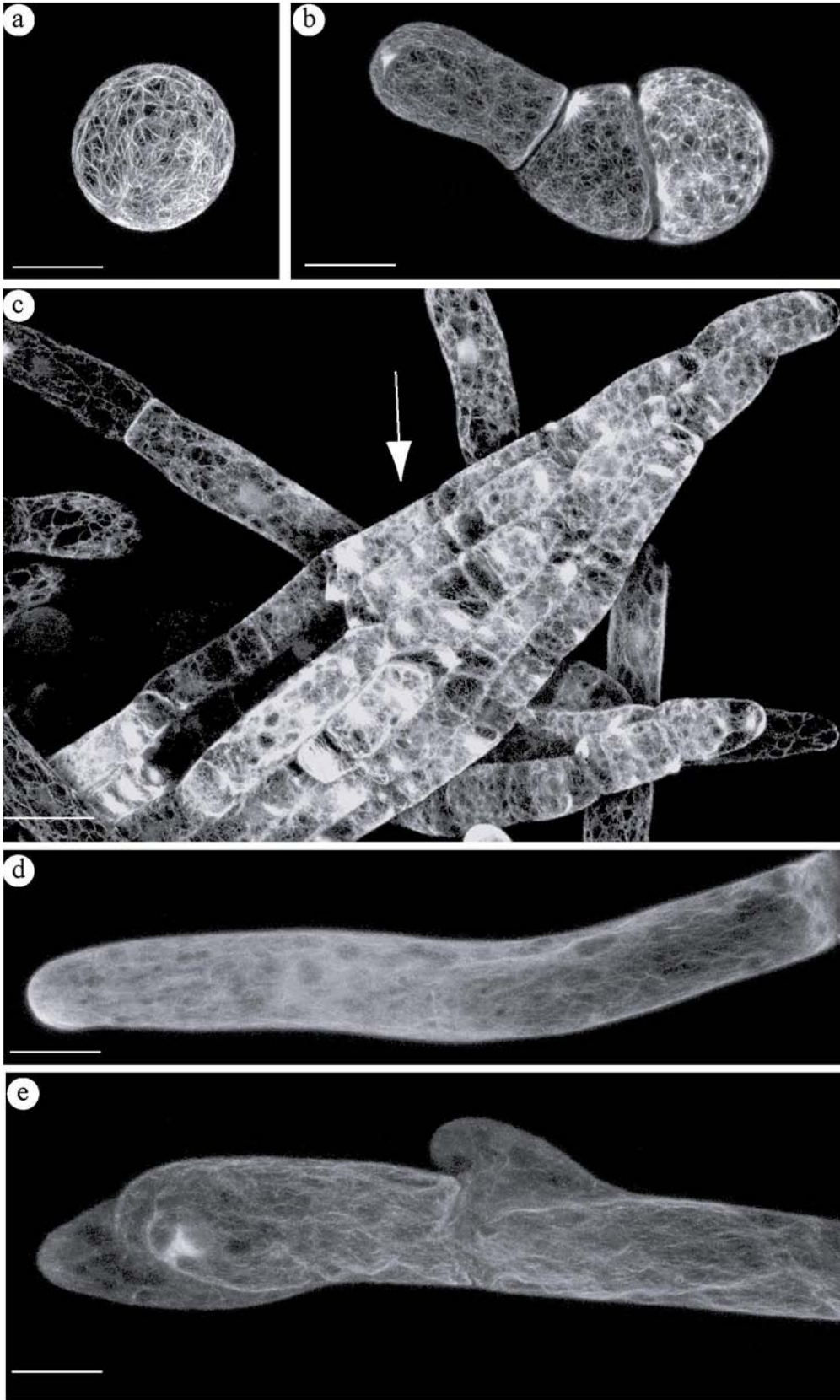
Bars: 100 μ m

strain. Thus we demonstrate that optimized heat-shock induces a complete and transient labeling of F-actin in moss cells, and that the intensity and the duration of the labeling is proportional to the number of plasmid copies integrated in the genome.

2.6 High levels of GT caused cease of growth in protonemal cells

We were interested in inducing GT in order to examine F-actin labelling at different developmental stages of moss. We found that the aforementioned one hour heat-shock at 37°C enabled to visualise F-actin network in protoplasts, protonemal cells and gametophores (Fig. 8a-8c). Detailed confocal imaging of apical caulonemal cell revealed a fine meshwork of densely intertwined F-actin strands converging toward an accumulation point at the very cell apex (Fig. 8d).

It has already been documented that strong overexpression of GT driven by pollen specific promoter caused retardation of growth in the pollen tubes of tobacco (Kost et al., 1998). In order to verify whether apical caulonemal cells can support the permanent presence of GT, we induced accumulation through repeated thermal treatment. We applied two one hour heat-shocks on the HGT1 protonemal colony with a 24 hour recovery period between each treatment. As a consequence, we observed swelling and misshapen morphology of the caulonemal cells, displacement of apical caps and of the fine actin network, as well as microfilament aggregations into thicker cables (Fig. 8e). As a control, the same treatment was applied to wild type and 35S-GT6 plants; it did not visibly result in any similar morphological alterations (cell swelling) confirming that the observed effect is likely to be caused by the overloading of GT and not by heat stress (Fig. 8f).



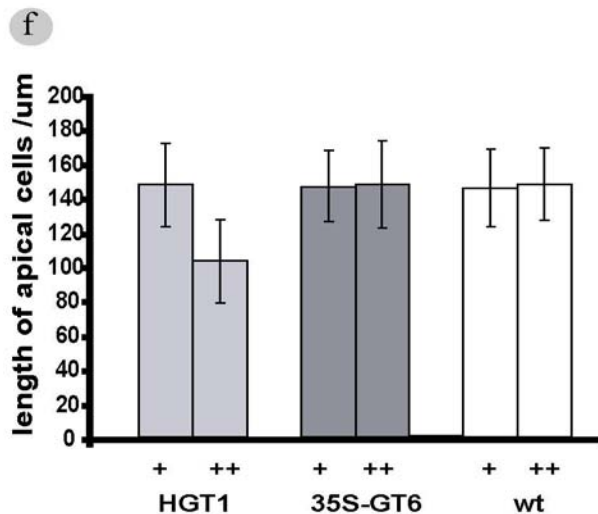


Figure 8. (a) Confocal image of a protoplast 16 hours upon induction. Upon isolation the protoplasts were submitted to heat stress for one hour. The network of actin cables is present. (b) Three days old protonemal colony regenerating from protoplast. Note the apical accumulation of F-actin. (c) Part of young gametophore with labeled juvenile leaf (arrow). (d) Confocal image of caulonemal cell taken 16 hours after single heat induction. (e) Confocal image of caulonemal cell taken after two heat inductions in the period of 24 hours. Image is taken 16 hours after second heat.shock. (f) Graph shows average length of apical caulonemal cells in HGT1, 35S-GT6 and wild type strains after one (+) or two (++)consecutive heat stress.

Bars: (a) , (b) and (d) 20 µm; (c) 40µm

2.7 Acetyl-salicylate induction was localized in juvenile cells of moss protonemal tissue

It has been demonstrated that expression of the GUS reporter protein placed under *GmHsp17.3* promoter at 25°C could be achieved in the presence of acetyl-salicylate (ASA). One hour treatment at 0.8 mM of ASA resulted in a six fold lower expression of GUS, than the one hour heat shock treatment at 38°C. We tested the HGT1 strain under both conditions. One hour induction at 38°C resulted in a remarkably uniform labelling of the majority of the *P. patens* chloronemal cells. In contrast, one hour exposure to 0.8 mM ASA at 25°C resulted in efficient labelling mostly of apical cells, and poor labelling of differentiated subapical cells (Fig. 9). This suggests that the complexity of the cell wall can limit the penetration of ASA into older cells. Yet, indistinguishable clear patterns of actin filaments are obtained following the two types of treatments (not shown), demonstrating that ASA induction is a viable alternative to heat-shock induction of proteins in plant, when heat-shock conditions must be avoided.

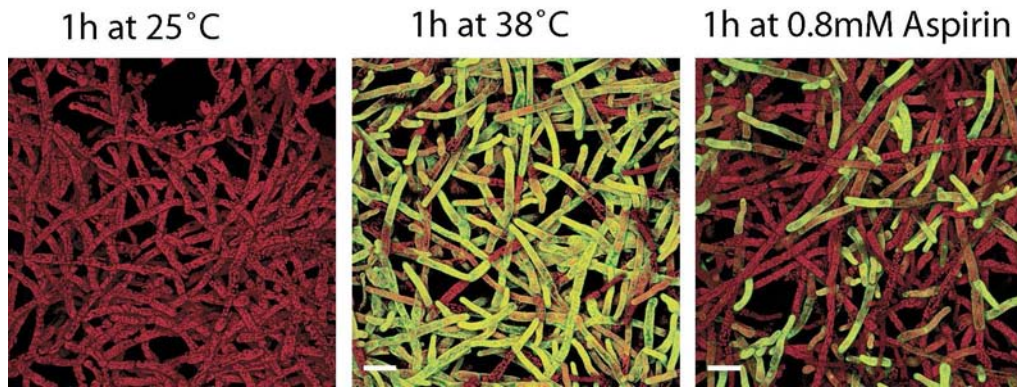


Figure 9. Heat-shock induced GFP-Tn causes overall labelling of moss tissue compared to ASA induction. Protonemal moss tissue is uniformly labeled upon heat-stress (left), whereas ASA (middle) induces GFP-Tn expression only in apical and adjacent subapical cells. Untreated protonemata (right) are not labeled. Detailed images of apical chloronemal cells show no differences in morphology and cytoskeletal organisation. Confocal projections represent merged GFP signal and chloroplast autofluorescence. Bars: (a) 100 μm ; (b) 20 μm

3. Discussion

We have generated two types of transgenic lines of moss *P. patens* expressing GFP-Talin either under the constitutive 35S CaMV promoter or heat-inducible soybean Hsp17.3 gene promoter. In HGT strains, the entire moss tissue has been labeled following one hour thermal treatment at 37°C followed by 16 hours recovery at 25°C, whereas in 35S-GT strains the labelling has been observed in old cells, but not in regenerating protoplasts, juvenile protonemal cells and young gametophores.

It has been shown in transgenic strains containing the GUS gene driven by Hsp17.3 promoter that GUS activity was very low at room temperature and was induced over up to 3 orders of magnitude following heat-shock (Saidi et al., submitted). This work also demonstrated that maximal expression levels in these strains were 300 and 30 fold higher than those measured in transgenic strains carrying the GUS gene driven by the 35S and *act-1* promoter, respectively. These data strongly indicate that the 35S promoter is a rather weak promoter in moss cells. In addition, we demonstrate here that the activity of 35S promoter is reduced in darkness, whereas the *act-1* promoter is still active.

Some reports describing spatio-temporal expression of 35S-GFP in whole plant failed to detect fluorescence in early stage of embryo development in cotton (Sunilkumar et al., 2002), whereas GFP was absent from mature leaves of *M. truncatula* (Zhou et al., 2004). In 35S-GFP-Talin transgenic *Arabidopsis*, successful labelling of actin structures was limited to developed trichomes, leaf cells and root hairs, whereas constitutive over-expression of GFP-Talin in pollen tubes inhibited pollen growth (Kost et al., 1998) (El-Assall et al., 2004). Three reasons can account for these observations: (a) the expression profile of the 35S promoter is not uniform in plants, (b) the stoichiometric balance between GFP-talin and F-actin amounts may not allow efficient labelling of F-actin in cells with high actin turnover, as during differentiation, and (c) high GT expression may reduce the dynamics of the actin cytoskeleton, thus limiting the growth of over-expressing transgenic plants. Our data support the idea that the strength of 35S promoter is insufficient to label F-actin in juvenile cells with a high actin turnover, whereas differentiated older cells have accumulated enough GT to label F-actin. On the other hand, the strength of the GmHsp17.3 promoter allows the labelling of F-actin in every cell including the juvenile one. Additionally, this promoter induces a transient

expression of GT, which prevents the toxic effect resulting from constitutive high expression of GT.

We propose that temporary labelling of filamentous actin network by GT can be achieved without affecting morphology using a heat stress promoter. In contrast, prolonged exposition of the cell to GT was leading to cellular aberrations. Upon induction, HGT strains tolerate the temporary peak expression of GT expression without any obvious interference with the cell morphology. To the contrary, the permanent presence of GT blocks growth of apical protonemata confirming the toxic effect found in growing tobacco pollen tubes (Kost et al., 1998). Our unsuccessful attempts to produce a stable transgenic moss having GT driven by the strong constitutive rice *act-1* promoter (Mcelroy et al., 1991) most likely failed due to this toxicity of a permanently high concentration of GT (Finka, unpublished observation), although low copy number of this expression cassette could be supported (Sato, personal communication)

Our plasmid constructs as well as the moss transgenic plants we obtained are very powerful tools to examine the plant actin cytoskeleton. Specifically, forward and reverse genetic assays could identify the proteins involved in upstream regulation of actin polymerization as well as the elements that regulate the actin cytoskeleton in cell morphogenesis and development. Furthermore they could be applied in the rapid screening for compounds that elicit heat receptors as well as the characterization of the receptors by themselves (Saidi, submitted). To conclude, using the inducible heat-shock promoter *Gmhsp17.3* we have achieved complete labelling of *Physcomitrella* HGT transformants by GT in a spatial and temporary reversible manner.

4. Materials and methods

4.1 Construction of integrative heat-shock inducible GT vector

All plasmid manipulations and bacterial transformations were performed by standard techniques (Sambrook et al., 1989). In order to put the GT cassette under the control of the 507 bp upstream activating region of the gene encoding the soybean heat shock protein (GenBank Acc. No.: X01104), the GT cassette, excised by Nco/EcoRI from pYSC14, was inserted in a Nco/EcoRI digested p*Gmhsp17.3*-GUS vector (Saidi et al., submitted) to generate p*GmHGT*. The pBS-BMAH108 vector (see [Annex 1](#) for construction) containing the hygromycin cassette driven by the rice actin promoter (Mcelroy et al., 1991) along with 2 kb of *108* genomic locus (Schaefer and Zryd, 1997) was digested by NotI. The resulting 4.7 kb fragment was placed into the single NotI site of p*GmHGT* backbone thus generating the p*GmHGT*-AH108 vector used in moss transformation.

4.2 Isolation and Detection of DNA

Genomic DNA was isolated using the cetyltrimethylammonium bromide method (Schaefer and Zryd, 1997). The genomic DNA (3 µg per lane) was digested by *EspI* (Fermentas), separated on a 0.7% agarose gel and blotted on Zeta-Probe membranes (BioRad). Labelling of the probes (Amersham) and probe hybridisation was performed according the manufacturer's protocols. High-stringency genomic DNA hybridisation was performed in Church buffer (0.25 M sodium phosphate; pH 7, 7% SDS) at 65°C and washed three times with 0.1x SSC (20x SSC is 3 M NaCl and 0.3 M sodium citrate) and 0.1% (w/v) SDS. Finally, the membranes were exposed to X-Omat AR film (Kodak).

4.3 Plant tissue culture, protoplast transformation and isolation of transgenic lines

P.patens was grown axenically either on solid minimal medium (Ashton and Cove, 1977) or on minimal medium supplemented with 2.7 mM ammonium-tartrate (Merck) and 25 mM glucose (Fluka). The standard growing conditions were defined as 16 hr of light and 8 hr of darkness at 25°C, whereas a light intensity used in this study was 80 µmol m⁻²·sec⁻¹ (white light).

Isolation of protoplasts, polyethylene glycol-mediated transformation and regeneration and hygromycin selection were performed as described previously (Schaefer and Zryd, 1997), (Girod et al., 1999).

35S-GT lines were generated by co-transformation of equimolar amounts of pYSC14 and pGL108 that was linearised by *Cla I*, whereas HGT lines were obtained upon transformation by the pGmHGT-AH108.

4.4 Immunoblotting

Plant tissue (~100 mg) was ground directly in 100 µl of sample buffer (100 mM Tris; pH 6.8, 20 mM EDTA; pH 6.8, 20% glycerol, 4% SDS, 20 mM β-mercaptoethanol), incubated for 1 hour at 40°C and briefly centrifuged. Proteins were quantified by Lowry assay (Lowry et al., 1951) and 20 µg were loaded on a 12% polyacrylamide gel. Polypeptides were separated by SDS-PAGE and electrotransferred onto a 0.2 µm nitrocellulose membrane (Biorad) at 100 V for 1 hour in transfer buffer (25 mM Tris, 192 mM glycine and 20 % methanol). The membrane was briefly stained in 2% Ponceau S (Sigma) to confirm equal loading and protein transfer and then blocked for 1 h in TTBS buffer (20 mM Tris; pH7.6, 1.37 M NaCl, 0.1% Tween 20) containing 1% non-fat dry milk, and subsequently incubated for 1 h in monoclonal anti-GFP primary antibody (1:2,000; Roche). Following three 10-min rinses in TTBS, the membrane was incubated in anti-mouse horseradish peroxidase-conjugated secondary antibody in TTBS (1:2,000; Sigma) for approximately 1 h. The membrane was washed and developed using the chemiluminescent Immunstar™ Kit (Bio-Rad) according to manufacturer's instructions. Upon detection of GT, the blot was stripped (100 mM 2-mercaptoethanol, 2% SDS, 62.5 mM Tris-Cl pH 6.7) at 50°C for 30 minutes. Following washing and blocking, the blot was probed with the monoclonal anti-actin antibody C4 (1:1000, ICN Biomedicals) overnight at 4°C and developed as above.

4.5 Heat-shock treatment

Cellophane disks containing moss tissue were transferred to preheated solid medium agar plates at 37°C, which were sealed with parafilm and placed into the cabinet at the same

temperature. After treatment, disks were returned onto the original plates and placed in a growth chamber.

4.6 Live cell microscopy and image analysis

For confocal microscopy, carefully excised pieces of cellophane containing undamaged moss tissue were transferred into the glass slide chamber (Lab Tek II, Nunc) in inverted position and covered by a block of solid agar medium. Confocal microscopy was performed on a TCS SP2 system using an inverted microscope (Leica-DMRE). A krypton-argon laser (488-nm line) was used for excitation. To distinguish between the GFP fluorescence and red autofluorescence of chloroplasts, the bandwidth mirror settings for discriminating between the two signals were 504/531 for GFP and 634/696 for TRITC (chloroplasts). The two channels were allocated false green (GFP) and red (TRITC) colours. The projections of image stacks were processed using Photoshop 6.0 software (Adobe Systems).

ACKNOWLEDGEMENTS

We thank Dr. Nam-Hai Chua for kindly providing of pYSC14 plasmid. This work was supported in part by Swiss National Science Foundation (Grant # 31-51853.97).

Chapter II: Distinct spatio-temporal F-actin assemblies are present at different developmental stages in the moss *Physcomitrella patens*

ABSTRACT

The actin cytoskeleton plays a crucial role in cellular differentiation. In the previous chapter, we developed optimal conditions of F-actin labeling in the moss *Physcomitrella patens* by using heat-shock induced GFP-Talin (GT) expression. By confocal microscopy, we examined the spatio-temporal organization of F-actin at all developmental stages. The observed structures including patches, star-like structures, converging apical arrays, subcortical network of thin, randomly organized actin strands in juvenile cells, and networks of thick actin bundles in differentiated cells. In regenerating protoplasts, apical protonemal cells and rhizoids, converging actin arrays were densely accumulated at the growing tip and connected with dispersed fine F-actin mesh, whereas undulating network of actin cables were found at the final stage of cell differentiation. The cortical star-like structures are widespread in the meristematic cells of developing bud and young gametophores but not in adult leaves. In addition, during redifferentiation of mature leaf cells into protonemal filaments the rather stagnant web of actin cables is replaced by diffuse actin meshwork.

Altogether, our results show that different assemblies of actin microfilaments reflect their particular role in morphogenetic and developmental status of different moss cell types.

1. Introduction

Studies of cellular growth and morphogenesis highlighted the involvement of the actin and microtubule cytoskeleton in these processes (for reviews see (Wasteneys and Galway, 2003); (Smith, 2003). For decades, spatiotemporal organisation of actin cytoskeleton in plant cells was examined in fixated tissues followed either by indirect immunofluorescence or by rhodamine-phalloidin staining (Traas et al., 1987), (Doris and Steer, 1996), (Olyslaegers and Verbelen, 1998), (Wasteneys et al., 1997). A non-invasive method of overexpression of GFP conjugated to the F-actin binding domain from mouse talin revolutionized studies of actin microfilaments in living cells (Kost et al., 1998). Thus research conducted on the plant F-actin and its relations with cell morphogenesis put emphasis on single cell systems of angiosperms such as root hairs, pollen tubes and trichomes (Kost et al., 1999), (Hepler et al., 2001), (Mathur et al., 1999). The F-actin bundles are longitudinally oriented in tip-growing root cells from *Arabidopsis* and tobacco pollen tubes. A network of fine actin strands is found in the apical region of terminally differentiated root hairs and in sub-apical region of pollen tubes (Baluska et al., 2000) and (Hepler et al., 2001). Besides, labeled microfilaments form a network around nucleus, and extend through cytoplasmic strands (Kost et al., 1998). In the early stages of *Arabidopsis* trichome development GFP-decorated microfilaments are diffusely distributed, becoming organised into the characteristic strands in later stages (Mathur et al., 1999).

The mosses represent suitable models for studying cytoskeletal organisation because they can be examined in a complete cell lineage at the single cell level (Schnepf et al., 1986). Studies of actin cytoskeleton in mosses have been limited to the analysis of fixated protonemal tissue showing longitudinally oriented actin cables in dark grown caulonemata from *Physcomitrella patens* (Doonan et al., 1988) as well as in protonemata of *Ceratodon purpureus* (Walker and Sack, 1995); (Meske and Hartmann, 1995) and *Funaria hygrometrica* (Quader and Schnepf, 1989). The actin strands have not been visualized in the very tip of caulonemata of *Ceratodon* (Meske and Hartmann, 1995). In *Funaria*, particular F-actin arrays have been detected at the prospective outgrowing sites during side branching initiation (Quader and Schnepf, 1989). Cell cycle studies have shown a phragmoplast composed of two rings of interconnected microtubules and actin filaments (Doonan et al., 1988). In addition,

functional studies have frequently been conducted using pharmacological agents that specifically interfere with microtubules and microfilaments. These essays demonstrated that actin filament disrupting drugs like cytochalasins abolish tip-growth in *P. patens* (Doonan et al., 1988) whereas the antimicrotubule drugs oryzalin and cremart generate subapical protrusions and lateral branching in mosses (Doonan et al., 1988); (Meske and Hartmann, 1995).

In the previous chapter, we achieved overall moss labelling by GT using heat-shock induction. Since the organisation of actin microfilaments during moss development remained totally unknown, we attempted to describe it in detail by using confocal microscopy. Our report demonstrates the existence of subcortical actin patches, star-like structures, and complex arrays in actively growing cells, whereas a network of actin bundles was predominant in differentiated cells. We show existence of labeled network around nucleus and presence of GT in cytoplasmic strands. In protonemal cells and rhizoids, apical distribution of F-actin determined new cell outgrowth. Furthermore, re-differentiation processes were followed by cytoskeletal rearrangement. Finally, the application of cytoskeletal inhibitors targeted selectively F-actin arrays of moss protonemata. As a whole, our detailed description of F-actin structures shed a new light on the role of F-actin during moss growth establishing *P. patens* as a model for studying cytoskeletal organisation in plants.

2. Results

2.1 Polarized accumulation of F-actin was localized at the growing pole of regenerating protoplasts

We initiated our developmental description of F-actin on regenerating protoplasts of HGT1 strains. Freshly isolated unlabeled protoplasts were embedded in solid medium, placed for 24 hours in darkness and then regenerated in light. Each of the following five days, we treated a portion of such embedded protoplast with optimized heat shock. We followed the localization of GFP-mTn in regenerating cells after every treatment. Using epifluorescence microscopy we estimated that approximately 95% of the spherical protoplasts had uniform distribution of fluorescence across their surface. At the single cell level, detailed confocal imaging revealed a subcortical network of cables that corresponded to a labeled subcortical microfilament network (Fig. 10a). Over the following next 24 hours, the distribution of fluorescence became polarized and it was found that F-actin was accumulated as a bright cortical array at the growing pole of pear shaped regenerating cells (Fig. 10b). In divided protoplasts, polar F-actin array was present at the growing side, whereas accumulation of GFP-mTn was detected on both sides of the cell wall separating two cells (Fig. 10c). After six days, multicellular chloronemal colonies displayed the previously described cap of F-actin at the tip zone of apical cells. In the subsequent four to five subapical cells, we often found similar lateral cortical structures at the presumptive site of new side branches (Fig. 10d). The position of the new cell outgrowth could be confirmed after 48 hours (data not shown). These data indicated that apical F-actin accumulation was tightly linked to polar outgrowth.

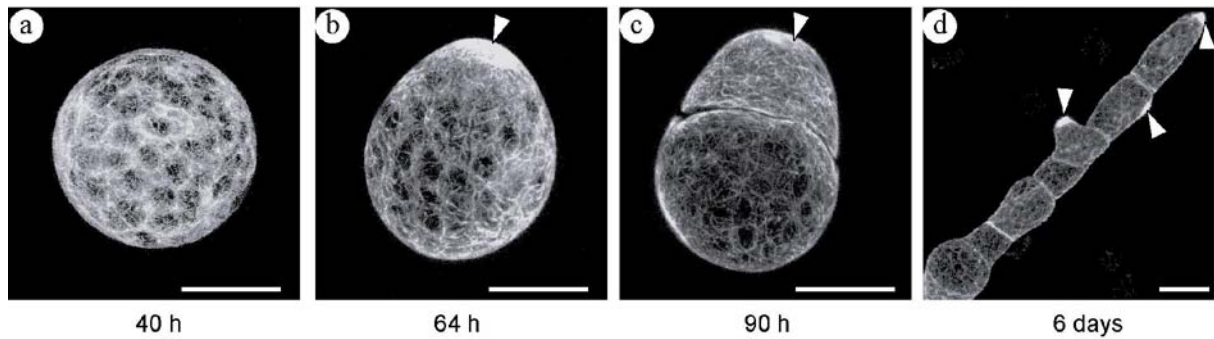


Figure 10 . Apical arrays of F-actin determine cell outgrowth

Freshly isolated protoplasts were kept for 24 hours in darkness and then GFP-mTn was heat induced during different developmental phases. CLSM images showing only the GFP signal were taken 16 hours post-induction. The given time corresponds to cell age after isolation. (a) Spherical protoplast showing random distribution of actin strands. (b) An asymmetric, pear-shaped protoplast with actin accumulation at the growing tip (arrowhead). (c) The apical daughter cell obtained by division of an asymmetric cell continued to maintain tip actin accumulation. (d) Newly formed protonemal filament containing accumulated F-actin at the very tip of apical chloronemal cell. Prominent F-actin accumulation is also visible in subsequent subapical cells determining outgrowth of lateral cell (arrowheads). Bars: 20 μ m Step size (A)-(C):160 nm; (D): 630 nm

2.2 Different microfilament assemblies were present in protonemal cells

We proceeded to make a detailed description of F-actin assemblies in protonemal cells. Confocal imaging of apical chloronemal cells (Fig. 11a) revealed stellated feature of cap structure followed by a rather diffuse subcortical actin network that was interspersed with small patches. In subapical cells at the site of new cell outgrowth, we frequently observed small distinct cortical star-like structures or microfilament organising centres (MFOCs) that were directly interconnected with actin cables. Following further development of chloronemal filaments, subapical chloronemal cells that were positioned at least six cells away from the apex (Fig. 11d) contained a well defined network of subcortical undulating actin bundles that were parallel to the long cell axis, although MFOCs were observed less frequently. In the interior of the cell, the nucleus was surrounded by a mesh of fine actin filaments. Labeled F-actin could also be observed in cytoplasmic strands connecting the nucleus to the cell cortex (Fig. 11e). Finally, we observed that chloroplasts, which were mainly located in the cell periphery, were also surrounded by a mesh of fine F-actin and interconnected by cytoplasmic strands containing F-actin.

In apical caulonemal cells, the F-actin cap was also localized in an apical zone, whereas a dense network of longitudinally-oriented intertwined actin strands were intensely

amassed at the tip growing part of the cell (Fig. 11b). In the subapical caulonemata the numerous thick actin bundles were aligned in parallel displaying clear polar distribution (Fig. 11c).

Our images suggest that observed differences in spatiotemporal organisation of F-actin structures were related to morphology of protonemal cells. Our next interest was to depict the organisation of actin networks during the formation and the development of moss organs by caulinary growth.

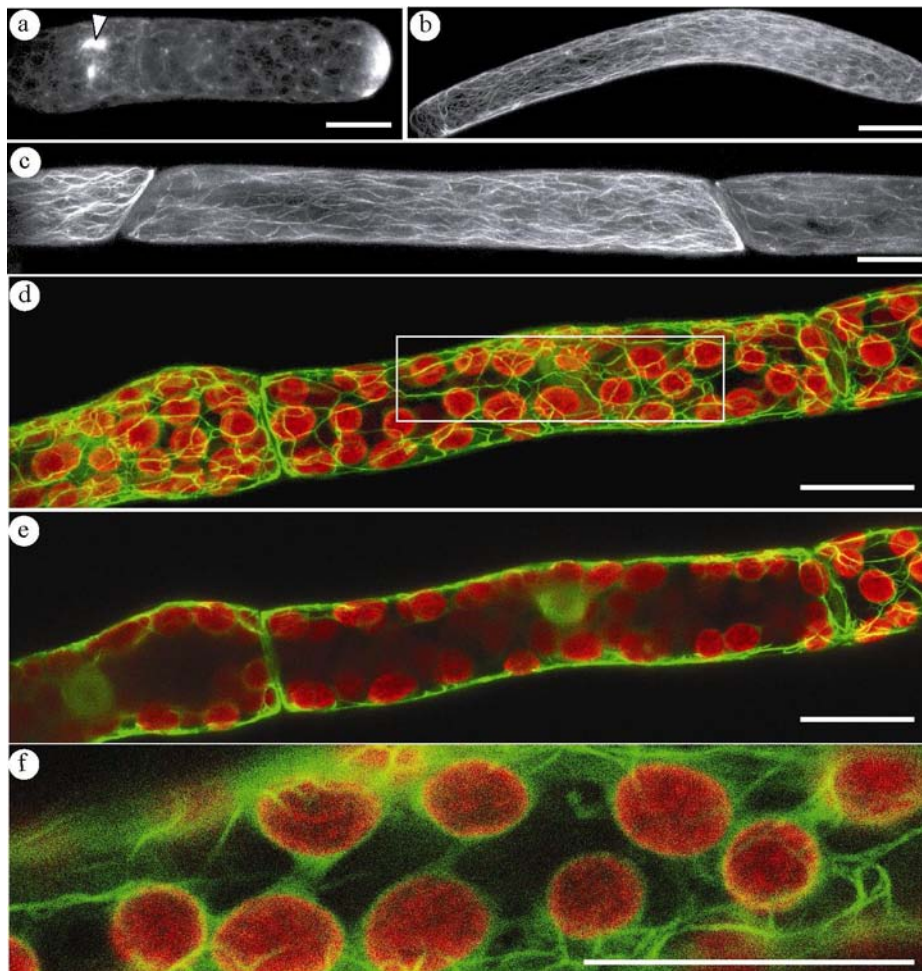


Figure 11. Various actin arrays are present in growing and differentiated protonemal cells. (a) In apical chloronemal cell, F-actin forms radial cap structure at the very tip of the cell followed by dispersedly localized patches throughout the cell. Smaller star-like MFOCs are visible in the subsequent cell. (b) Juvenile caulonemal cell containing apical cap structure and having dense network of actin cables. (c) Differentiated caulonemal cell with apicobasal distribution of actin bundles. (d) Chloronemal subapical cell with a defined network of undulating actin bundles. (e) Confocal projection of 30 optical sections from the medial region representing the F-actin mesh around nucleus and cytoplasmic strands. (f) Single confocal section representing the boxed region of (d) displaying F-actin mesh around chloroplasts and connections between them. Figures 2d-2f present merged confocal projection between GFP and chloroplast signals. Bars: 20 μm . Step size: (a), (b), (c), (e) and (f):160 nm

2.3 Gametophores exhibited differential labelling during their development

We continued our observations on tissue older than two week, grown on solid minimal medium. The observations were made 16 hours after one-hour heat-shock induction of GT. In the emerging buds, we noted that the youngest meristematic cells contained a dense network of randomly oriented microfilaments with two or three prominent actin arrays per cell (Fig. 12a). The phragmoplast was visualised as a dense band determining the future plane of the cell wall between these cells. The cells that formed the base of the gametophore as well as those in the surrounding meristem had a distinct network of actin cables with detectable actin patches. Following further development, the juvenile leaves of gametophores (Fig. 12b) contained MFOCs and actin bundles that were more often transversally positioned along the longitudinal axis of the cell. Finally, in adult leaf of a one month old gametophore (Fig. 12c), we identified isolated star-like structures mainly in the basal part of the leaf. The actin network in these cells was made from subcortical actin bundles without preferential orientation. Apical rhizoids that emerged from the base of the gametophores possessed a network of undulating cables converging at the cell apex in a cap structure similar to caulonemal cells (Fig. 12d and 12e). These data showed that transition from unidirectional to caulinary development included formation of complex F-actin arrangements depending on the specific morphogenetic stage of each cell. The homogeneous presence of bundled actin network in every leaf cell represented the final step in differentiation.

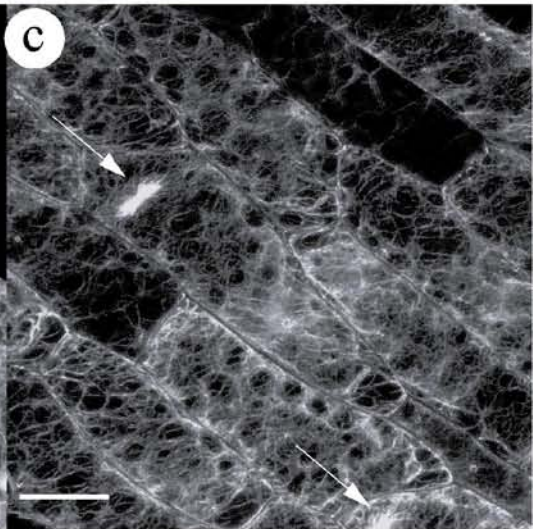
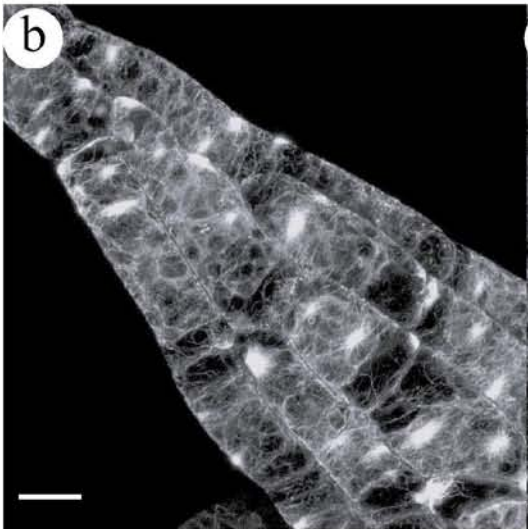
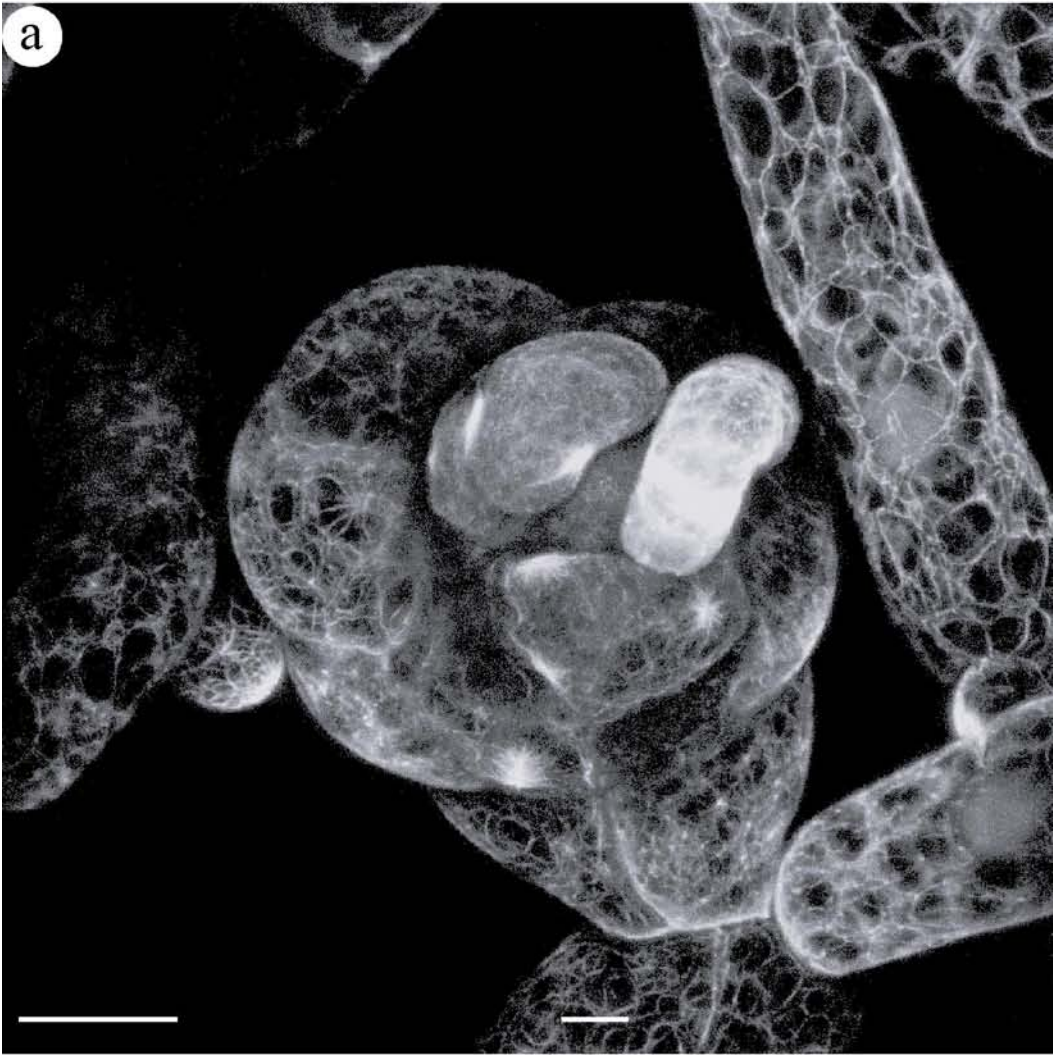


Figure 12. Labelled F-actin networks during development of gametophore. (a) Proliferating bud showing complex organization of actin network. The areas of dense and diffuse actin as well as the MFOCs are present more often in the youngest meristematic cells compared to other cells. (b) Labeled leaflet of juvenile gametophore in which every cell contains elongated MFOCs. (c) Detailed image of part of the leaf of adult gametophores displaying structural organization of actin bundles in leaf cells. Only few MFOCs are visible (arrows). (d) Transmission image of rhizoid filament with tip cell (e) containing apical actin array. Bars: 20 μm . Step size: (a), (b), (c), and (e):160 nm

2.4 Redifferentiation of leaf cells required replacement of bundled F-actin networks with fine meshworks

In order to determine whether redifferentiation required disassembly of actin bundles, we dissected and placed 20 adult leaves of five gametophores on solid minimal medium supplemented with ammonium and glucose. After two days we induced GFP-mTn in these leaves. In early dividing cells, we distinguished a diffuse mesh of actin fibres (Fig. 13a). These cells contained half sized chloroplasts compared to undivided neighbouring cells. In order to monitor the destiny of these cells we followed ten such spots on three leaves. After three days, we could see four protonemal filaments protruding from dedifferentiated leaf cells (Fig. 13b). In the proliferating apical cells, the actin network included apical actin arrays followed by diffuse F-actin strands, which were similar to the previously described apical chloronemal cell. On the contrary, the cytoplasmic content of undifferentiated leaf cells remained enclosed by the cage of actin bundles.

These results indicated that processes of redifferentiation and rapid growth required substitution and spatial rearrangement of thick actin strands into dense microfilament network in order to begin outgrowth of protonemal cells.

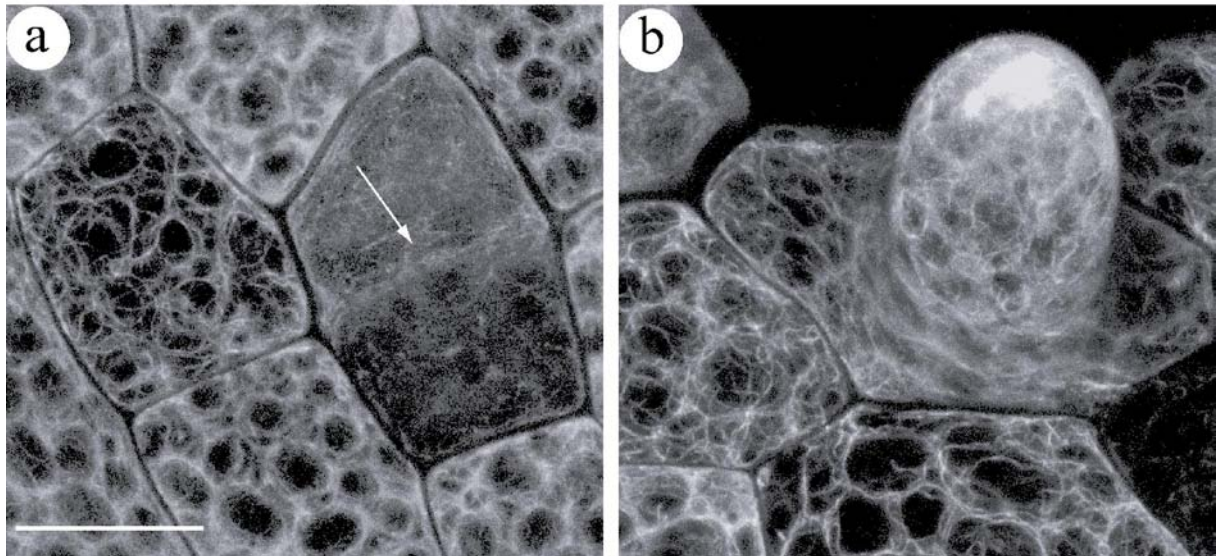


Figure 13. The actin bundles are substituted by diffuse actin meshworks and arrays during redifferentiation processes of leaf cells. (A) Confocal projection displays diffuse GFP fluorescence in newly divided cells (right) compared to the neighbouring cell where cable network is still visible (left). New cell wall is also noticeable (arrow). (B) CLSM image shows differentiating chloronemal cell having prominent apical F-actin array. Bars: 20 μm . Step size: (A) and (B): 160 nm

2.5 The networks of actin bundles in chloronemal cells can be disturbed by cytoskeletal disorganizing drugs

In order to confirm that GT labeled microfilaments were susceptible to cytoskeletal inhibitors, F-actin disrupting drug cytochalasin B and microtubule disrupting drug oryzalin were applied on heat-shocked protonemata at final concentrations of 10 μM and 3 μM , respectively. In cells treated by cytochalasin B we did not observe F-actin caps in the emerging cells, whereas the actin cable network was seriously distorted in subapical cells (Fig. 14a). Further incubation with cytochalasin B resulted in newly formed cells, which were approximately half as long as in untreated controls (not shown).

Treatment with 3 μM oryzalin induced characteristic bulging in growing protonema 14 hours after the beginning of the experiment. In confocal microscopy, the characteristic F-actin cap appeared at the bulged end, whereas a network of bundled actin cables was reoriented toward the tip actin array (Fig 14b).

Here we confirmed that cytochalasin B has a specific deleterious effect on F-actin structures such as bundles and apical arrays. On the other hand, oryzalin induced misoriented

tip growth without affecting the actin structures associated with this process. This data confirm previous observations with cytoskeletal inhibitors

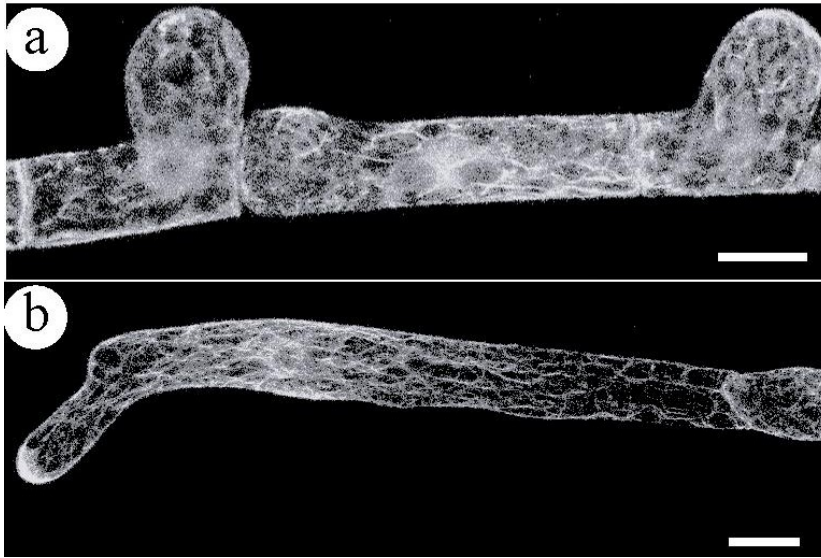


Figure 14. Effect of cytoskeletal disrupting drugs on microfilament network

(A) Disruption of microfilaments by Cytochalasin B causes loss of actin caps in outgrowing cells and destroys cable network. (B) Oryzalin provokes appearance of F-actin cap at the bulging site reorienting of actin cables.

Bars: 20 μm

3. Discussion

The GFP-mTn expressed under the control of the heat-shock *GmHSP17.3* promoter efficiently visualizes F-actin organisation *in vivo* during moss unidirectional and caulinary development without phenotypic alterations. For the first time, GFP-mTn labelling reveals the existence of several categories of F-actin assemblies including small actin patches, individual MFOCs, tip arrays, meshes of fine F-actin and networks of bundled actin that are distributed in different cell types according to their cellular morphogenetic status.

The small cortical patches appear in cells where a dense network of actin cables has not been yet completely formed. In fission yeast, as in budding yeast, F-actin patches and cables are the primary F-actin structures containing components of the Arp2/3 complex and other actin-interacting proteins that are necessary for F-actin polymerization (Pelham and Chang, 2001). These patches coincided with the sites of cell wall deposition in *S. cerevisiae* (Pruyne and Bretscher, 2000). These patches could represent nucleation centers for the establishment of more complex structures required later for differentiation.

The establishment of a polar axis precedes polar outgrowth during moss protoplast regeneration (Cove, 1992). Our results on F-actin localization during the polarization process demonstrate the involvement of F-actin in establishing the polarity axis at the unicellular stage of moss development. This reinforces earlier studies conducted on the embryos of *Fucus* and *Pelvetia* by rhodamine-phalloidin staining where it has been shown that F-actin accumulates at the prospective site of rhizoid pole when unilateral light was applied to induce zygote regeneration (Kropf et al., 1989); (Alessa and Kropf, 1999). These microfilament arrays as well as the star-like actin arrays in subapical chloronemal cells determine the position of cell outgrowth of protonemal cells and rhizoids. Similar actin arrays visualized by rhodamin-phalloidin are described in *Funaria* during side branch initiation in protonema cells (Quader and Schnepf, 1989). In growing pollen tubes and root hairs of higher plants, actin cables have never been detected at their very tip (Kost et al., 1998), (Baluska et al., 2000), but they are present in the apices of terminally developed root hairs. Finally, various longitudinal actin networks have been detected in differentiated subapical chloronemal and caulonemal cells with a resolution that has never been achieved before. Thus their morphological differences (Schumaker and Dietrich, 1997) can be confirmed also at the level of actin cytoskeleton

enabling to further investigate the relation between the actin cytoskeleton and the different morphology and function of these two cell types.

The transition from filamentous growth to three-dimensional growth requires drastic changes in cellular cytoskeletal arrangement because previous apicobasal determination of growth is replaced by lateral interactions in multicellular buds and leaves. Similar to protonemal cell differentiation, spatiotemporal re-arrangement of F-actin takes place from the fine filaments in meristematic cells of buds and young leafy gametophytes toward spider web like cytoskeletal actin organisation in differentiated leaf cells of adult gametophores. Our data corroborate observations made in developing trichomes (Mathur et al., 1999) and in the epidermal cells of leaves of *Arabidopsis* where networks of bundled actin cables have been formed in final stage of differentiation (Kost et al., 1998).

Why is the abundance of thin actin filaments of vital importance for cells in the actively growing phase? If they were bundled at this stage, there would be fewer “tracks” necessary for trafficking of vesicles carrying cell wall material. As the microtubules determine the sites of cellular growth (Mathur and Hulskamp, 2002), the operability of microfilaments would also be reduced. This would diminish targeting of the vesicles and affect cell growth. Once the cell reaches the terminal stage of its physiological maturity, its contents would be “encaged” by actin cables. Such an actin-based cytoskeleton provides active support for movement of chloroplasts and other organelles (Kandasamy and Meagher, 1999) as we show in subapical chloronemal cells and adult leaf cells. On the other hand, redifferentiation processes are followed by the rapid turnover of the actin microfilaments, establishing an initial network necessary for polarized growth. Taken together, our results here confirm the universal principle of polarized distribution of actin microfilaments at the single cellular level as well as in the multicellular organism (Drubin and Nelson, 1996); (Nelson, 2003).

Our studies also established the susceptibility of the actin cortical network decorated by GFP-Talin to cytoskeleton disrupting drugs indicating that they could be used in other experimental manipulations. Additionally, the transgenic plants will be used to show the role of the proteins involved in upstream regulation of actin polymerisation as well as the elements that reinforce the cytoskeleton in cell morphogenesis and development.

4. Materials and methods

4.1 Plant tissue culture

HGT1 strain of *P. patens* B.S.G was grown axenically on either solid minimal medium (Ashton and Cove, 1977) or solid medium supplemented with 2.7 mM ammonium-tartrate (Merck) and 25 mM glucose (Fluka) and under defined light conditions of 16 hr of light and 8 hr of darkness at 25°C. The light intensity used in this study was $80 \mu\text{mol m}^{-2}\text{sec}^{-1}$ for white light. Plants were subcultured every 7 days. Isolation of protoplasts was performed as described previously (Schaefer and Zryd, 1997). Chloronemal cells were obtained on supplemented medium 5-6 days after inoculation. Monitoring of caulonemal cells and gametophore growth was performed on plants maintained on solid minimal medium.

4.2 Heat-shock treatments of plant material

The cellophane disks supporting moss tissue were transferred to preheated solid medium plates at 37°C, which were sealed with parafilm and placed into the cabinet at the same temperature. After treatment, the disks were returned onto the original plates and placed in standard growth conditions. The isolated protoplasts were embedded in solid medium, placed 24 hours in darkness and further regenerated in standard growth conditions. Every day over five days, one part of the cellophane disk containing the protoplasts was thermally treated as described above. We followed the localization of induced GFP-mTn in regenerating cells 12-16 hours after the inducing treatment.

4.3 Live cell microscopy and image analysis

For confocal microscopy, carefully excised pieces of cellophane containing undamaged moss tissue were transferred into the glass slide chamber (Lab Tek II, Nunc) in inverted position and covered by a block of solid agar medium. Confocal microscopy was performed on a TCS SP2 system using inverted microscope (Leica-DMRE). A krypton-argon laser (488-nm line) was used for excitation. To distinguish between the GFP fluorescence and red autofluorescence of chloroplasts, the bandwidth mirror settings for discriminating between the two signals were 504/531 for GFP and 634/696 for TRITC (chloroplasts). The two channels

were allocated false green (GFP) and red (TRITC) colours. The projections of image stacks were processed using Photoshop 6.0 software (Adobe Systems).

4.4 Treatment with cytoskeletal affecting drugs

The microfilament and microtubule-depolymerizing drugs, cytochalasin B and oryzalin (Calbiochem), respectively, were dissolved in dimethyl sulfoxide at 4 mM and 100 mM and diluted to the required concentration with distilled water. The drug solution was directly applied to the moss protonemata after the heat shock. Observations were made 12-16 hours after drug application.

Chapter III: The *ARP3* gene is required for proper organisation of F-actin and for normal cellular elongation and differentiation in the moss *Physcomitrella patens*

ABSTRACT

The Arp2/3 complex is a highly conserved nucleation factor of actin microfilaments. We have isolated the genomic sequence of ARP3 of moss *Physcomitrella patens* and generated mutants by allele replacement. The Arp3 knock-out moss strains, displayed a complex developmental phenotype. The filamentous protonema is composed exclusively of shortened, almost cubic chloronemal cells. Caulonemal cells are absent from the protonema and buds differentiate from chloronemata to form stunted gametophores. They carry normally differentiated leaves whereas rhizoids never differentiated from epidermal cells of the gametophores. In order to visualise the F-actin organization in these cells we created the *arp3* mutations in previously described HGT1 strain, which expressed GFP-Talin after optimized mild heat shock. This mutation was associated with loss of apical cap structures in all juvenile cells and disorganisation of actin network in chloronemal cells. We show that overproduction of Arp3 homologue of *Physcomitrella* and *Arabidopsis* efficiently complemented this mutation indicating high degree of protein conservation between land plants.

1. Introduction

The ARP2/3 complex is an essential component of the actin network. This seven-subunit protein complex along with formins represent the two separate nucleation factors of actin subunits, that are required for the reorganization and dynamics of the actin cytoskeleton (Chang and Peter, 2002). Upon activation, the ARP2/3 complex promotes actin polymerization and nucleates novel filaments at the side of already existing ones, generating branched network of actin microfilaments. The complex comprises two evolutionary conserved actin related protein ARP2 and ARP3, which share about 45% identity with actin (Mathur et al., 2003a; McKinney et al., 2002) along with five other polypeptides called ARPC1-5 (Cooper et al., 2001).

In unicellular yeasts such as *Saccharomyces cerevisiae* and *Schizosaccharomyces pombe*, the ARP2/3 complex is essential for cellular growth and is required for the generation of actin patches associated with the sites of cell wall deposition (Pruyne and Bretscher, 2000; Winter et al., 1997). The ARP3 mutations in *Drosophila* and *Caenorhabditis elegans* lead to embryo lethality (Hudson and Cooley, 2002); (Sawa et al., 2003). In *Arabidopsis*, several reports reveal typical mutational phenotypes linked to mutations in *ARP2*, *ARP3* (Le et al., 2003; Li et al., 2003; Mathur et al., 2003a), *ARPC2* (El-Assall et al., 2004) and *ARPC5* (Mathur et al., 2003b) genes. In general, these mutations lead to misplaced localization of cortical F-actin cytoskeletal network that result in a reduced expansion of cell lobes in leaf epidermal pavement, leaf trichomes and hypocotyl cells, whereas the process of cell elongation is not seriously affected in pollen tubes and root hairs.

The moss *Physcomitrella patens* is a useful model organism in the study of plant development at the cellular level. The simple morphology allows both apical and caulinary growth to be studied at the single cell level during gametophytic development. The sequence of development of the gametophyte involves a two dimensional growth of protonemal filaments composed of tip-growing chloronemal and caulonemal cells followed by a three dimensional growth of gametophores or leafy shoots, which become attached to the substrate by filaments of rhizoid cells (Schumaker and Dietrich, 1997). The chloronemal cells are mainly involved in assimilation and propagation, whereas the main role of caulonemal is the rapid colonization of the growing surface. Moreover, the predominance of homologous over illegitimate

recombination allows proper reverse genetics through allele replacement to be effectively used for biological investigations (Schaefer, 2002).

Up to now functional studies of moss actin cytoskeleton have been limited to the use of actin-interacting drugs, such as cytochalasins; the resulting interference with cellular organisation abolishes tip-growth in *P. patens* (Doonan et al., 1988). To study the function of *ARP3* gene from *P. patens*, we generated *Pparp3* knockouts through gene disruption. We demonstrate here that loss of function of the *ARP3* gene dramatically affects protonema development, impairing the elongation of chloronemal cells and blocking further differentiation of caulonemata and rhizoids, without seriously affecting gametophore development. At the ultrastructural level, this phenotype is associated with a disorganised actin network and the absence of actin cytoskeletal arrays.

2. Results

2.1 Cloning and Analysis of *P. patens* ARP3

A partial cDNA of the moss *ARP3* gene was isolated from a cDNA library of one week old protonema built in Lambda UNI-ZAP XR (Girod and Schaefer, unpublished), using the *Arabidopsis ARP3* genomic sequence as a probe. This partial cDNA was used to isolate the complete *ARP3* genomic locus from a lambda-FIX-II genomic library of *Physcomitrella patens* (PEP, Leeds). The sequence of the genomic fragment was established ([Annex 2](#)) and Southern blot analysis confirmed that the isolated gene is unique in the moss genome (Fig. 15).

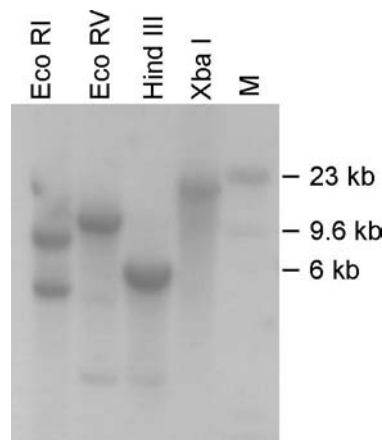


Figure 15. High-stringency Southern blot analysis of *PpARP3*. 3 μ g of genomic DNA of *P. patens* was digested with *Eco RI*, *Eco RV*, *Hind III* and *Xba I* and hybridised using an *Xba I* genomic fragment of *ARP3* as a probe. Marker was lambda DNA digested with *Hind III*.

A full length cDNA clone was identified in the moss EST collection and kindly provided to us by Dr. Mitsuyasu Hasebe (NIBB Okasaki, clone pphb36p18, accession BJ588569 and BJ183257). Comparison of the genomic and cDNA sequence established that the moss *ARP3* gene was encoded by ten exons. The same number of exons is present in the rice *arp3* gene ortholog (Genbank Acc. No. [AP004092](#)), whereas the *Arabidopsis ARP3* gene (Genbank Acc. No. [At1g13180](#)) has nine exons, the second exon corresponding to the second and third exon of rice and *Physcomitrella*. The individual size of the last five exons is equal in all of these

orthologues, but the sizes of the introns are different. (Fig. 16). The genomic structure of the moss *ARP3* gene is therefore highly similar to that of the *Arabidopsis* and rice homologues.

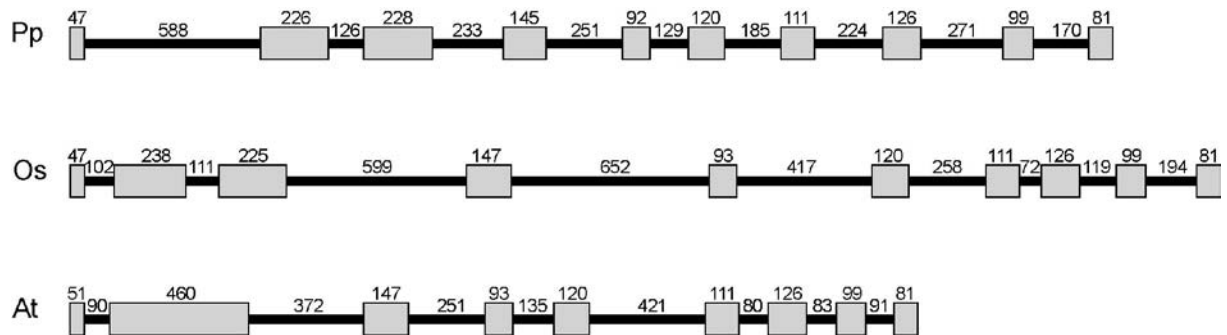


Figure 16. Schematic representation of the organisation of *ARP3* gene in *Physcomitrella* (Pp), rice (Os) and *Arabidopsis* (At) presented in Annex 1. The overall organisation of the 3 genes is highly similar except that the moss and rice exon II and III are encoded by a single exon in *Arabidopsis*. The rectangles represent exons. Introns are presented as lines. The numbers represent lengths in base pairs.

The derived amino acid sequence of *PpARP3* encodes a protein of 424 amino acids that displays 74 and 76% identity compared to the rice and *Arabidopsis* orthologues, respectively (CLUSTALW alignment). Sequence identity with *ARP3* orthologues from other eukaryotes ranges between 55 and 60% (Fig. 17, see also Table 1 in General Introduction). Thus, the predicted *Physcomitrella* *ARP3* protein sequence is closely related to its orthologs in other kingdoms. The main region of variability between the plant and the other eukaryotic sequences is at the N-terminal part. In *PpARP3* this region spans from Asn³⁹ to Val⁵⁹. From crystallographic data of the bovine Arp2/3 complex (Robinson et al., 2001) we can predict that this variable stretch corresponds to an external domain of the complex.

```

PpArp3 1 MDATQRPAAVIDNGTGYTKMGFAGNVVPCFIIPPTVVA NESPLGQ SAP---KAGTAATHNAG-----VMADLDFYIGDE
AtArp3 1 MDPHSRPAIVIDNGTGYTKMGFAGNVVPCFIIPPTVVA NESPLNQSKS-SSKATVQTOHNAG-----VMADLDFYIGDE
OsArp3 1 MDAA SRPAVIDNGTGYTKMGFAGNVVPCFIIPPTVVA VNDTEAGQIRANITKGNVMAQHSAG-----VMADLDFYIGDE
HsArp3 1 -MAGRLPACVVDCTGYTKLGTAGNTEPQFIIPPCIAIKESAK-----VGDQAQRVMK-----GDDLDFYIGDE
SpArp3 1 -MAGFNVPIINDNGTGYSKLGVAGNDAPSYVPEPTVIATRSAGASSGPAVSSKPSIMASGSGHLSSKRATEDLDFYIGND

PpArp3 72 ALAKQHSS-ATILSYPIRQGGQENWDIMERFWQQCFNYLRCDDPDHYMLLTESPLTAPENREYVGEIMPETPNVPGLYI
AtArp3 74 ALAKSRSSSTHNLHYPIEHGQVEDWDAMERWQQCFNYLRCDDPDHYFLLTBSPLTPPE SREYTGELIPETPNVPGLYI
OsArp3 75 ALAKSRSSNTYNL SYPIEHGQVENWDIMERFWQQCFNYLRCDDPDHYFLLTBSPLTPPE TREYTGEMIPETPNVPGLYI
HsArp3 66 ALERP---H--HATKMPIRHGIVEDWDLMERERLEQVLFKYLRAEPEDHYFLLTEPPLNTPENREYTABIMPESPNVPGLYI
SpArp3 80 ALKKNASLG--HSLDYPIRHGQENWDIMERFWQQSIFPKYLRCDDPDHYFLLTEPPLNTPENREYTABIMPESPNVPGLYI

PpArp3 151 ATQAVLVLAAGYTTSKL---EMTGVVVDAGDGMTHVVPVADGYIIGSSIKSIPVAGRDLSENFVQQLMRERGERVPPEDSL
AtArp3 154 AVNSVLALAAAGYTTSKC---EMTGVVVDVGDGATHVVPVAGYVIGSCKISPIACKDVTLFIQQLMRERGERVPPEDSF
OsArp3 155 ACQAVLVLAAGYTTTKC---EMTGVVVDVGDGATHVVPVADGYVIGSSISIPITGKDVTOFIQQLKERGERVPPESF
HsArp3 142 AVQAVLVLAASVTSRQVGERDTCGVVDSGDGVTHVVPVAGYVIGSCKIHEPIAGRDTYFIQQLRDRVGVLPPEOSL
SpArp3 158 AVQAVLVLAASVTSKVTDRSITCGVVDSGDGVTHVVPVAGYVIGSSIKMPLAGRDTVYFVQSLLRDRNE---PPSSL

PpArp3 228 DIARRVKEMYCYTCADIAKEFGKHKDKPAKYIKQKGNNSKTGAPPSCDI GYERFLAPEVFFSPEIYSSDFTTLPPEVVD
AtArp3 231 DVARRVKEMYCYTCDIVKBFNKHKDKPAKYIKQKGNNSKTGAPPSCDI GYERFLGPEVFFSPEIYSSDFTTLPPEVVD
OsArp3 232 DVARRVKEMYCYTCDIVKBFNKHDEBNKYIKHWSGKPKTGAKITCDI GYERFLGPEIFFSPEIYSSDFTTLPPEVVD
HsArp3 222 ETAAVKEKRYVYVCEDEVKBFNKYDTGSKWIKQYTGDNATSKKPESSIDVGYERFLGPEIFFSPEIYSSDFTTLPPEVVD
SpArp3 235 KTAERIKKECCYVCPDIKBFNSRFDREPDYIKKYS--ESITGHSITIDVGERFLAPEIFFSPEIYSSDFTTLPPEVVD

PpArp3 308 NCIQSAPIDVRRALYKNIIVLSGGSTMFKDFGRRLQRLDKKRVDA RTSASEKSGGCHKSCAVEVNVVCHPMQRFAVWFGG
AtArp3 311 KCIQSAPIDVRRALYKNIIVLSGGSTMFKDFGRRLQRLDKKIVDARLANNARTGGEITSQPVENVVSHPMQRFAVWFGG
OsArp3 312 KCIQSSPIDVRRALYKNIIVLSGGSTMFKDFGRRLQRLDKKIVDARLANNARTGGAKQPIEVNVVSHPMQRFAVWFGG
HsArp3 302 EVIQNCPIVRRALYKNIIVLSGGSTMFKDFGRRLQRLDKKIVDARLKI SEELSGGRLKPKPIIDVQVITHEMQRFAVWFGG
SpArp3 313 NVVQSSPIDVRRALYKNIIVLSGGSTLFPKFNQRLQRLDKKIVDERIHRSEMLSG--AKSGGVVNVVSHKQRFAVWFGG

PpArp3 388 SLLASTPDPFNACHTKAIEYEEYGSICRINPVFKGML
AtArp3 391 SVLSTPEFFASCTKIEYEEYGSICRINPVFKGMY
OsArp3 392 SVLASTPEFFAECTKAIEYEEYGSICRINPVFKGMY
HsArp3 382 SMLASTPEFYQVCHTKIEYEEYGSICRINPVFKGMS
SpArp3 391 SLLAQTPEFGSYCHTKAIEYEEYGSIAIRYQIFGNL

```

Figure 17. Clustal W alignment of *Pp*ARP3 amino acid sequence with its orthologues from *Arabidopsis* (NP_172777), rice (AK101163), human (NP_005712) and fission yeast (NP_592898). Note that the region of poor homology is at the N-terminus.

The protein sequence of ARP3 orthologs were aligned and used to construct a phylogenetic tree using TREEVIEW program. In this tree, animal, fungi and plant kingdoms are clearly separated leaving protozoan organisms as the outgroups (Fig. 18). Taken together these results demonstrate that the *ARP3* gene of *Physcomitrella* is unique in the moss genome, and probably monophyletic in the plant kingdom, and that it encodes an ARP3 protein of 424 aa that shares a high level of sequence identity with ARP3 proteins from other eukaryotes. This also supports the concept that the ARP3 function is highly conserved within land plants.

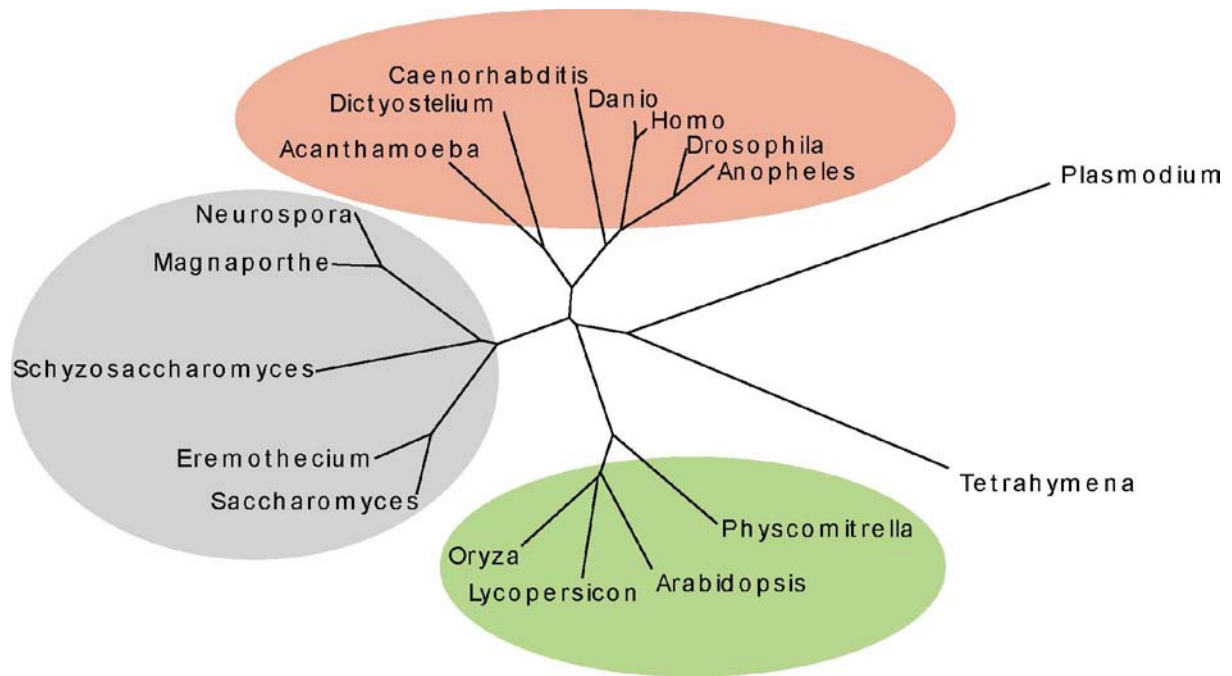


Figure 18. Unrooted phylogenetic tree of PpARP3 homologues in plants (green), fungi (grey) and animals (red). *Plasmodium* and *Tetrahymena* ARP3 correspond to the outgroups. Multiple alignments of PpARP3 orthologs were done with Clustal W and the tree was created with TREEVIEW. For GenBank accession numbers see Annex 2.

2.2 Disruption of ARP3 alters cellular elongation and blocks differentiation of caulonemata and rhizoids

To investigate the role of *PpARP3* in moss development, loss of function mutations were generated by targeted mutagenesis in the WT strain (KO strains SS) as well as in the previously described GFP-talin expressing strains 35S GT-6 (KO strains GS) and HGT1 (KO strains HS)(c/f Chapter 1). These strains were transformed with a replacement vector (Fig. 19) and antibiotic resistant strains were selected as previously described. More than 100 similar phenotypic mutants could be readily identified visually during the selection process. Whereas juvenile protonema regenerated from WT protoplasts spread evenly on the agar surface and were composed of elongated chloronema and caulonema, juvenile protonema from putative ARP3 knock-out were extremely compact and apparently composed of a single type of almost cubic cells (see fig 24). At this stage we could confirm that this phenotype was associated with the effective disruption of the moss *Arp3* gene by Southern blot analysis (Fig 20).

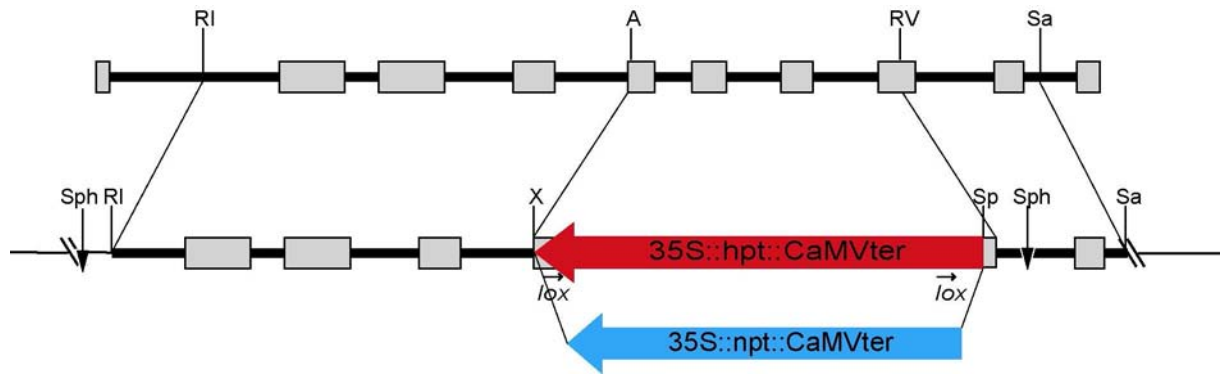


Figure 19. Schematic representation of the ARP3 knock-out constructs. The genomic ARP3 *Eco RI* (RI) / *Sac I* (Sa) fragment was cloned in pGEM-T-Easy and the *Ava I* (A) / *Eco RV* fragment was deleted and replaced by the Hygromycin or the kanamycin resistance cassette to generate pGAKO-hygro and pGAKO-neo, respectively. WT was transformed with the hygro vector, GT6 and HGT1 with the neo vector.



Figure 20. Southern blot analysis of *arp3* knock-out lines. 3 μ g of genomic DNA of *P. patens* was digested with *Hind III*. Entire ARP3 cDNA was used as a probe. Wild-type band detected at 6 kb is not present in two tested strains SS12 and SS13

A detailed phenotypic characterisation of the mutants over the entire life cycle was performed. Further observation of the protonema revealed that it was exclusively composed of chloronema which were unable to elongate properly (Fig 21). This was supported by morphometric analyses which showed that the width to length ratio of mutant chloronema was 1:1 whereas this ratio is 1:6 in WT chloronema. The absence of caulonema in mutant protonema was also supported by the lack of filamentous growth in dark grown tissue (Fig 22c and d), since caulonema are the only cell type of moss protonema that can grow and divide in darkness. Consequently, buds differentiated directly from chloronema side branch initials in the mutant whereas they develop from caulonema side branch initials in wild type.

Bud formation occurred simultaneously and at equal frequencies in the mutants and in wild type, and their morphology was apparently not affected (Fig 21c and d). These buds further differentiated into leafy shoots that were similar to wild type shoots except for two features: mutant gametophores were slightly stunted and had smaller leaves, and aerial and basal rhizoids never differentiated on mutant gametophores (Fig 21e).

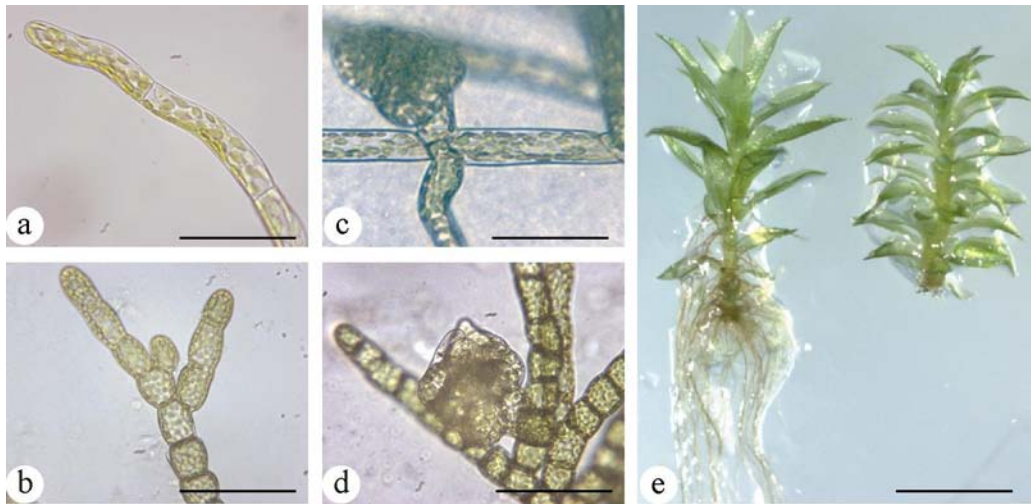


Figure 21. Comparison of the phenotypic characters of wild type *Physcomitrella* and *arp3*-KO mutant at different developmental stages. (a) Chloronemal filament of wild type consists of elongated cells. (b) *arp3*-KO mutant has filament made of short, almost cubic chloronemal cells. In wild type(c), buds appear on caulonemal cell with oblique cell walls, whereas in (d) *arp3*-KO buds appear directly on the shortened chloronema cells, with no caulonemal phase (e) Wild-type gametophores (left) have a rich rhizoid cell network at their basis, while *arp3*-KO gametophore lacks rhizoid filaments. Bars: (A)-(D), 100 μ m; (E) 1mm

The size alterations in the gametophores were measured on more than twenty wild-type and mutated SS12 lines grown for six weeks on solid minimal medium. In fully differentiated shoots, the mean length of the internode was 0.20 ± 0.02 mm in wild type and 0.15 ± 0.02 mm in the mutant, whereas the area of adult leaves were 0.85 ± 0.2 mm² and 0.53 ± 0.1 mm² in wild type and the mutant, respectively. Yet the number of cells per internode and per individual leaves was similar in both strains (not shown). We therefore concluded that the stunted aspect of the ARP3 mutant was associated with reduced expansion of shoot and leave cells. Finally fully differentiated mutant colonies were grown for several months on minimal medium in short day (8 hours light a day) and low light intensity ($15 \mu\text{E} / \text{m}^{-2} \cdot \text{s}$) to induce

sporogenesis: antheridia and archegonia differentiated normally but we never observed any differentiated spore capsule (not shown). This suggested that the mutation did not affect the development of reproductive organs but could impair fertilisation and further formation of the spore capsule.

Mosses exhibit directional growth in response to external stimuli such as light phototropism, (Jenkins and Cove, 1983) or gravity (gravitropism). In polarized light, wild type protoplasts regenerate into protonema filaments growing parallel to the electrical vector. We checked the phototropic and photopolarotropic responses of regenerating protoplasts of *Pparp3* mutants. Both tropisms are conserved in the mutant (Fig. 22a and b). Simultaneously, we investigated the gravitropic response and tested the formation of caulonemal cells in both the *arp3* mutants and the wild type in dark grown tissue. No caulonemal filament was produced in the mutant strains, whereas emerging etiolated buds were negatively geotropic as they are in wild type plants grown under the same conditions (Fig. 22c and 22d).

Finally differentiation of caulonemal cells could be induced by auxin, such as 1-naphtaleneacetic acid (NAA) in light grown chloronemal tissue (Imaizumi et al., 2002). Protonemal cells of *Pparp3* mutants were treated with 1-NAA in concentrations ranging from 1-10 μM to try to induce caulonema differentiation. These treatments did not induce the formation of caulonemal cells (not shown) suggesting that the execution of auxin-mediated signalling was blocked.

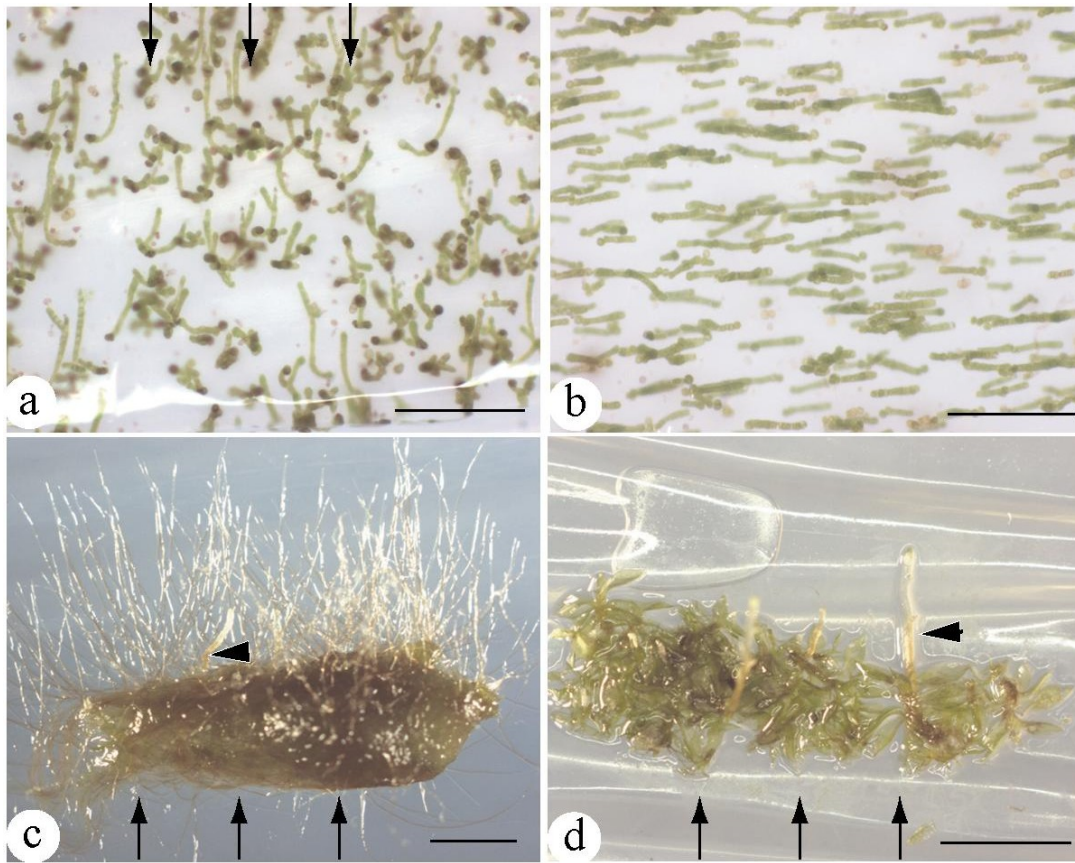


Figure 22. Tropic responses are preserved in *arp3* knock-out lines. (a) and (b) Primary chloronemata regenerated from protoplasts. In phototropic response (a), at low illumination moss filaments grow toward light source. (B) Cell filaments are aligned parallel in polarotrophic response. (c) and (d) 10 days old dark grown moss tissue. Caulonemal filaments are present in wild type (c) but absent from *arp3* KO lines (d), whereas etiolated buds are negatively gravitropic (arrowheads). The light direction (a), and the gravity vector (c) and (d) are presented by arrows, whereas the electrical vector of polarized light is parallel to bar (b). Bars: (a) and (b), 500 μm; (c) and (d) 10 mm.

Our data show that disruption of *PpARP3* gene impaired cellular elongation of chloronemal cells and completely arrested their further differentiation into caulonemata in the protonema. Gametophores were less affected by the mutation but displayed a stunted phenotype associated with smaller cells whereas filamentous rhizoids did not differentiate from stem epidermal cells. Noticeably, the mutation also induced a sterility phenotype. We also showed that the mutation did not affect tropic responses. The main consequence of the absence of caulonemata and rhizoids was the inability of moss to rapidly colonize growing surface and to fix the plant to the substrate.

2.3 Actin organisation in arp3-KO lines is affected

The effect of the loss of *ARP3* gene function on the organisation of the actin cytoskeleton was studied in the *HS* strains, which conditionally express GFP-Talin. In protonemal cells, apical cap structures, actin patches and putative MFOC which are present in WT cells were not observed in the mutant. Furthermore subcortical actin filaments were shorter, thicker and appeared more diffused with no preferential orientation in the mutant (Fig 23 a and b). Similarly, the numerous actin arrays observed in WT bud were absent in the mutant (Fig 23 c and d). In contrast, the patterns of the actin bundles network found in cells of adult leaves from the *arp3* mutants and from the HGT1 clone were visually indistinguishable.

Our data indicate that the lack of the actin arrays present in the chloronemal cells and meristematic cells of the bud is directly related to *arp3* mutation. The absence of those arrays resulted in dramatic alterations of the actin networks that in turn influence the morphology and further differentiation of tip growing cells.

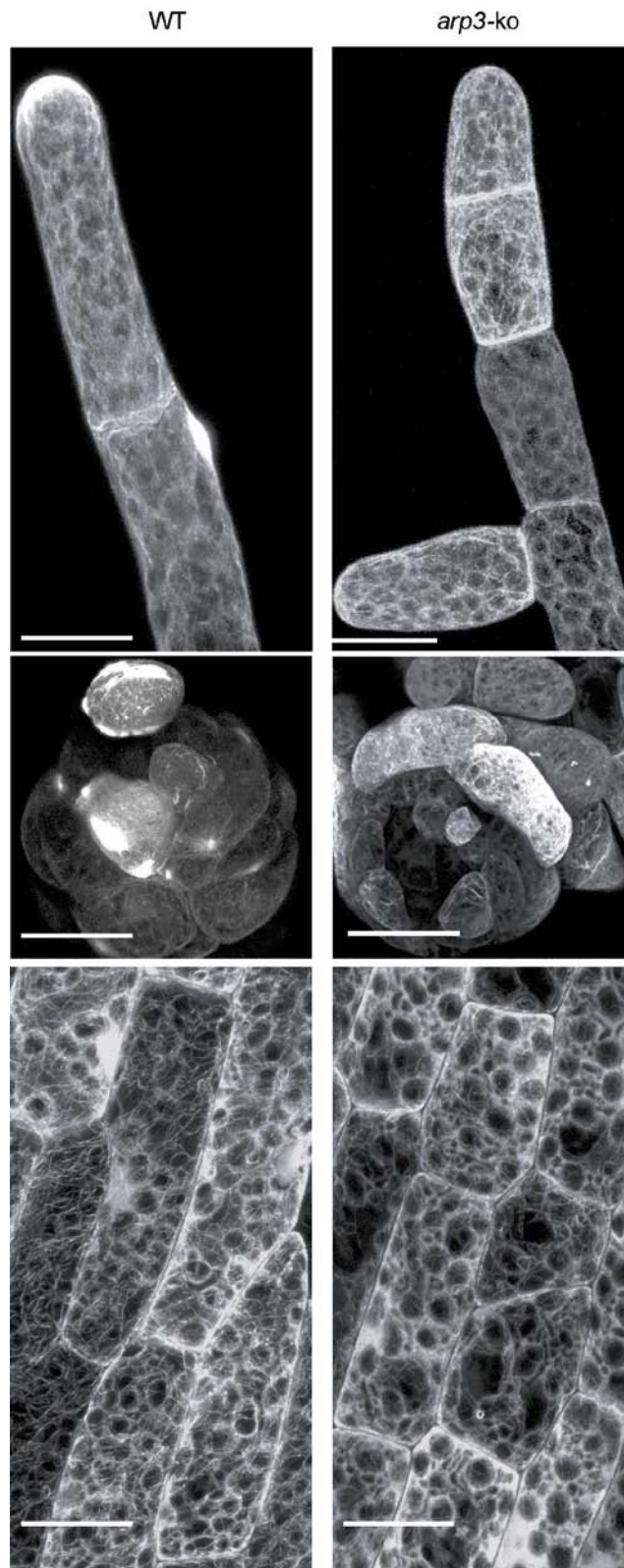


Figure 23. Comparative CLSM images of *arp3* mutant and wild type overproducing GFP-talin at protonemal (left), bud (middle) and leaf stage of development (right). Note that apical structures (arrowheads) present in protonemal and bud cells of wild type are not present in *arp3* mutant. Bars: 20 μ m.

2.4 Complementation of the *arp3* mutation was achieved by expression of the moss and *Arabidopsis* ortholog

Complementation of the moss *arp3* mutation with the moss ARP3 gene and with the homologue from *Arabidopsis* and fission yeast was attempted to address the level of functional conservation of the protein between different species. We constructed the vectors containing the cDNA of ARP3 from *Arabidopsis*, *Physcomitrella* or *S. pombe* driven by the strong constitutive maize ubiquitin-1 gene promoter, a kanamycin resistance cassette and part of 108 genomic loci for the purpose of targeted integration (Fig. 24).

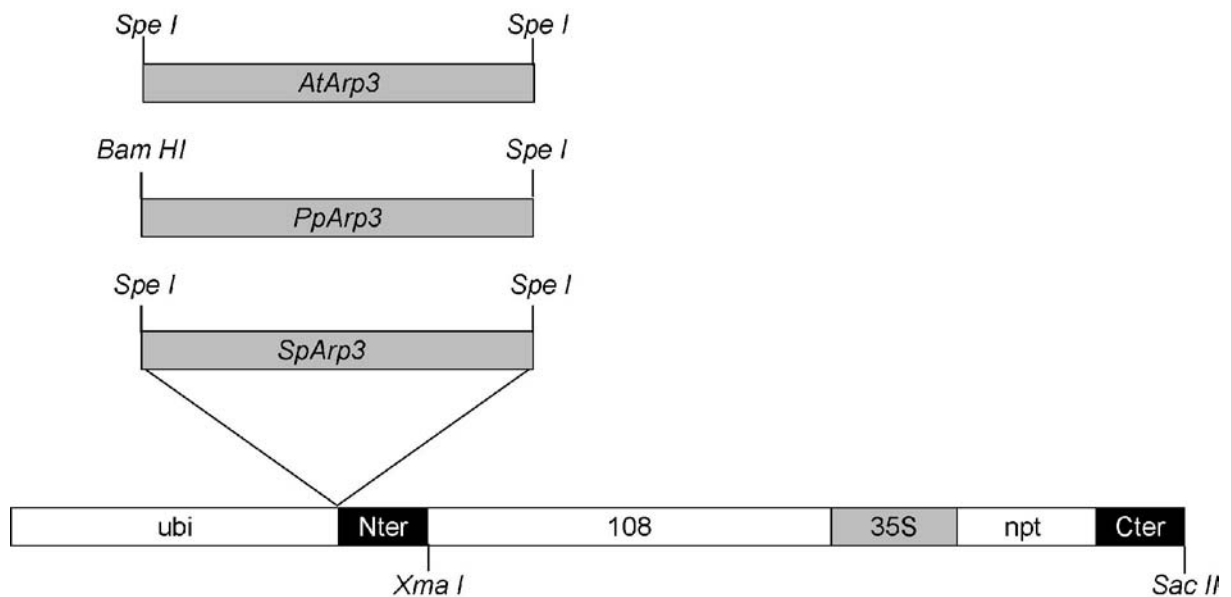


Figure 24. Schematic representation of vector used for ectopic expression of cDNAs encoding for ARP3 homologues from *Arabidopsis* (AtARP3), *Physcomitrella* (PpARP3) and *Schyzosaccharomyces pombe* (SpARP3) in *Pparp3* mutant. Restriction sites used for the insertion of each ARP3 sequence in expression cassette as well as cloning of targeting and selective cassette are indicated. *ubi*; maize ubiquitin promoter, *Nter*; nopaline synthase polyadenilation signal, *108*; 2 kb portion of genomic locus 108, *35S*; 35 promoter from cauliflower mosaic virus (CaMV), *npt*; neomycin phosphotransferase, *Cter*; CaMVter terminating sequence.

The strains GT6 (hygroR) and GSS1 (*arp3* KO in GT6, neo and hygroR) were used for the complementation assay. Expression of the three ARP3 genes tested here had no phenotypic impact on the normal developmental pattern of strain GT6 nor on the previously described

actin structures observed in this strain (c/f Chapter 1), indicating that there was no ARP3 overexpression phenotype in a wild type background (data not shown). The strain GSS1 carries a kanamycin selectable cassette flanked by two LoxP sites that needs to be eliminated to permit the complementation assay. Previous work in our lab showed that the elimination of floxed selectable markers could easily be achieved following transient expression of the Cre recombinase and selection of antibiotic sensitive strains (A.Finka and D.Schaefer, unpublished data). Transient expression of the vector pAct-Cre-NOS was performed in protoplasts from 2 GSS strains and in 10 SS strains (carrying a lox-Hygro cassette) and single protoplast derived antibiotic sensitive colonies were selected. The loss of antibiotic resistance observed in the different strains ranged from 3% up to 79% (Table 2).

strain	No. of colony tested	Antibiotic	Loss of resistance	%
GSS1	103	G418	13	12.6%
GSS2	96	G418	3	3.1%
SS11	101	Hyg	12	11.9%
SS12	102	Hyg	14	13.7%
SS13	97	Hyg	15	15.5%
SS13 (MOCK)	99	Hyg	0	0%
SS14	96	Hyg	59	61.5%
SS16	106	Hyg	3	2.8%
SS17	109	Hyg	12	11.0%
SS18	100	Hyg	5	5.0%
SS19	93	Hyg	8	8.6%
SS20	100	Hyg	79	79.0%

Table 2. Loss of the antibiotic resistance in generated *arp3* mutants after transient overexpression of Cre recombinase.

Finally, we re-transformed one of the G418 sensitive clones derived from line GSS1 with the aforementioned vectors constitutively expressing *ARP3* orthologues. After selection of kanamycin resistant colonies, we found that the expression of *ARP3* from *Arabidopsis* and *P. patens* completely restored the wild-type phenotype in the *ARP3* KO GSS1 line (Fig. 25). In the complemented strains, the protonema was composed of normal elongated chloronema and caulonema, buds differentiated from caulonemal side initials, filamentous growth of caulonema in dark grown cultures was similar to the WT strain and gametophores did not display anymore the stunted phenotype observed in the *ARP3* mutants. These data

demonstrate that the phenotype described here was effectively associated with ARP3 loss of function and that the *Arabidopsis* ARP3 gene can fully complement the mutation in *Physcomitrella*. In contrast, the fission yeast ARP3 expression cassette could not re-establish wild-type phenotype.

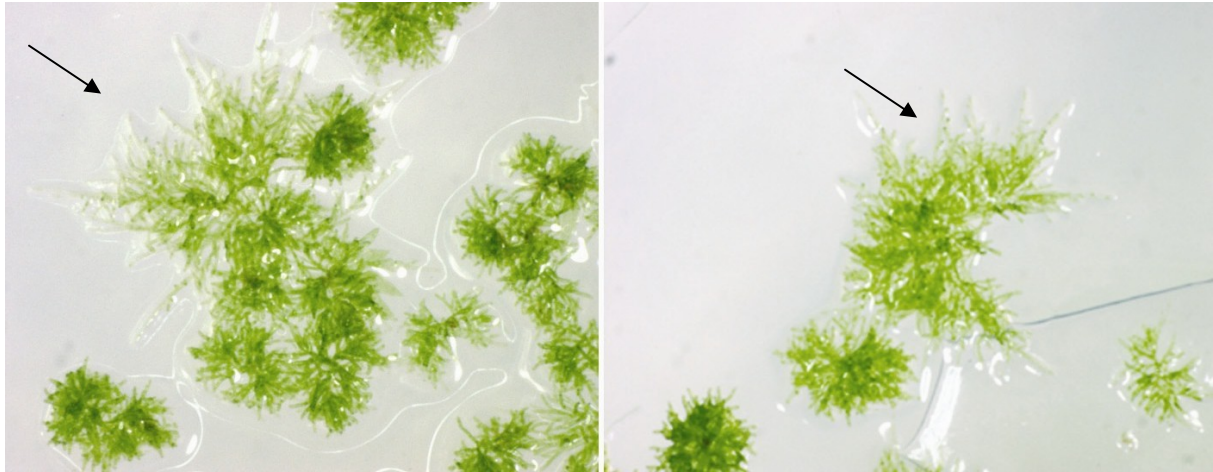


Figure 25. Complementation of *arp3* mutation in *P. patens* with AtARP3 (left) and PpARP3 right. Big colonies are complemented.

3. Discussion

We have identified a genomic sequence encoding for the ARP3 subunit of putative ARP2/3 complex of *P. patens* that agreed with the database predictions and fit into the phylogenetic analysis (McKinney et al., 2001). The disruption of this genomic sequence demonstrates that the ARP2/3 complex plays a crucial role in the cellular morphogenesis of moss protonema and to a lesser extent in leafy gametophores. Tip growth is seriously affected in chloronemata and their differentiation into caulonemata, as well as the formation of rhizoids from gametophores epidermal cells is blocked. Thus, disruption of *ARP3* gene affects mainly tip-growing cells of moss indicating that functional ARP2/3 complex is required for their polar growth. In angiosperms, pollen tubes and root hairs represent counterpart of apically growing moss protonemata and rhizoids as they exhibit apical elongation (Geitmann and Emons, 2000). In mutants of *Arabidopsis* disrupted in the *ARP2* and *ARP3* genes (Le et al., 2003; Li et al., 2003; Mathur et al., 2003a), only expansion of unicellular trichomes and epidermal cells has been altered, whereas the apical growth of root hairs and pollen tubes is not affected despite the fact that their growth is strictly dependent on F-actin (Gibbon et al., 1999).

Why is the effect of the ARP2/3 mutations not the same in all types of plant tip-growing cells? It is known that cytochalasins block F-actin dependent vacuolar movement that is required for the deposition of new cell wall material (Preuss et al., 2004; Uemura et al., 2002). Cytochalasin also affects tip-growing cells of both bryophytes (Doonan et al., 1988; Geitmann et al., 1996; Meske and Hartmann, 1995; Miller et al., 1999) and angiosperms (Doonan et al., 1988; Geitmann et al., 1996; Meske and Hartmann, 1995; Miller et al., 1999); (Mathur et al., 1999). Additionally, the altered vacuolar morphology and cellular localization observed in the distorted trichomes of ARP2/3 subunit mutants of *Arabidopsis* can be phenocopied by treatment of the wild-type with cytochalasins. It is suggested that the ARP2/3 complex is necessary for the integrity of the vacuolar movement only in certain types of cells, whereas members of the formin family may accomplish this actin polymerization dependent process in other types of cells. This is further supported by the effect of the overexpression of the *Arabidopsis* formin AtFH1 in tobacco pollen tubes which leads to strong alteration of pollen growth (Cheung and Wu, 2004). To synthesise these data, one may hypothesise that tip

growth in moss cells depends more on the integrity of the ARP2/3 complex whereas tip growth in spermatophytes relies more on formin functions. The availability of formin related moss full length cDNAs in the RIKEN collection should allow addressing this question experimentally.

Moss protonemata are known to both sense and respond to gravity and light stimuli. Our experiments show that *arp3* mutants are positively phototropic in unilateral light and align to the electrical vector of polarized light similarly as the wild type (Jenkins and Cove, 1983). We also observed that dark grown mutant gametophores are normal and negatively gravitropic. These observations suggest that these processes are independent on ARP2/3 mediated actin polymerization.

At the ultrastructural level, the mutation of the ARP3 protein is followed by the loss of apical structures of F-actin and disorganisation of actin cable network preferentially in chloronemal cells. The *in vivo* studies and immunolocalization of ARP2/3 complex has confirmed its role in the creation of cortical actin patches, which are concentrated at sites of polarized cell growth (Pelham and Chang, 2001). It has been shown that the mutation in actin gene results in defects of apical cell growth in filamentous fungi *Neurospora crassa* and reduces average colony growth four times in comparison with wild type (Virag and Griffiths, 2004). In moss, the presence of caulonemata is required for rapid moss colonization. Taking together those informations we suggest that the activity of ARP2/3 complex mediates moss propagation.

Our complementation essays in moss *arp3* mutant reveal the effectiveness of *Arabidopsis* ortholog in restoring of wild-type phenotype. In contrast, the ARP3 subunit of fission yeast is not able to complement the *arp3* mutant of moss. Our first hypothesis assumes that the moss ARP2/3 complex containing heterologous ARP3 moiety from *S. pombe* is not functional due to the improper interactions between subunits. This inability of Sp ARP3 to be effective in plant cells may be due to the poor homology of 20 amino acids at N-terminal part of protein between plant and yeast homologue. Swapping these domains between yeast and moss ARP3 proteins followed by overexpression of the recombinant protein would confirm or reject this hypothesis. Our second hypothesis is based on the possible differences between the mechanisms that regulate the activators of the ARP2/3 complex in plants. Regulation of

activators determines when and where in cells ARP2/3 complex nucleates actin assembly. Upon interaction with an activator (also called a nucleation-promoting factor), ARP2/3 complex is thought to undergo conformational changes that result in rearrangement of the ARP2 and ARP3 subunits to form an actin dimer-like nucleus for polymerization. In mammalian cells and yeasts the ARP2/3 complex can be activated by ActA, WASP/SCAR/WAVE family members, cortactin, Abp1, type I myosins, and Pan1 (Welch and Mullins, 2002). The Wiskott-Aldrich syndrome protein (WASP) subfamily contain a Cdc42/Rac-interactive binding (CRIB) motif that is bound by activated Rho GTPases, mainly Cdc42. The plant homologues of WASP and Cdc42 are not known, although eleven members of Rho-related GTPase-of- plants (ROPs) are identified. Their relationship with the activation of ARP2/3 complex is not yet deciphered. It is possible that the ARP2/3 complex possessing Sp ARP3 will not be properly activated in plant due to the lack of interaction between plant nucleation promoting factor and the yeast ARP3 moiety.

The members of the other subfamily, SCAR/WAVE, do not contain a CRIB motif and therefore do not interact directly with Rho GTPases. Five predicted WAVE homologues are found in *Arabidopsis*, whereas no functional data exist regarding these genes (Brembu et al., 2004). Purified bovine WAVE complex contain WAVE1, Abi2, PIR121, NAP1, and HSPC300 (Eden et al., 2002), but only *PIR*, *NAP* and *HSPC300*-like genes are easily identified in plant sequence databases. T-DNA inactivation of *NAPP* and *PIRP* results in distorted trichomes, similar to ARP2/3 complex mutants (Brembu et al., 2004). It is demonstrated that their functions are interchangeable with human homologues (El-Assal et al., 2004) and (Basu et al., 2004), respectively. The genetic evidence for a HSPC300 plant ortholog is found upon characterization of maize *brick* mutant that exhibits a similar disorganisation of epidermal cells as it is shown in the *ARP2/3* mutant alleles in *Arabidopsis* (Frank and Smith, 2002). Altogether, one should expect more drastic phenotypical changes as a result from uncontrolled activation of ARP2/3 complex (Deeks and Hussey, 2003). However in plants, based on analogy in animal cells, inactivation of these subunits would probably result in rapid degradation of WAVE homolog and the ARP2/3 complex would remain inactive (Brembu et al., 2004). Since the moss homolog of HSPC300 is deciphered (Perroud personal communication), genetic and biochemical analysis of this subunit and the

other interaction partners would contribute to the additional informations in process of regulation of ARP2/3 mediated actin nucleation.

4. Materials and methods

4.1 Plant tissue culture, transformation of protoplasts and selection of resistant clones

P.patens was grown axenically on solid minimal medium (Ashton and Cove, 1977) supplemented with 2.7 mM ammonium-tartrate (Merck) and 25 mM glucose (Fluka) and under defined light conditions of 16 hr of light and 8 hr of darkness at $25^{\circ} \pm 1^{\circ}\text{C}$. Gametophores growth was conducted on solid minimal medium without supplement. Isolation of protoplasts and polyethylene glycol-mediated transformation were performed according to (Schaefer and Zryd, 1997). For the gravitropic experiments, fragments of 10 day old moss tissue composed of protonema and juvenile gametophores were grown in darkness on solid minimal medium supplemented with ammonium-tartrate and glucose in vertically positioned Petri dishes. For the phototropic and polarotropic experiments, freshly isolated protoplasts were embedded in top agarose and regenerated on solid protoplast medium. Low intensity white light ($5 \mu\text{E} / \text{m}^{-2} \cdot \text{s}$) was provided unidirectionally for the phototropic response. Embedded protoplasts were regenerated in glass Petri dish covered with a polarisation filter in the polarotropic assays. Light intensity under the polarising filter was around ($5 \mu\text{E} / \text{m}^{-2} \cdot \text{s}$).

4.2 Isolation and Detection of DNA

Genomic DNA was isolated using the cetyltrimethylammonium bromide method (Schaefer and Zryd, 1997). The digested genomic DNA ($3 \mu\text{g}$ per lane) was separated on a 0.7% agarose gel and blotted on Zeta-Probe membranes (BioRad). Labelling of the probes (Amersham) and membrane DNA blotting were performed according the manufacturer's protocols. High-stringency genomic DNA hybridisation was performed at 65°C in 0.25M NaPO_4 pH 7.2, 7% SDS overnight and the membranes were washed 2 x 20 minutes with 0.1xSSC, 0.1% (w/v) SDS. Finally, the membranes were exposed to X-Omat AR film (Kodak).

4.3 Cloning of *Physcomitrella* ARP3 encoding gene

All plasmid manipulations and bacterial transformations were performed by standard techniques (Sambrook et al., 1989). *Arabidopsis* genomic DNA (gDNA) was used as a template to generate *AtARP3* fragment by PCR with primers *AtARP3-FW160* (5'-

TGGCAAACCTCAGCACAAC-3') and *AtARP3-R1073* (5'-GCAAGAACACGAGCATCAAC-3'). Resulting 2173 bp fragment was ³²P-labeled and employed as a probe to screen *Physcomitrella* λZAP cDNA library (Girod et al., 1999) at low stringency. Partial cDNA was obtained (data not shown) and used as a probe to screen *Physcomitrella* λFIXII genomic library [constructed by Stavros Bashiardes as part of The *Physcomitrella* EST Programme (PEP) at the University of Leeds (UK) and Washington University in St Louis (USA)]. Positive lambda clones plaques were propagated and phage DNA was isolated from positive clones by Nucleobond® AX kit (Macherey-Nagel) according to manufacturer instruction followed by digestion with XbaI. Corresponding fragments of 6.7 kb and 2 kb were cloned into a vector pBS-SK (-) (Stratagene) and sequenced.

4.4 Construction of ARP3 gene disruption vectors

The 3 kb EcoRI/SacI portion of *PpARP3* gene was inserted in the vector EcoRI/SacI digested pGEM-T Easy vector (Promega) to generate pGEM3.0/EcoRI-SacI. The pBSMDII vector (Michel Laloue, not published) bears neomycin phosphotransferase driven under 35S promoter of *Cauliflower mosaic virus* [CaMV] and CaMV polyadenylation signal [CaMVter]). This neomycin cassette is flanked by *loxP*-sites that allow recycling of the markers. The XhoI/NotI (blunted) fragment of pBSMDIIIb (Murielle Uze, not published) containing hygromycin cassette (35S-hygromycine phosphotransferase flanked by *loxP*-sites) was inserted into AvaI/EcoRV of pGEM3.0/EcoRI-SacI, replacing native 900 bp, to yield pGAKO-Hyg with preserved XhoI site. To construct pGAKO-neo, XhoI/SpeI fragment of pBSMDII that carries neomycin transcription unit was ligated into the XhoI/SpeI digested pGAKO-Hyg backbone.

4.5 Construction of pActCreNOS

The pMM23 (Dale and Ow, 1990) was digested with SacI/PstI and fragment bearing *cre-nos3'* was ligated in pBS-SK (-) to generate pBSCreNOS. The XhoI/PstI digested pCOR105 (Mcelroy et al., 1991) fragment bearing actin rice promoter was inserted into XhoI/PstI cut of pBSCreNOS to create pActCreNOS.

4.6 Construction of integrative vectors for overexpression in *Physcomitrella*

The entire 2kb fragment representing part of 108 genomic loci was excised by XhoI/XbaI from pBS2k108 vector and placed into XhoI/XbaI cut of pBNRF bearing neomycin resistance cassette. The maize ubiquitin 1 promoter, first exon and first intron (Christensen et al., 1992) was excised as HindIII/BamHI fragment of pUbiGUS (Uze, not published) and inserted in HindIII/BamHI pBS-SK (-) to generate pBSUbi. The expression vector pBSUbiNOS was constructed by insertion of SpeI/NotI *nos* polyadenylation sequence from pG35SDT (Finka, not published) into SpeI/NotI cut of pBSUbi. The cDNAs encoding ARP3 from *Physcomitrella* (gift of M. Hasebe; Genbank Acc. No. BJ183257) was used as a template to generate PCR fragment with forward oligo 5'-CACCTGTTCTGAGATCTGATGCTACTCAACGTCCT-3' and reverse oligo 5'-GGATCCTAACATACCCTGAAGACCGG-3'. Similarly *Arabidopsis* ARP3 cDNA (RIKEN pda08187, Genbank Acc. No. AY093149) was amplified with primers 5'-AATGATCAATGGATCCGACTTCTCGA-3' and 5'-TTACTAGTTCAATACATTCCCTTGAA-3'. The ARP3 sequence *S. pombe* (kindly provided by K. Gould) was amplified with 5'-AATGATCAATGGCTTCGTTTAATGTT-3' and 5'-TTACTAGTTTAAAGAGAATTTC CAAA-3' (primer sequence in bold corresponds to ARP3 coding sequences). All obtained PCR fragments were cloned in pGEM-T-easy (Promega) and sequenced. They were all cut by *SpeI* and 1.3 kb fragment that represented corresponding ARP3 was placed in *SpeI* cut pBSUbiNOS resulting in overexpression vectors pBSUbiAtARP3, pBSUbiPpARP3 and pBSUbiSpARP3, respectively. Finally, the XmaI/SacII fragment of pBNRF108 bearing neomycin resistance cassette and 2 kb portion of 108 genomic locus was placed in the equally cut of ARP3 overexpression vectors giving rise to the integrative vectors.

4.7 Live cell microscopy and image analysis

The moss tissue was photographed using a Leica Diaplan microscope (Leica) coupled with DC300 digital camera (Leica) and acquired by IM50 software (Leica). The measurement of cell and tissue length as well as leaf area was made by ImageJ software (<http://rsb.info.nih.gov/ij/>). For confocal microscopy, carefully excised pieces of cellophane containing undamaged moss tissue were transferred into the glass slide chamber (Lab Tek II,

Nunc) in inverted position and covered by block of solid medium. Confocal microscopy was performed on a TCS SP2 system using inverted microscope (Leica-DMRE) as it was previously described. The projections of image stacks were processed using Photoshop 6.0 software (Adobe Systems).

Chapter IV: General discussion

There are two main objectives of this thesis: a) labelling of the cytoskeleton of actin microfilaments (F-actin) in order to characterize its structure in all cells of the moss *Physcomitrella patens* and b) characterizing the phenotype induced by loss of function of the *ARP3* gene on moss development and on the organisation of the actin cytoskeleton

It has been demonstrated that GFP-Talin (GT) fusion protein labels F-actin *in planta* (Kost et al., 1998). In order to achieve it in the moss, we have created two types of transgenic strains of the moss *P. patens* expressing GT either under the heat-inducible soybean *Gmhsp17.3* gene promoter or the constitutive CaMV 35 S promoter. In the HSP-GT lines at room temperature, GT presence can not be detected by fluorescence microscopy or immunochemical methods. After one hour mild heat-shock at 37°C followed by 16 hours recovery at 25°C fluorescently labelled actin structure can be observed in all cells of moss tissue. In contrast, labelling of actin by 35S-GT was incomplete and accumulated in older differentiated cells without regard to growth conditions. In transgenic moss strains containing the beta-glucuronidase (GUS) gene driven by the *Gmhsp17.3* (Saidi et al., submitted), it has been shown that the maximal activity of heat-induced GUS was thousand fold higher than its basal activity and at least two orders of magnitude higher than the levels observed with a 35S-GUS construct. Taken all this in consideration, we concluded that rather weak expression level of the 35S promoter in *Physcomitrella* is insufficient for labelling actin structures in cells with highly dynamic actin turnover (i.e. juvenile cells). Nevertheless the 35S promoter enables labelling of the actin cytoskeleton in fully differentiated cells in which the actin cytoskeleton has acquired its final structuration stage.

In addition, the level of fluorescence drastically diminishes after 48 hours following heat-shock induction demonstrating the transient nature of labelling without deleterious effect on the plant. On the other hand, we showed that high amounts of GT that are produced by two consecutive thermal inductions over a period of 24 hours interfere with cellular growth and morphogenesis. These data support the idea that high amount of GT blocks the dynamics of the F-actin cytoskeleton producing aberrant growth pattern. To conclude, using the heat-shock

inducible promoter *Gmhsp17.3* we have achieved a complete labelling of *Physcomitrella* F-actin structures. We propose that this labelling system may be used in other plants whenever the circumstances do not allow complete spatiotemporal labelling. Moreover, the transient over production of desired recombinant protein may overcome its negative impact on cellular functioning.

These moss strains expressing GT in a inducible manner are very powerful tools to examine the organisation of the F-actin cytoskeleton. Using confocal microscopy we demonstrate existence of distinct actin patches, star-like structures, converging apical arrays, subcortical network of thin, poorly organized actin strands in juvenile cells, and networks of thick actin bundles in differentiated cells. In yeasts, actin patches are localized at the growing pole and represent nucleation centers for the establishment of more complex structures required later for differentiation (Pruyne and Bretscher, 2000). We speculate that a similar process precede the formation of apical actin arrays during cellular polarization in protoplasts, protonemal and meristematic cells.

Large star-like actin arrays have been observed in every cell type of *P.patens*. Similar arrays have been previously visualized in *Funaria* during side branch initiation in protonema cells (Quader and Schnepf, 1989). Yet, their role has to be further investigated during moss caulinary growth. In angiosperms, a similar structure has not been described during the development of caulinary growing organs. This may indicate that these actin arrays may be specific to the three-dimensional growth of moss. Cap structures observed at the apices of protonemal cells are most likely structurally and functionally similar to the cap structure described in root hairs of angiosperms and associated with tip growth.

The organization of subcortical actin strands and bundles is quite different in juvenile and differentiated cells. Juvenile cells have a rather diffuse network of thin cables, whereas thick actin bundles are characteristic of fully differentiated cells. In older chloronemal cells, using time lapse video (not shown) we observe a rather immobile “cage” of cortical actin bundles supporting chloroplasts oscillations. This indicates a differential role of F-actin, which allows the rapid transportation of the vesicles carrying new cell wall material on thin cables in proliferating cells, whereas bundled cables provide mechanical support for organellar movement. In older chloronemal cells and leaf cells, the network of bundled actin

cables did not show any preferential orientation and we occasionally observed the cables traversing two adjacent cells (not shown). In contrast, the organization of thin actin strands in older caulonema displays a clear apicobasal distribution. We hypothesize that these F-actin strands are indispensable for the intracellular transport in rapidly growing caulonemal cells. Cellular redifferentiation of adult leaf cells into chloronemata requires F-actin rearrangements that reinitiate the cellular mechanisms necessary for apical polar growth. Although these mechanisms are unknown, they probably involve activity of actin depolymerization factors in the initial phase of cytoskeletal rearrangements, but further investigations have to be made to determine the fate of cytoplasmic actin subunits. Taking together, our transgenic strains overexpressing GT may serve as a valuable tool for the studies involving biotic and abiotic factors regulating dynamic organization of cytoskeleton during cellular morphogenesis and development.

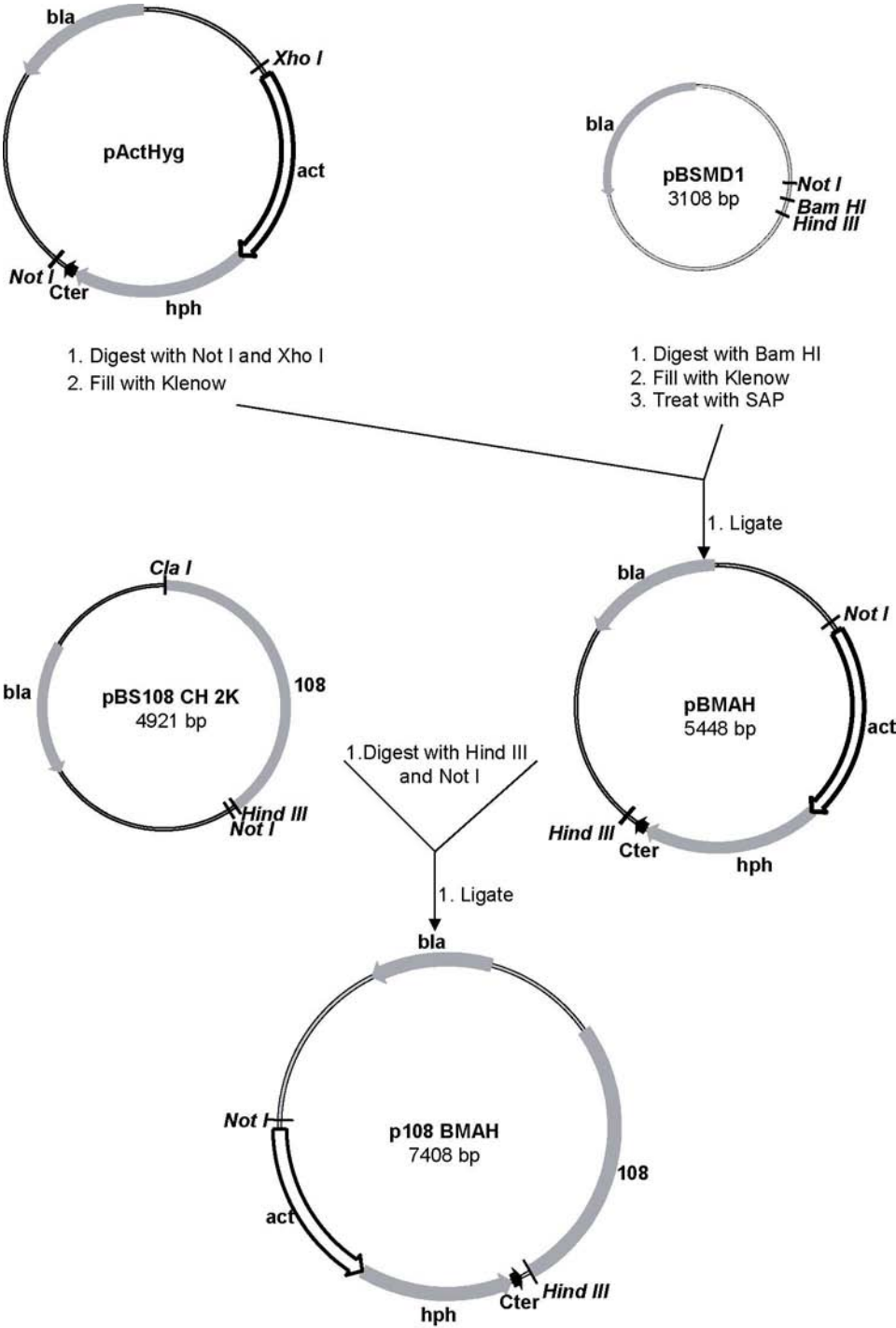
In this work we show that GT and HGT plants can be advantageously used to decipher the organisation of actin cytoskeleton in morphologically affected *arp3* mutants. The confocal imaging proves the absence of every previously described stellated F-actin structure at all developmental stages and an obvious disorganisation of the network of actin cables in chloronemal cells. These data suggest that the Arp2/3 complex may be located in the different actin arrays, but that these arrays have different physiological function in different cell types. Disruption of the *ARP3* gene, a component of the Arp2/3 complex, resulted in shortened chloronemata. On the other hand the development of moss organs by caulinary growth was slightly affected. The most marked observation is the complete absence of caulonemata and rhizoids. The same phenotype has been observed in moss *ARPC3* knock-out (Perroud, personal communication). This strongly supports that the observed phenotype is associated with loss of function of the *ARP2/3* complex. Our results indicate that this complex is essential for growth and differentiation of moss protonema cells. Thus, disruption of *ARP3* gene affects mainly tip-growing cells of moss indicating that functional *ARP2/3* complex is required for their growth and differentiation.

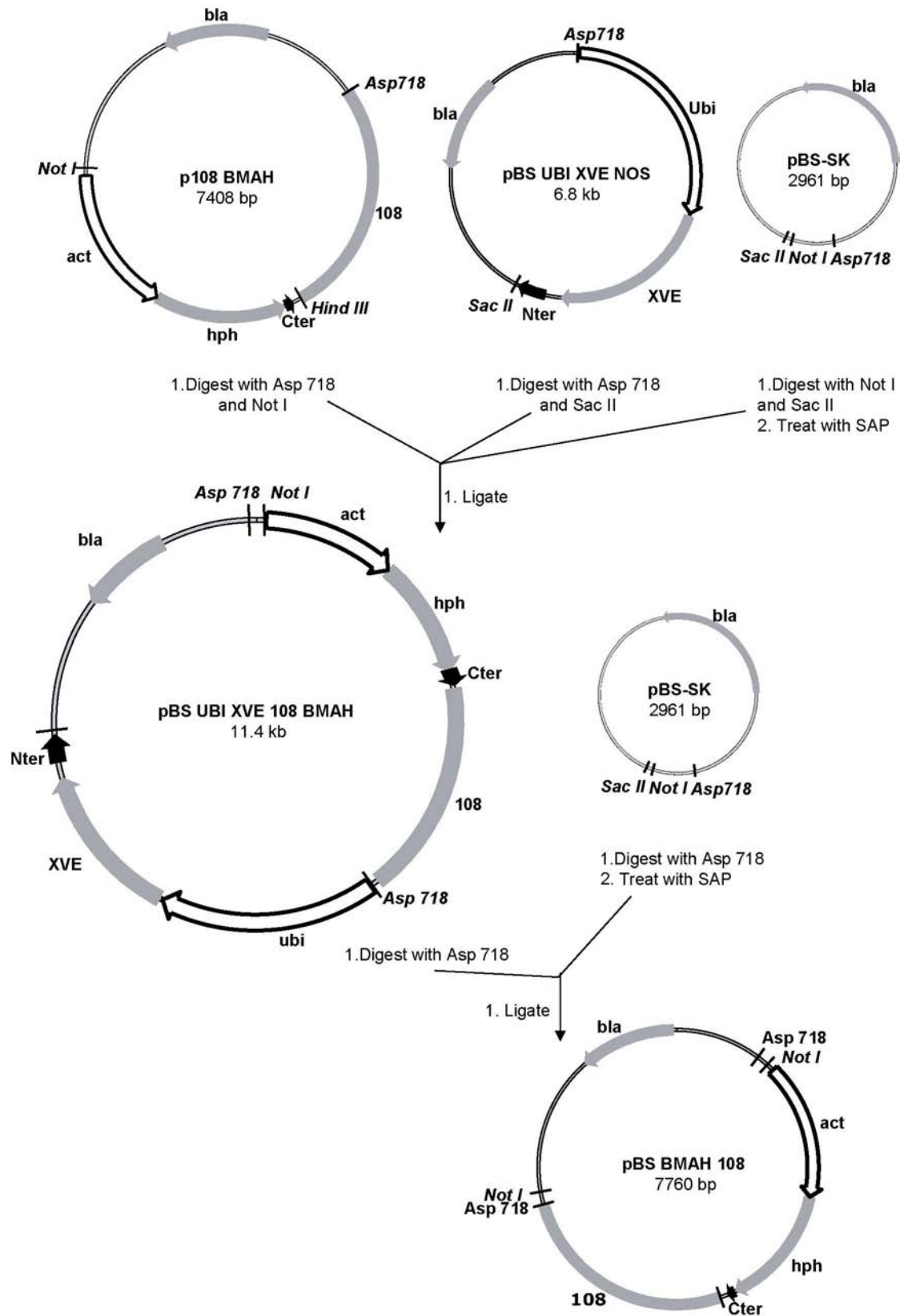
We suggest that the other actin nucleating factors such as formins may play crucial role in cellular morphogenesis of the cell types whose differentiation does not depend on Arp2/3 complex. Additionally, microtubular cytoskeleton may be more involved in the

processes of three-dimensional growth and differentiation than the actin cytoskeleton. In order to complement *arp3* mutation we demonstrate that the expression of *Physcomitrella* and *Arabidopsis* orthologs of Arp3 complement this defect. The Arp3 subunit of *S. pombe* is not functional probably due to the inability to interact with other subunits of Arp2/3 complex or nucleation promoting factors. This suggests that the functional role of the Arp2/3 complex between the plant orthologs is conserved.

Annex 1

Construction of pBS-BMAH108 vector





Legend: , *act*; rice actin 1 promoter, *hph*; hygromycin phosphotransferase, *108*; 2 kb portion of *Physcomitrella* genomic loci, *Cter*; *CaMVter* terminating sequence, *bla*; beta-lactamase, *ubi*; maize ubiquitin promoter, *XVE*; an estrogen receptor-based transactivator (Zuo et al., 2000)s, *Nter*; nopaline synthase polyadenylation signal.

Annex 2

Arp3 genomic DNAs from *Physcomitrella patens*, *Oryza sativa* and *Arabidopsis thaliana*

>*Physcomitrella patens*

ATGGATGCTACTCAACGTCCTGCTGTTGTTCATCGACAATGGCACCCGGTATGTTTGTTCATTACCCAGC
TTTTGTTTTGCTGTGTTTTGTATTGCTTTCTATGCATTCCTTCTCATTGTTCGATCGGTGAATCCTTTTGTAGG
TTTCGAGGCGTGACGCTGGGAGATTGCTTGTGCTGTGTTGGTTGCATCGTTGGTTGTGGGTTTTTCGGTCTG
AGAGTGGGCATGTGGATTGTTGGAATGAGGCTGGCTGAGAGAGGGTTAGAAGCGTGGTTGTGATGCCGTCGT
GAGACGTTTTGTTGGACCTGTGTAGTCCGATTGGTTTCGATGAGAATTAGGGTTATGAGTAGCATCAATTGCGG
TGGATTGTGACTTTTTGCTGAACGTTGCGTGGGGGGTTGGTGAATCCCGTCGTGCTGGGTTAAGAAATTCAGAG
CGTTGCTACGCCTCGTGAACCTTGGTTGGGGTTGATCATATGCAAGTACCTAGAGGTTACGTATCGCTCTGA
TGTATTCTAACGGTTCACTCAGTGACGATCGTCTTTAAAGATCGTCTTTAAAGATCGTGAGACATGGTATT
TGTAGCTCAATTTGACGGCATATTGAGCCTACATAGAATCTCACGACATGAATATGTAGGTATACGAAGATG
GGATTCGCAGGGAATGTGGAGCCCTGTTTTATTATTCTACAGTAGTGGCACTCAATGAGTCCTTTTTGGGC
CAGTCGGCTCCAAAGGCAGGCACAGCTGCATATACAATGCAGGAGTAATGGCTGATCTCGATTTCTACATT
GGCGAAGAGGCACTTGCGAAGCAACTCAAGTGCCTACTCTTAGTTATCCATTCGACAAGGCCAGGTA
CACGTATCCAACCTCCGCATTCTGGGGTACTTCTTTACGTGAAGTTAAGTGGTTGTGGTCGTAATATTTT
CGCACTACTGAAGGGTGTTTAATGTCCGACAGCCTTCGTTCTTTTTGCAGATTGAAAATTTGGGATACGATG
GAGAGATTTTGGCAGCAATGCCTCTTCAACTATCTGCGATGCGATCCAGAAGATCATTATATGTTACTCACT
GAGAGCCCCTTGACAGCACCAGAGAATCGTGAATACATGGGAGAAAATCATGTTTCGAGACTTTCAACGTGCCA
GGATTGTATATCGCAACTCAAGCAGTGTAGTTCTAGCAGCTGGCTACACGACCTCCAAGCTGAGTTTGGCT
ATTTTGGGTTCTTTCTGGTGTCTCCCGTGAATCATTGATAATGGAGTCTTTTGATTTCGTGAATTGATAAGTGT
ATTGAAGTAGCCCTGGTTGTTTCTGAGGTCCATGACCTACGATCTGTATGGATTTACTACTGTTGGCTTCGAC
TGGTAGTGAAAAGAAAGTGCAGTCTGGTTGAGTGTAGGGATCTTGGTGGCTTTAATGTGTTGGGAACTGAA
TGCAGCTGGAAATGACGGGCTTGGTGGTGGATGCCGGGGATGGAATGACTCATGTTGTTCCAGTGGCGGGATG
GTTACATCATTGGTAGCAGCATCAAGTCAATTCCTGTGCGAGGCCGGGATCTCTTAATTTTCGTTCAACAGC
TAATGCGAGTAGCAGCCAAAACCTTACCTCTCCTAGCACCTCAATGACAACTAATACTCAGCTTCATAATGTG
ATAGAATCATTCTGATATGATGCATCGGGCAGAATTGGTCGATAATTGTAGCTGATCCACGTAATAGCTTG
TCACTCCAGATTGTTTCTGTGGCGGTTTGAATCGATTGAATAGCCTATAAAAGATATTTGAAAAGTAGGAAT
TTTTTGGAGTAGGTGACTTACAAGTGTACATGTTTATTCTAGGAACGAGGCGAACCTGTGCCCCCGAGGA
TTCTTGGATATTGCCAGGAGGGTGAAAGAAATGTATTGCTACACATGTGCTGATATTGCGAAGGTAATATC
CATTTTTATCTCATCATATGAAGCTATAGTCATAGGAATACTGGGATCTCATTGATTATCTGGAACATATTG
TTGCAATGGCTGCTCGGCTGCTCACTTGGTAGAACTGCATGTGTTGCAGGAGTTTGGTAAGCATGATAAGGA
ACCTGCCAAATACGTTAAGCAGTGGAAAGGAAACAATTCGAAAACCTGGAGCGCCCTTTTCTTGTGATATTGG
ATATGAGAGATTTTTGGCGCCCGAGGTCAGCGTCTGGACCCGCTCTCGCAAAGAGAGCGAAAAGAGAGGGAGAG
ATTGAACTTTACCCTTCAATTGATATTAGACAATTTCTTTACTTACTTAGGGTTTGATCACATGCTGAGAA
ATATTTTTATCCTGATACAGTTTATTTTATTTTGAACCTGACACGTTTGATTTTTGAGTTTCGACAGGTATTC
TTCTCACCAGAGATTTATAGCAGTGATTTCAACAACCTTTGCCAGAGGTGGTTGATAACTGCATACAATCG
GCTCCTATTGATGTTTCGTCGAGCCCTATAACAAGGTTAGTTTCATTTGTTCTGTCATCACTGTATGCAGCTCC
TATTACCTACTGCGGTCTATTGTTTACGATGTGTTATGTCCACCTGCATCTCATTGTCTGAGGTTGTCTGGT

TTGACCATATAATCCGCCTTTGATATGCCATGTTATATTTAGAGGATTGTTTTGTAGAATTAGTCTTTTGAA
CTGAATTGAATATTGACATACTCCTTGTTTCATTCCAACAGAATATTGTCCTTTCCGGGGGGTCTACAATGT
TCAAGGATTTTCAAAGAAGATTGCAACGAGATATCAAGAAACGTGTAGATGCGCGGACTTCAGCTTCAGAAA
AGAAATCTGGAGGTGACCACAAAGTAAGCCTATTCTATTTAATAGCAGTTCCTTTGTATGATTACAGCCTCT
TCCATGACGACTCAGATCATGTTTCATGCCGAGGTGGAGAATGCACCAATATATTGGCGAACATAGGGCCTG
AGCTTCCTTGTTGTCCCTGGTGCATTTGCATGCTTTGTCTGCTTTCTCAGTTCCTGCCTAGCTGCCTCTTCT
TTTAAGCTTTAGGTATGATATGCTGGTTTGAAAGTTGTTTCAGCAACTTGTTTGTGAAGACATGGCTATTTGT
CTACAGTCTCAGGCAGTTGAAGTAAATGTGGTGGGACATCCCATGCAACGATTTCGCTGTCTGGTTTGGAGGC
TCGCTCTTGGCTTCCACGCCAGATTTTTATAATGTATATCTATCACCCATCTTTATCTGCTTCTCTTTCT
TTAATATTTAATTTTTGCAAGTAACTTTCATGTGAGCAGCATGTCCGATGAGCTCTAGATTGCAAGTGGTTT
TTCGTATGCATCGAGATCTAATTTGGCTTAGCATGCTTTCTGGACCTTTCATCTACAGGCTTGCCATACCA
AAGCTGAATACGAAGAATATGGCTCCAGTATATGCCGTCTCAATCCGGTCTTCAAGGGTATGTTATAA

>*Oryza sativa* (AP004092)

ATGGACGCCGCCTCCCGCCCCGCGTGCATCGACAACGGCACCGGGTAAGCCTCCCTCTCTCTCTCTCTT
TCCAGATCTGCGCGCGGAGAGCGTGCGCCGCGGCAATCTGAGGCGGGTGATGAGAATGGGTGGCGCGCGCG
CGCAGGTACACGAAGATGGGGTTCGCCGGGAACGTGGAGCCCTGCTTCATCACCCCCACCGTCGTCGCCGTC
AACGACACCTTCGCCGGCCAGACCAGGGCCAACACCACCAAGGGGAACTGGATGGCGCAGCACAGCGCCGGC
GTCATGGCCGATCTCGACTTCTTCATCGGGGAGGACGCCCTGGCCCGCTCCCGCTCCAGCAACACCTACAAC
CTCAGCTATCCAATTCACAATGGCCAGGTTTTGTGCGCGCGCGCGGAGCGAGCGTAAATTTCTCTTCTGAC
ACTCTGCGTTGCTATCTTAGTTTTGCGGAGCTTCATTTACTCAAGCTGATATGGGCTAGATATTCAGGTTGAG
AATTGGGACACCATGGAGAGGTTCTGGCAGCAGTGCATTTTTCAATTACCTGCGGTGTGATCCGGAGGATCAC
TATTTCTGCTCACCGAGAGCCCCCTGACTCCTCCCGAGACCCGAGTACACCGGGGAGATCATGTTTGAG
ACTTTCAATGTGCCTGGTCTGTACATAGCGTGCCAGCCGGTTCTTGCCTCGCAGCAGGATACACCACCACA
AAGGTTAGTAGAGCAAGAATTCCTTGAGATGAGAACATGAATTTTCGTTCTCAAGGCCATGTTTATGTTGTAG
TTGAACTGTTTTATTACACGCTTTCAATATGCAATATTTCTGCTTAACCTTAATTTGATAGGTGAAAGAGAC
TACATTATTGAAATATTTACGTTTCCAATAAATTTAATTTCTATAGTGGTTTTTCTGTTTCATTTGAAAGCT
CATTGTGTTGGCATCTTATTTCTAGCCATGCATGGACTCTTGAGCTTCGTAGTTGTGCTTAGTTTGTCTTAC
AATACTCCTTCCATCCCACAATACTGTCTTTCTGGTTTTGTTTAGCACAAATTAAGGTTTAGCAATCAAAGAC
TAAAGTGCCTCTCATTTGAATGGAATTGTGAGGTTGTTGAGGATAGAATGTGTAGAAATTTGAATAGGAGGT
GATTGATTGGACATATAGTACTCTTAAGTGACAAGTATTGTGGGATAAATTTTAAACCTTAAAGAGACAAC
ATTTTGGGACGGAGGAAGTACTACATTATTTGCCCTCTTTTTCTTTTCGTTCTATGTTGAGAGATATATTTA
TGAGGAATTTTCATGCTTTGTTTTAGTGTGAAATGACAGGTGTTGTAGTCGATGTGGGTGATGGGGCTACCC
ACATTGTTCTGTTGCTGATGGTTATGTTATAGGAAGCAGCATCAGATCAATTCCAATTACAGGCAAGGATG
TTACCCAGTTTATTACGCAACTCTTAAAGGTAGTTACCATTGCTTTCTTGTGGCCGTCACAAGATAGTACT
TAACCTTCTATTTGTCAACAGATGTCACTGATCTTACATTACTGTGGATCTATGCCTTTGAGAGTCCAAATG
TCCATCATAACTGCACAAGGAAATCAAAGATTCATGAAAATAACAGCCACAAATAATGAAAGGGATAAAATG
CATGAAATAGAGGTAGAATTGGTGGAAAGTAACTGTCAATTTTTATCTAATGATGCACAATAAATTTCCACTC
AAAGTTTTACAAGCAACTCCAGCCTGCAGCTGCAATCATGCGCCATGGCAAATTTTGTAAACACACCTGAGA
TTATTTGAGTCACCTCACCGTGGTTGTCAAATAAGCATATCAAGTATATCATTTCTGAACAAATGAATACACA
TGTTAAGACTAGAGGACAAGCTGAAATTATCGTTACCTGTATGTGATGAGAGAGACAACCTTCTCTTCTTGT

GCCATTTAACCTGCATGTGAAATTGACTTGGGACTTGGGAGTGTGATATATCAAGAAAGGATATATAAATAT
ATAACAAGTTTACCTCATAATTTTCTTGAGATTTTCATATTTTATATAGCGAATCTGCATAATGGCAGTGCA
CTTATAAGTCACTGAGCCAATTAGTTCTTGACAGGAAAGAGGTTGAGCACATTCACCAGAAGAATCTTTTGAT
GTGGCAAGGAGAGTGAAGAAATGTACTGCTATACATGTTTCAGATATTGTGAAGGTATTAACTACTACAATA
AATACATGAACTGTCAATTATTGAAACATGGATAGTATATGTTCTCGTTTATTCTAGGATGAGTGTACTTC
AAAAGGAAGGATTGCTTTTACCTCATAATAGCATTGCAGTTGACTGACTGTCACAGTTATAGCAGCCTAGGC
ATTGGCATTTAAGGCTTACCCTGCCTGGAATCTAATTTTGTAAAGCACTGTTCCAGCATGCTTGATGTCAA
CAATGCATCTGCTTTCTCTGATTCACTTTTTCTGCAACTGGTGATTGTTTTTCAGTATCGAATATGTTGTC
TCGGTTCTTCCAGCTTTGAACCATTGACTTTGTTATTTGTACGACAAAAAATAGAGTCCCTAAGAGATGAA
AAGAAAAATAATAATATAACTTTATTGTTGCCTTTTTAGGAATTTAATAAGCATGACAGAGAGCCCAATAAG
TACATAAAGCACTGGAGTGGCATCAAACCAAAAACTGGTGCCAAATACACCTGCGACATTGGATATGAACGC
TTCCTAGGGCTGAGGTAATTGATTTTGCATTAATGTGTTTACCATTAACTGTGGCTTCTACAATGTAACAT
TTGATTTAGGTTCAAACCTTAACTGCGATCATAATTTAACTCCAATTCATGGATAAACAGTTTGAGTTCAG
GCTTTATGTTTATAAATAAATACTGCTTTGTACATGATATCTCTAGTAGTTCTGATGCATTTTCTAACTAAAC
ATTTTGATTGCACTATCATTTTAATCTAATTTCCACAGTTGCTGTGAACCATGCAGATTTTCTTCCACCCT
GAGATTTACAACAATGACTTACCCTCCTTTGCATGTAGTTATTGACAAGTGCATCCAATCATCCCAATT
GACACAAGAAGGGCTCTTTATAAGGTTTGTGTTATCAAAATGCCGTCTTATGATTCAAAATATCACAGTGGT
TCTGAGTTTCATTTTATTGGACAGAATATTGTCTTGTCCGGGGATCAACTATGTTTAAAGATTTCACAGG
AGGCTGCAGCGGACCTAAAAAGATAGTGGATGCACGAGTCTTGCATCTAATGCTCGACTTGGTGGAGAT
GCAAAGGTACAAACTTTTCATGTTTGTCTGCTCTCTCCTGATTGCAGAAAGAACTGGCCAAACCAGAAA
CTTTATTGTGATATTGGAACCTGGAAGCTACAGCTACATTCTGTTTATTTCAGGCCCAACCTATAGAAGTAA
ATGTAGTTAGCCATCCTATTCAAAGATATGCTGTCTGGTTTTGGTGGTTCTGTGCTTGCTCTACCGCTGAAT
TCTACGAGGTATTCAAACCTTCTATTTCTATGTACAGTAGTAATGAACACTCATATCACTTGAAACTAGTGCA
TAGCGTTTACTTTTGCAAGTTGTTTCCAAAGCTTAAATTTTTTTGTTGGAATATATCCCATATTCGGGGTT
TCTTTTTCTTTTTCCATTTTAGAAATTAAGCTAATTTCTGGTAGTTTCCCAACCAGGCTTGCCACACAAA
AGCAGAGTATGAAGAGTATGGCGCAAGCATCTGCCGGACGAATCTGTTTTCAAAGGGATGTACTAA

>*Arabidopsis thaliana* (At1g13180)

ATGGATCCGACTTCTCGACCCGCTATTGTCATCGACAATGGAAGTGGGTACGTTCAATGATAGGTTTGATTT
GTTTATGCGCTTAACGTGTTTCGATGAAATGCTGCAATTAGATTCAATCTTGTGTGTGTGTGATTGCAGGGTA
TACTAAAATGGGATTTGCGGGTAATGTAGAGCCATGTTTTATCTTACCAACAGTAGTTGCAGTAAACGAGTC
GTTTTTGAATCAATCCAAGAGTTCTTCTAAGGCAACTTGGCAAACCTCAGCACAAACGCTGGAGTTGCTGCGGA
TCTCGATTTCTATATTGGAGATGAAGCTCTTGCGAAATCGCGGTCTAGTAGTACTCATAATCTTCATTATCC
AATTGAGCATGGTCAAGTTGAGGATTGGGATGCTATGGAGAGATATTGGCAGCAGTGTATATTTAACTATTT
GAGATGTGATCCTGAGGATCATTATTTTCTTCTTACTGAAAGTCTCTTACTCCTCTGAAAGTCGAGAATA
TACTGGAGAAATTTTGTGTTGAGACTTTTAATGTTTCTGGGCTTTACATTGCTGTTAATTCAGTTCTTGCACT
TGCTGCTGGCTACACAACATCAAAGGTATGTTACACATTTCTTTTTCTCCAAGTATTTACGTTGTTGCTGTG
ATGAAATGCTATGTATTAGCCTACTTGCTGTGATGAAATGATATGTATTTAAGTTGTTTGTGCTGGGATGAAAT
GATATGTATTTAGGCTATTAGTTGTTTAAAGTTTGTCTGTAGACTGTGTGAATCCTTAAATCAAGTCATAATT
ATACTTTATTCAGTTTTGGTTTTAGGGACTGAGTCTCAAGAATAGGTTAGTGTAACTCACCAACATTAGAC
AATTTCCGAGCTTTGTGGGATTTAGCAAATATTAACATGTTCTCTTGTTTTTTGTCTGTCTCGTTATGCT

CGCCTCGCCTCTTAATTTGACTTACAATTCTTCTTAGTGTGAGATGACAGGGGTGTAGTAGATGTTGGAGA
TGGGGCAACTCATGTTGTACCTGTTGCAGAAGGTTATGTCATCGGGAGCTGTATCAAATCGATTCCAATTGC
TGGCAAAGATGTCACCCTCTTTATCCAGCAACTCATGCGGGTATGCACTAATTTATTATCTTAATATTAGTC
TTGGTCTTCTTTTGTAGTTGGTTTTTCATTCTTTCTCTGTGACATTTTAAAGATTTTAAAGGCACAGAAGTTAA
ATGTGTTAAATCCAAGCTTTGAGTATGGTAGCTAGGCTTCTGTTTATTTGTTTTAGATGTTGTGCTCATAT
GCTTAGAGAGGGTGTACTGTTTTAGATTAATGTATTAACCTTCATGTAACCTCTCGTTTCAATGTTTACTG
TAGGAAAGAGGTGAGAATATACCACCAGAAGATTCATTTCGATGTAGCCCGTAAAGTGAAGGAAATGTACTGC
TACACTTGTCTGACATCGTAAAGGTAATCCTTAGTGGTGAATATTCAAGTCAGATAATATTAATATATACT
CTTCTGAAAATTTATTACTGGCCTGTATGCTGAAATCGCTTGAAAAGAATATAGGAATATTGATAAAGAACA
TTCATATGGTTGCAGGAGTTTAAATAAACATGACAAAGAACCAGCAAAGTATATTAACAATGGAAAGGTGTA
AAGCCAAAGACTGGTGCACCATACACTTGCACGTGGGATATGAACGATTCCTTGGACCCGAGGTTTGTTAC
CATCTATCTGTTATAAAAAGTTGTAAGTTGATAAGATAACCAGAATCGGAGACTGGATATCTTTACTGGTGC
ATGAGTTTCTAGTATGTCAGTGTGAGCTGTTTCATGATTTGTTATCGATTATAAGATATTTTCAGCACTCTGTTT
TGATTACTGAACGGTACTGATATAAACTATGCTCTCTCAGAACTCAAATTAGGTAATTACTTAGTCCATT
ATGTTAACTGGAAGTCTGGAACATAATTCTTATCTAGTTAGAATTCAGCTGTCACTACTGGACCCATAGGAAG
CTAATCTCCTTTGTATCTCTATACCAAGAGAGTAACTGGAAAGTGGAACATAATTTCTTTATTGTTCTTGC
GTTTTTGTCTGCTATTACCGATGAGTAATGTTGAGATTTTGTGTGTTACAGGTGTTCTTTAATCCAGAGAT
ATACAGCAATGACTTCACAACACTTTTACCAGCTGTGATAGACAAATGTATTCAGTCTGCACCAATTGACAC
ACGAAGAGCTTTATATAAGGTTTGAAACGCCAAAGACTGGTCAGAGTTTTAAGATAATTTCCAATCCGCAAT
ACTGATGAATTTGTGAAATCATTTAGAATATAGTGTGTCCGGAGGTTCAACTATGTTCAAAGATTTCCGGA
AGAAGTTACAAAGGGACCTCAAGAAGATTGTTGATGCTCGTGTCTTGCTAATAACGCTCGTACTGGTGGT
GAAATTACGGTAAGAAAATTGTATGATATTCTGGAAAATAAAAGTGATAACCAGTTTTCTTAATCTGAGGTG
ATATTTATTTATAACCACAGTCTCAACCGGTGGAGGTTAATGTCTGTGAGCCATCTGTCCAGAGGTTTGCAG
TTTGGTTTGGAGGCTCTGTGCTTTTCACTCAACTCCTGAGTTTTTTCGCGGTATGCAAACCTAGTTTAGAGATCCG
CTAGTTTGAAGCTAAACCTCATGGCTTGATCGTGTTTTGAACAAGATGTATTTTGTGTTGCAGAGTTGC
AGAACGAAAGAGGAGTATGAGGAATATGGAGCAAGCATATGCCGCACGAATCCGGTGTTC AAGGGAATGTAT
TGA

Annex 3

Arp3 homologous proteins predicted by conceptual translation:

>*Physcomitrella patens* (BJ183257.1)

MDATQRPAAVVIDNGTGYTKMGFAGNVEPCFIIPTVVALNESFLGQSAPKAGTAAAYHNAGVMADLDFYIGEEA
LAKQHSSAYTLSYPIRQGGQIENWDTMERFWQQCLFNLYLRCDPEDHYMLLLETESPLTAPENREYMGEIMFETFN
VPGLYIATQAVLVLAAGYTTSKLEMTGLVVDAGDMTHVVPVADGYIIGSSIKSIPVAGRDLNPNFVQQLMRE
RGEVPPPEDSLDIARRVKEMYCYTCADIAKEFGKHDKEPAKYVVKQWKGNNSKTGAPFSCDIGYERFLAPEVF
FSPEIYSSDFTTPLPEVVDNCIQSAPIDVRRALYKNIVLSGGSTMFKDFQRRLQRDIKKRVDARTSASEKKS
GGDHKSQAVEVNVVGHMPQRFAVWFVGGSLLASTPDFYNACHTKAEEYEEYGSSICRLNPVFKGML

>*Acanthamoeba castellanii* (AAA93068.1)

MSRSGLPAAVVIDNGTGYTKMGYAGNTEPQYIIPTAIATKGAIEDPRCRARRWCPWAAGKNIADLDFFIG
DEAYENSKVYQITMPVRHGQVENWTHMEQFWEHCIFKYLRCPEPDHFFLLTEPPLNAPENREYTAEIMFE
TFNVPGLYIAVQAVLALAASWTSKQVTEKTLTGTVIDSGDGVTHVIPVAEGYVIGSSIKHIPLAGRDITN
FVLQLLRERNEKIPPAETLEVAKRIKETFSYVCPDIVKEFKKYDTEPKWFKTYEGIESVGKKPNVNDVG
YERFLGPEIFFNPEIFSSDFLTPLPKVVDETIQSCPIDTRRGLYKNIVLSGGSTMFKDFGKRLQRDIKRA
VDYRIKRSEELSQGRIKSKAVDVKVISHHMQRFVAVWFVGGSMMLASTPEFYKVCCHTKQQYDEVGSPICRHNP
VFGAMTM

>*Anopheles gambiae* (XP_313987.1)

MTGRLPACVIDVGTGYTKLGFANKEPQFIIPSAIAIKESAKVGDQSARRVTKGVEDLDFYIGDEAFDATGY
SVKYPVRHGLVEDWDLMERFLEQCIFKYLRAEPEDHFFLLTEPPLNTPENREYTAEIMFETFNVPGLYIAVQ
AVLALAASWASRPVEERTLTGIVVDSGDGVTHVIPVAEGYVIGSCIKHIPIAGRNIITSFIQSLLREREVGI
PEQSLETAKAIKERYSYICPDIAKEFAKYDAEPTKWMRHYEGINAITKQPFVGVYERFLGPEIFFHPEFS
NPDFTTPLSEIVDVTIQNCPIDVRRPLNNIVLSGGSTMFRDFGRRLQRDIKRSVDARLRISENLSEGRIP
KPIDVSVISHHMQRVAVWFVGGSMMLASTPEFYQVCHTKAAEYEEYGPICRHNPVFGTMT

>*Arabidopsis thaliana* (NP_172777.1)

MDPSTRPAIVIDNGTGYTKMGFAGNVEPCFILPTVVAVNESFLNQSKSSSKATWQTQHNAGVAADLDFYIGD
EALAKSRSSSTHNLHYPIEHGQVEDWDAMERYWQQCIFNLYLRCDPEDHYFLLLETESPLTPPESTREYTG
EILFE
TFNVPGLYIAVNSVLALAAGYTTSKCEMTGVVVDVGDGATHVVPVAEGYVIGSCIKSIPVAGKDVTLFIQQL
MRERGENIPPEDSFDVARKVKEMYCYTCSDIVKEFNKHDKEPAKYIKQWKGVKPKTGAPYTCVGYERFLGP
EVFFNPEIYSNDFTTTLPVIDKCIQSAPIDTRRALYKNIVLSGGSTMFKDFGRRLQRDLKIVDARVLANN
ARTGGEITSQPVEVNVVSHPVQRFAVWFVGGSVLSSTPEFFASCRTKEEYEEYGASICRTNPNVFKGMY

>*Caenorhabditis elegans* (NP_491066.1)

MSAHQLPACVIDNGTGYTKLGYAGNTEPQFIIPSAIAVKDKVASSNSQAMRWNNRVGAGIDDLDFFIGDEAL
SPAATNYTVKYPPIRHGIVEDWDLMERYWEQCIFKYLRAEPEDHFFLLTEPPLNTPENREYTAEIMFESFNVP
GLYIAVQAVLALTASWNSREANERSLTGLVIDSGDGVTHCIPVADGYVIGSCIKHIPIAGRDIITYFIQSLLR

DREHTIPAEQSYEVAKMIKEKFCYVCPDVMKEFVKYDTDAAKWLRTYDGINSTITKKPFNVVDVGYERFLGPEI
FFHPEFCNPEFTTPIISDTIDTLIQQCPIDVRRGLYENIVLSGGSTMFKDFARKLQRDVKRLSDGRLQMSETL
SGGRLKPKPIDVQVISHKMQRVAVWFGGSMLASTSEFYQVSHTKAEYMERGPSICRYNPVFGALT

>Danio rerio (NP_001003944.1)

MAARLPACVVDCGTGYTKLGYAGNTEPQFIIPSCIAIKESAKVGDQAQRMMKGVDDLDFFIGDEAIDKPTY
ATKWPIRHGIVEDWDLMERFMEQVIFKYLRAEPEDHYFLLTEPPLNTPENREYTAEIFFESFNVPGLYIAVQ
AVLALAASWTSRQVGERTLTGTVIDSGDGVTHVIPVAEGYVIGSICKHIPIAGRDITYFTQQLLREREVGI
PEQSLETAKAVKERFSYVCPDLVKEFSKYDTDGSKWIKQYTGINTISKKEFTIDVGYERFLGPEIFFHPEFA
NPDFTQPISEVVDEVIQNCPIDVRRPLYKNIVLSGGSTMFRDFGRRLQRDLKRTVDARLKLSEELSGGKLP
KPIDVQVITHHMQRVAVWFGGSMLASTPEFYQVCHTKKDYEEIGPSICRHNPVFGVMS

> Dictyostelium discoideum (CAA86553.1)

MNPASGLPAVIDNGTGYTKMGYAGNNDPSFIIPPTTIATQSSKQKQTAASQKKGVEDLDFFIGDEAIANSKT
YDMTNPVKHGQIENWTHMEQYWEHCVFKYLRCEPEDHYFLLTEPPLNAPENREFTAEIFFETFNVPGLYIAV
QAVLALAASWTSKNAEKTLTGTVIDSGDGVTHVIPISEGYVIGSSICKHIPIAGRDISSYVQQIMREREPNIP
PAESLEIAKRVKEQYSYVCPDIVKEFGKYDSEPKWIKTINAQDSVTKKPFSDVGYERFLGPELFFNPEIA
SSDYLTPLPKVDDTIQSCPIDCRRGLYKNIVLSGGSTMFKDFGKRLQRDVKRSVDYRIKRSEELSGGKIK
VPLAVNVI SHNMQRVAVWFGGSMLASTPEFYQVCHTKAQYDEIGPSICRFNTVIGGIN

>Drosophila melanogaster (NP_523968.1)

MAGRLPACVIDVGTGYSKLGAFAGNKEPQFIIPSAIAIKESARVGDNTNRRITKGIEDLDFFIGDEAFDATGY
SIKYPVRHGLVEDWDLMERFLEQCVFKYLRAEPEDHYFLLTEPPLNTPENREYTAEIFFETFNVPGLYIAVQ
AVLALAASWASRSAEERTLTGIVVDSGDGVTHVIPVAEGYVIGSICKHIPIAGRNITSFIQSLLREREVGI
PEQSLETAKAIKEKHCYICPDIAKEFAKYDTEPGKWIRNFSGVNTVTKAPFNVDVGYERFLGPEIFFHPEFS
NPDFTIPLSEIVDNVIQNCPIDVRRPLYNNIVLSGGSTMFKDFGRRLQRDIKRSVDTRLRISENLSEGRIP
KPIDVQVITHHMQRVAVWFGGSMLASTPEFYQVCHTKAAEYEEYGPSICRHNPVFGTMT

>Eremothecium gossypii (NP_985966.1)

MSYLNPAVMDNGTGLTKLGFAGNDSPSWVFPTAIATAQPSKTAKSSSMSGMGQSGSGMGAGGSAFFGNTT
SATSFTGFTSSSLMSNNLAGKRGTELDFFYIGNEALAAAQGPSYLSYPIRHGQVEDWNHMERFWENSIFKY
LRTEPEDHFFLLTEPPLNPPENREQVAEIFFESFNAGLYIAVQAVLALAASWTSKVTDRSLTGTVIDSGD
GVTHVIPVAEGYVIGSAIKHIPIAGRDITLFIQSLLRERGEVDTSLRTAERIKQEYCYVCPDIVKEFNKFD
DATKFAQFIVENKEKTQKKVVDVGYERFLAPEIFFNPEIASSDFLTPLPTVVDQTIQACPIDVRKGLYNNIV
LSGGSTMFKDFGRRLQRDLRSIVNRIAQSELLSGTKSTGVEVQVISHRRQRNAVWFGGSLLAQTAEFKSYC
HTKKDYEEYGPQIVRNFSLFNMV

>Homo sapiens (NP_005712.1)

MAGRLPACVVDCGTGYTKLGYAGNTEPQFIIPSCIAIKESAKVGDQAQRVMKGVDDLDFFIGDEAIEKPTY
ATKWPIRHGIVEDWDLMERFMEQVIFKYLRAEPEDHYFLLTEPPLNTPENREYTAEIFFESFNVPGLYIAVQ
AVLALAASWTSRQVGERTLTGTVIDSGDGVTHVIPVAEGYVIGSICKHIPIAGRDITYFIQQLLRDREVGIP

PEQSLETAKAVKERYSYVCPDLVKEFNKYD TDGSKWIKQYTGINAISKKEFSIDVGYERFLGPEIFFHPEFA
NPDFTQPISEVVDEVIQNCPIDVRRPLYKNIVLSGGSTMFRDFGRRLQRDLKRTVDARLKLSEELSGGRLKP
KPIDVQVITHMQRYAVWFGGSM LASTPEFYQVCHTKKDYEEIGPSICRHNPVFGVMS

>*Lycopersicon esculentum* (BT013825)

MDPSTSRPAVVIDNGTGYTKIGFAGNVEPCFILPTVVAANESFVNQPRALTKNSNWL AQHSAGVMADLDFFI
GDEALTRSKSSSNYNLTYP IQHGQVDNWD SMERFWQQCIFNYLRCDPEDHYFLLTESPMTAPENREYTGEIM
FETFNVPGLYIAVQPV LALAAAGYTASKCEMTGVVVDIGDGATHVVPVAEGYVIGSSIKSIPVSGKDVT LFWQ
QLMKERGEHVPAEDSFEIARKVKEMHCYTCSDIVKEFNKHDKEPGKYIKHWRGTPKPKTGAPYSCDVGYERFL
GPEVFFSPEIYNSDFTSPLPEVIDKCIQSAPIDTRRALYKNIVLSGGSTMFKDFHRRLQRDLKKIVDDRILA
SDARLGGNVKAQPVEVNVVSNPIQRCAVWFGGSVLASTPEFFAACHTKAEYEEYGASICRTNPVFKGMY

>*Magnaporthe grisea* (XP_361405.1)

MDNGFAGNDSPSFVFP TAIATKSAGASGGTSGRPAVANKPSFLTGGAGPGGHL SGKRGTEDLDFFIGDEAI
AASSGPGYGLHYPIRHGQIENWDHMERFWSNSIFKYLRVEPEDHFFLLTEPPLNPPENRENTAEIFFESFNC
AGLYIAVQAVLALAA SWTSSKVHDRSLTGTVIDSGDGVTHVIPVAEGYVIGSSIKSIP IAGRDITYFVQSLL
RDRGEPDSSLKTAQEIKEEYCYVCPDIVKEFTKFRDRSRFARHVVSQPGGREVGVDVGYERFLAPEIFFNP
EIIYSSDFLTPLPVVVDGVIQSSPIDVRRGLYKNIVLSGGSTLYKDFGRRLQRDIKQLVDARIRASEMRSGGA
KSGGLEVQVITHKRQRHGPWFGGSLLGQTPEFRSYCHTKAEYQEYGP GIVRRFALLGGPGGS

>*Neurospora crassa* (XP_328195.1)

MANTTPAVVMDNSSSSAGFAGNDSPSFVFP TAIATKSPSAGTGGSGSGRPAVANKPSFLTGGAGPGGHL SAK
RGTELDLYFIGDEAVAAANGPGTHGQIENWDHMERFWSNSIFKYLRVEPEDHFFLLTEPPLNPPENRENTAE
IFFESFN CAGLYIAVQAVLALAA SWTSSKVQDRSLTGTVIDSGDGVTHVIPVAEGYVIGSSIKSIP IAGRDI
TYFVQSLLRDRGEPDSSLKTAQEIKEEYCYVCPDIVKEFAKYDRDRSRFLKHTITQPGRQVTVDVGYERFM
APEIFFNPEIYSSDFLTPLPVVVDGVIQSSPIDVRRGLYKNIVLSGGSTLYKDFGRRLQRDIKQLVDTRIKA
SEVRSGGAKSGGLDVQVITHKRQRHGPWFGGSLLGQTPEFRSYCHTKAEYQEYGPSIVRRFALLGGPGGS

>*Plasmodium falciparum* (NP_702012.19)

MSEEAVALVVDNGSGMVKSGLAGDDAPKCVFPSIVGRPKMPNIMIGMEQKECYVGDEAQNKRGI LTLKYPIE
HGIVTNWDDMEKIWHHTFYNELRVSP EHPVLLTEAPLNPKTNREKMTQIMFETFDPAMYVSIQAILSLYA
SGRTTGIVLDSDGDVSH TVPIYEGYVLP HAINRIDMAGRDLTYHMMKLF TERGHFTTTAEREIVRDIKEKL
CYIAMDYDEELKRSEEHSD EIEEIIYELPDGNLITVGSERFRCPEALFNPTLIGRECPGLHITAYQSIMKCDI
DIRKELYNNIVLSGGTTMYNNIGERLTKEMTNLAPSSMKIKVIAPPERKYSVWIGGSILSSLSSTFQQMWITK
EEYEDSGPSIVHRKCF

>*Oryza sativa* XP_466542.1

MDAASRPVVIDNGTGYTKMGFAGNVEPCFITPTVAVVNDTFAGQTRANTTKGNWMAQHSAGVMADLDFFIG
EDALARSRSNTYNSYPIHNGQVENWDTMERFWQQCIFNYLRCDPEDHYFLLTESPLTPPETREYTGEIMF
ETFNVPGLYIACQPV LALAAAGYTTTTKCEMTGVVVDVGDGATHIVPVADGYVIGSSIRSIPITGKDVTQFIQQ
LLKERGEHIPPEESFDVARRVKEMYCYTCSDIVKEFNKHDREP NKYIKHWSGIKPKTGAKYTCDIGYERFLG

PEIFFHPEIYNNDFTTPLHVVIDKCIQSSPIDTRRALYKNIVLSGGSTMFKDFHRRLQRDLKKIVDARVLAS
NARLGGDAKAQPIEVNVVSHPIQRYAVWFGGSVLASTAEFYEAUGHTKAEEYEEYGASICRTNPVFKGMY

>*Saccharomyces cerevisiae* NP_012599.1

MSYLNNPAVVMNDNGTGLTKLGFAGNDSPSWVFPTAIATAAPSNTKKSSGVBGAPSAVSNEASYFGNSTSATNF
NGATGGLLSNNLSGKRGTELDIFYIGNEALVASQGPSYLSYPIRHGQVENWDHMERFWENSIFKYLRTEPE
DHFLLTEPPLNPPENREQVAEIFFESFNCAGLYIAVQAVLALAASWTSSKVTDRSLTGTVIDSGDGVTHVI
PVAEGYVIGSAIKNIPIAGRDITLFIQSLLRERGEADTSLRTAEKIKQEYCYVCPDIVKEFNKFDKDPKFA
QFVVENQEKTRRKVV DIGYERFLAPEIFFNPEIASSDFLTPLPTVVDQTIQACPIDVRKGLYNNIVLSGGST
MFKDFGRRLQRDLKSIVNNRIAQSELLSGTKSTGVDVSVISHKRQRNAVWFGGSLLAQTAEFKGYCHTKKDY
EEYGPEIVRNFSLFNMV

>*Schyzosaccharomyces pombe* (NP_592898.1)

MASFNVPIIMDNGTGYSKLGAGNDAPSYVFPTVIATRSAGASSGPAVSSKPSYMASKGSGHLSSKRATEDL
DFFIGNDALKKASAGYSLDYPPIRHGQIENWDHMERFWQSLFKYLRCEPEDHYFLLTEPPLNPPENRENTAE
IMFESFNCAGLYIAVQAVLALAASWTSSKVTDRSLTGTVVDSGDGVTHIIPVAEGYVIGSSIKTMPLAGR DV
TYFVQSLLRDRNEPDSSLKTAERIKEECCYVCPDIVKEFSRFDREPDRLKYASESITGHSTTIDVGFERFL
APEIFFNPEIASSDFLTPLPELVDNVVQSSPIDVRKGLYKNIVLSGGSTLFKNFGNRLQRDLKRIVDERIHR
SEMLSGAKSGGVDVNVISHKRQRNAVWFGGSLLAQTPFEFGSYCHTKADYEEYGASIARRYQIFGNSL

>*Tetrahymena thermophila* (AAN73250.1)

MDNKCFIENKVAIIDNGTGYSKMGWGGNIEPTYDIPTVIVSDNSDKNSVQVSKNYNEQLDFCIGNDALNQQVK
TYPMKSGIVTDWTLMEKFWQKSIFDYLRCDPDETTFVLTTEPPMNPPENRENIAEIFFETFNKSIYIGVQAV
LALYSNQMHQNAQTGNKLTGCVLDSGDGVTHIIPVSDGYVIGSCIKHIPLAGRDI TNFIAQMIRDRGEKVN
NQDINRISAEIKEKYGYVAPKGLLQEFERYDKPGQDGKPSNFKQYTFESQVDKKQYTMVGYERFLGPPEMF
FYPEFFDSKWRTSIDESIDNAIQGSPIDTRRHLYSNIVLSGGSTMFEFGFTDRLQSAIQKRVDRLRLRYSTAL
SKPQPIVVQVAQNPHQRFSVWQGGSLLSIKPGFEKVKSRQEYLEYGPSIVRQNAVLSGSM

REFERENCES

- Ainley, W. M. and Key, J. L.** (1990). Development of a Heat-Shock Inducible Expression Cassette for Plants - Characterization of Parameters for Its Use in Transient Expression Assays. *Plant Molecular Biology* **14**, 949-967.
- Aizawa, H., Sameshima, M. and Yahara, I.** (1997). A green fluorescent protein actin fusion protein dominantly inhibits cytokinesis, cell spreading, and locomotion in Dictyostelium. *Cell Structure and Function* **22**, 335-345.
- Alessa, L. and Kropf, D. L.** (1999). F-actin marks the rhizoid pole in living *Pelvetia compressa* zygotes. *Development* **126**, 201-209.
- Ashton, N. W. and Cove, D. J.** (1977). Isolation and Preliminary Characterization of Auxotrophic and Analog Resistant Mutants of Moss, *Physcomitrella-Patens*. *Molecular & General Genetics* **154**, 87-95.
- Balasubramanian, M. K., Feoktistova, A., McCollum, D. and Gould, K. L.** (1996). Fission yeast Sop2p: A novel and evolutionarily conserved protein that interacts with Arp3p and modulates profilin function. *Embo Journal* **15**, 6426-6437.
- Baluska, F., Jasik, J., Edelmann, H. G., Salajova, T. and Volkmann, D.** (2001). Latrunculin B-induced plant dwarfism: Plant cell elongation is F-actin-dependent. *Developmental Biology* **231**, 113-124.
- Baluska, F., Salaj, J., Mathur, J., Braun, M., Jasper, F., Samaj, J., Chua, N. H., Barlow, P. W. and Volkmann, D.** (2000). Root hair formation: F-actin-dependent tip growth is initiated by local assembly of profilin-supported F-actin meshworks accumulated within expansin-enriched bulges. *Developmental Biology* **227**, 618-632.
- Baluska, F., Vitha, S., Barlow, P. W. and Volkmann, D.** (1997). Rearrangements of F-actin arrays in growing cells of intact maize root apex tissues: A major developmental switch occurs in the postmitotic transition region. *European Journal of Cell Biology* **72**, 113-121.
- Bamburg, J. R.** (1999). PROTEINS OF THE ADF/COFILIN FAMILY: Essential Regulators of Actin Dynamics. *Annu. Rev. Cell Dev. Biol.* **15**, 185-230.
- Baskin, T. I., Wilson, J. E., Cork, A. and Williamson, R. E.** (1994). Morphology and Microtubule Organization in Arabidopsis Roots Exposed to Oryzalin or Taxol. *Plant and Cell Physiology* **35**, 935-942.
- Basu, D., El-Assal, S. E.-D., Le, J., Mallery, E. L. and Szymanski, D. B.** (2004). Interchangeable functions of Arabidopsis PIROGI and the human WAVE complex subunit SRA1 during leaf epidermal development. *Development* **131**, 4345-4355.
- Bibikova, T. N., Blancaflor, E. B. and Gilroy, S.** (1999). Microtubules regulate tip growth and orientation in root hairs of Arabidopsis thaliana. *Plant Journal* **17**, 657-665.
- Blancaflor, E. B.** (2000). Cortical actin filaments potentially interact with cortical microtubules in regulating polarity of cell expansion in primary roots of maize (*Zea mays* L.). *Journal of Plant Growth Regulation* **19**, 406-414.
- Brembu, T., Winge, P., Seem, M. and Bones, A. M.** (2004). NAPP and PIRP Encode Subunits of a Putative Wave Regulatory Protein Complex Involved in Plant Cell Morphogenesis. *Plant Cell* **16**, 2335-2349.
- Chalfie, M., Tu, Y., Euskirchen, G., Ward, W. W. and Prasher, D. C.** (1994). Green Fluorescent Protein as a Marker for Gene-Expression. *Science* **263**, 802-805.
- Chang, F. and Peter, M.** (2002). Cell biology - Formins set the record straight. *Science* **297**, 531-532.

- Chen, C. Y., Wong, E. I., Vidali, L., Estavillo, A., Hepler, P. K., Wu, H. M. and Cheung, A. Y.** (2002). The regulation of actin organization by actin-depolymerizing factor in elongating pollen tubes. *Plant Cell* **14**, 2175-2190.
- Cheung, A. Y. and Wu, H.-m.** (2004). Overexpression of an Arabidopsis Formin Stimulates Supernumerary Actin Cable Formation from Pollen Tube Cell Membrane. *Plant Cell* **16**, 257-269.
- Christensen, A. H., Sharrock, R. A. and Quail, P. H.** (1992). Maize Polyubiquitin Genes - Structure, Thermal Perturbation of Expression and Transcript Splicing, and Promoter Activity Following Transfer to Protoplasts by Electroporation. *Plant Molecular Biology* **18**, 675-689.
- Cooper, J. A., Wear, M. A. and Weaver, A. M.** (2001). Arp2/3 complex: Advances on the inner workings of a molecular machine. *Cell* **107**, 703-705.
- Coue, M., Brenner, S. L., Spector, I. and Korn, E. D.** (1987). Inhibition of Actin Polymerization by Latrunculin-A. *Febs Letters* **213**, 316-318.
- Cove, D.** (1992). Regulation of Development in the Moss, *Physcomitrella patens*. In *Development. The molecular genetic approach*, (ed. V. E. A. Russo S. Brody D. Cove and S. Ottolenghi). Berlin: Springer-Verlag.
- Cubitt, A. B., Heim, R., Adams, S. R., Boyd, A. E., Gross, L. A. and Tsien, R. Y.** (1995). Understanding, Improving and Using Green Fluorescent Proteins. *Trends in Biochemical Sciences* **20**, 448-455.
- Dale, E. C. and Ow, D. W.** (1990). Intramolecular and Intermolecular Site-Specific Recombination in Plant-Cells Mediated by Bacteriophage-P1 Recombinase. *Gene* **91**, 79-85.
- Deeks, M. J. and Hussey, P. J.** (2003). Arp2/3 and 'The Shape of things to come'. *Current Opinion in Plant Biology* **6**, 561-567.
- Doonan, J. H., Cove, D. J. and Lloyd, C. W.** (1988). Microtubules and Microfilaments in Tip Growth - Evidence That Microtubules Impose Polarity on Protonemal Growth in *Physcomitrella-Patens*. *Journal of Cell Science* **89**, 533-540.
- Doris, F. P. and Steer, M. W.** (1996). Effects of fixatives and permeabilisation buffers on pollen tubes: Implications for localisation of actin microfilaments using phalloidin staining. *Protoplasma* **195**, 25-36.
- Drubin, D. G. and Nelson, W. J.** (1996). Origins of cell polarity. *Cell* **84**, 335-344.
- Eden, S., Rohatgi, R., Podtelejnikov, A. V., Mann, M. and Kirschner, M. W.** (2002). Mechanism of regulation of WAVE1-induced actin nucleation by Rac1 and Nck. *Nature* **418**, 790-793.
- El-Assal, S. E. D., Le, J., Basu, D., Mallery, E. L. and Szymanski, D. B.** (2004). Arabidopsis GNARLED encodes a NAP125 homolog that positively regulates ARP2/3. *Current Biology* **14**, 1405-1409.
- El-Assal, S. E., Le, J., Basu, D., Mallery, E. L. and Szymanski, D. B.** (2004). DISTORTED2 encodes an ARPC2 subunit of the putative Arabidopsis ARP2/3 complex. *Plant Journal* **38**, 526-538.
- Frank, M. J. and Smith, L. G.** (2002). A small, novel protein highly conserved in plants and animals promotes the polarized growth and division of maize leaf epidermal cells. *Current Biology* **12**, 849-853.
- Gatz, C.** (1997). CHEMICAL CONTROL OF GENE EXPRESSION. *Annual Review of Plant Physiology and Plant Molecular Biology* **48**, 89-108.
- Geitmann, A. and Emons, A. M. C.** (2000). The cytoskeleton in plant and fungal cell tip growth. *Journal of Microscopy-Oxford* **198**, 218-245.
- Geitmann, A., Wojciechowicz, K. and Cresti, M.** (1996). Inhibition of intracellular pectin transport in pollen tubes by monensin, brefeldin A and cytochalasin D. *Botanica Acta* **109**, 373-381.

- Gibbon, B. C., Kovar, D. R. and Staiger, C. J.** (1999). Latrunculin B has different effects on pollen germination and tube growth. *Plant Cell* **11**, 2349-2363.
- Gilliland, L. U., McKinney, E. C., Asmussen, M. A. and Meagher, R. B.** (1998). Detection of deleterious genotypes in multigenerational studies. I. Disruptions in individual Arabidopsis actin genes. *Genetics* **149**, 717-725.
- Girod, P. A., Fu, H. Y., Zryd, J. P. and Vierstra, R. D.** (1999). Multiubiquitin chain binding subunit MCB1 (RPN10) of the 26S proteasome is essential for developmental progression in *Physcomitrella patens*. *Plant Cell* **11**, 1457-1471.
- Haseloff, J., Siemering, K. R., Prasher, D. C. and Hodge, S.** (1997). Removal of a cryptic intron and subcellular localization of green fluorescent protein are required to mark transgenic Arabidopsis plants brightly. *Proceedings of the National Academy of Sciences of the United States of America* **94**, 2122-2127.
- Hepler, P. K., Vidali, L. and Cheung, A. Y.** (2001). Polarized cell growth in higher plants. *Annual Review of Cell and Developmental Biology* **17**, 159-187.
- Higgs, H. N. and Pollard, T. D.** (2001). Regulation of actin filament network formation through Arp2/3 complex: Activation by a diverse array of proteins. *Annual Review of Biochemistry* **70**, 649-676.
- Holtorf, S., Apel, K. and Bohlmann, H.** (1995). Comparison of different constitutive and inducible promoters for the overexpression of transgenes in *Arabidopsis thaliana*. *Plant Molecular Biology* **29**, 637-646.
- Hudson, A. M. and Cooley, L.** (2002). A subset of dynamic actin rearrangements in *Drosophila* requires the Arp2/3 complex. *J. Cell Biol.* **156**, 677-687.
- Imaizumi, T., Kadota, A., Hasebe, M. and Wada, M.** (2002). Cryptochrome Light Signals Control Development to Suppress Auxin Sensitivity in the Moss *Physcomitrella patens*. *Plant Cell* **14**, 373-386.
- Jenkins, G. I. and Cove, D. J.** (1983). Phototropism and Polarotropism of Primary Chloronemata of the Moss *Physcomitrella-Patens* - Responses of Mutant Strains. *Planta* **159**, 432-438.
- Kandasamy, M. K., Gilliland, L. U., McKinney, E. C. and Meagher, R. B.** (2001). One plant actin isoform, ACT7, is induced by auxin and required for normal callus formation. *Plant Cell* **13**, 1541-1554.
- Kandasamy, M. K., McKinney, E. C. and Meagher, R. B.** (2002). Functional nonequivalency of actin isoforms in Arabidopsis. *Molecular Biology of the Cell* **13**, 251-261.
- Kandasamy, M. K. and Meagher, R. B.** (1999). Actin-organelle interaction: Association with chloroplast in Arabidopsis leaf mesophyll cells. *Cell Motility and the Cytoskeleton* **44**, 110-118.
- Kang, F., Purich, D. L. and Southwick, F. S.** (1999). Profilin promotes barbed-end actin filament assembly without lowering the critical concentration. *Journal of Biological Chemistry* **274**, 36963-36972.
- Kelleher, J. F., Atkinson, S. J. and Pollard, T. D.** (1995). Sequences, Structural Models, and Cellular-Localization of the Actin-Related Proteins Arp2 and Arp3 from *Acanthamoeba*. *Journal of Cell Biology* **131**, 385-397.
- Kost, B., Mathur, J. and Chua, N. H.** (1999). Cytoskeleton in plant development. *Current Opinion in Plant Biology* **2**, 462-470.
- Kost, B., Spielhofer, P. and Chua, N. H.** (1998). A GFP-mouse talin fusion protein labels plant actin filaments in vivo and visualizes the actin cytoskeleton in growing pollen tubes. In *Plant Journal*, vol. 16 (ed., pp. 393-401).

- Kovar, D. R., Gibbon, B. C., McCurdy, D. W. and Staiger, C. J.** (2001). Fluorescently-labeled fimbrin decorates a dynamic actin filament network in live plant cells. *Planta* **213**, 390-395.
- Kropf, D. L., Berge, S. K. and Quatrano, R. S.** (1989). Actin Localization During Fucus Embryogenesis. *Plant Cell* **1**, 191-200.
- Kropf, D. L., Bisgrove, S. R. and Hable, W. E.** (1998). Cytoskeletal control of polar growth in plant cells. *Current Opinion in Cell Biology* **10**, 117-122.
- Le, J., El-Assal, S. E. D., Basu, D., Saad, M. E. and Szymanski, D. B.** (2003). Requirements for Arabidopsis ATARP2 and ATARP3 during epidermal development. *Current Biology* **13**, 1341-1347.
- Li, S. D., Blanchoin, L., Yang, Z. B. and Lord, E. M.** (2003). The putative Arabidopsis Arp2/3 complex controls leaf cell morphogenesis. *Plant Physiology* **132**, 2034-2044.
- Lowry, O. H., Rosebrough, N. J., Farr, A. L. and Randall, R. J.** (1951). Protein Measurement with the Folin Phenol Reagent. *Journal of Biological Chemistry* **193**, 265-275.
- Marc, J., Granger, C. L., Brincat, J., Fisher, D. D., Kao, T. H., McCubbin, A. G. and Cyr, R. J.** (1998). A GFP-MAP4 reporter gene for visualizing cortical microtubule rearrangements in living epidermal cells. *Plant Cell* **10**, 1927-1939.
- Mathur, J. and Hulskamp, M.** (2002). Microtubules and microfilaments in cell morphogenesis in higher plants. *Current Biology* **12**, R669-R676.
- Mathur, J., Mathur, N., Kernebeck, B. and Hulskamp, M.** (2003a). Mutations in Actin-Related Proteins 2 and 3 Affect Cell Shape Development in Arabidopsis. *Plant Cell* **15**, 1632-1645.
- Mathur, J., Mathur, N., Kirik, V., Kernebeck, B., Srinivas, B. P. and Hulskamp, M.** (2003b). Arabidopsis CROOKED encodes for the smallest subunit of the ARP2/3 complex and controls cell shape by region specific fine F-actin formation. *Development* **130**, 3137-3146.
- Mathur, J., Spielhofer, P., Kost, B. and Chua, N. H.** (1999). The actin cytoskeleton is required to elaborate and maintain spatial patterning during trichome cell morphogenesis in Arabidopsis thaliana. *Development* **126**, 5559-5568.
- McCollum, D., Feoktistova, A., Mophew, M., Balasubramanian, M. and Gould, K.** (1996). The Schizosaccharomyces pombe actin-related protein, Arp3, is a component of the cortical actin cytoskeleton and interacts with profilin. *EMBO J.* **15**, 6438-6446.
- McDowell, J. M., Huang, S. R., McKinney, E. C., An, Y. Q. and Meagher, R. B.** (1996). Structure and evolution of the actin gene family in Arabidopsis thaliana. *Genetics* **142**, 587-602.
- Mcelroy, D., Blowers, A. D., Jenes, B. and Wu, R.** (1991). Construction of Expression Vectors Based on the Rice Actin-1 (Act1) 5' Region for Use in Monocot Transformation. *Molecular & General Genetics* **231**, 150-160.
- McKinney, E. C., Ali, N., Traut, A., Feldmann, K. A., Belostotsky, D. A., McDowell, J. M. and Meagher, R. B.** (1995). Sequence-Based Identification of T-DNA Insertion Mutations in Arabidopsis - Actin Mutants Act2-1 and Act4-1. *Plant Journal* **8**, 613-622.
- McKinney, E. C., Kandasamy, M. K. and Meagher, R. B.** (2001). The Arabidopsis genome contains ancient classes of extremely complex and differentially expressed actin-related protein (ARP) genes. *Molecular Biology of the Cell* **12**, 180.
- McKinney, E. C., Kandasamy, M. K. and Meagher, R. B.** (2002). Arabidopsis Contains Ancient Classes of Differentially Expressed Actin-Related Protein Genes. *Plant Physiol.* **128**, 997-1007.
- Meagher, R. B., McKinney, E. C. and Kandasamy, M. K.** (1999). Isovariant dynamics expand and buffer the responses of complex systems: The diverse plant actin gene family. *Plant Cell* **11**, 995-1005.

- Meske, V. and Hartmann, E.** (1995). Reorganization of Microfilaments in Protonemal Tip Cells of the Moss *Ceratodon Purpureus* During the Phototropic Response. *Protoplasma* **188**, 59-69.
- Miller, D. D., de Ruijter, N. C. A., Bisseling, T. and Emons, A. M. C.** (1999). The role of actin in root hair morphogenesis: studies with lipochito-oligosaccharide as a growth stimulator and cytochalasin as an actin perturbing drug. *Plant Journal* **17**, 141-154.
- Miyawaki, A., Nagai, T. and Mizuno, H.** (2003). Mechanisms of protein fluorophore formation and engineering. *Current Opinion in Chemical Biology* **7**, 557-562.
- Morrell, J. L., Morphew, M. and Gould, K. L.** (1999). A mutant of Arp2p causes partial disassembly of the Arp2/3 complex and loss of cortical actin function in fission yeast. *Molecular Biology of the Cell* **10**, 4201-4215.
- Mullins, R. D., Heuser, J. A. and Pollard, T. D.** (1998). The interaction of Arp2/3 complex with actin: Nucleation, high affinity pointed end capping, and formation of branching networks of filaments. *PNAS* **95**, 6181-6186.
- Nelson, W. J.** (2003). Adaptation of core mechanisms to generate cell polarity. *Nature* **422**, 766-774.
- Olyslaegers, G. and Verbelen, J. P.** (1998). Improved staining of F-actin and co-localization of mitochondria in plant cells. *Journal of Microscopy-Oxford* **192**, 73-77.
- Pantoloni, D. and Carlier, M. F.** (1993). How Profilin Promotes Actin Filament Assembly in the Presence of Thymosin-Beta-4. *Cell* **75**, 1007-1014.
- Pelham, R. J. and Chang, F.** (2001). Role of actin polymerization and actin cables in actin-patch movement in *Schizosaccharomyces pombe*. *Nature Cell Biology* **3**, 235-244.
- Pollard, T. D.** (2001). Genomics, the cytoskeleton and motility. *Nature* **409**, 842-843.
- Ponappa, T., Brzozowski, A. E. and Finer, J. J.** (1999). Transient expression and stable transformation of soybean using the jellyfish green fluorescent protein. *Plant Cell Reports* **19**, 6-12.
- Prandl, R. and Schoffl, F.** (1996). Heat shock elements are involved in heat shock promoter activation during tobacco seed maturation. *Plant Molecular Biology* **31**, 157-162.
- Preuss, M. L., Serna, J., Falbel, T. G., Bednarek, S. Y. and Nielsen, E.** (2004). The Arabidopsis Rab GTPase RabA4b localizes to the tips of growing root hair cells. *Plant Cell* **16**, 1589-1603.
- Pruyne, D. and Bretscher, A.** (2000). Polarization of cell growth in yeast I. Establishment and maintenance of polarity states. *Journal of Cell Science* **113**, 365-375.
- Pruyne, D., Evangelista, M., Yang, C. S., Bi, E. F., Zigmund, S., Bretscher, A. and Boone, C.** (2002). Role of formins in actin assembly: Nucleation and barbed-end association. *Science* **297**, 612-615.
- Quader, H. and Schnepf, E.** (1989). Actin Filament Array During Side Branch Initiation in Protonema Cells of the Moss *Funaria-Hygrometrica* - an Actin Organizing Center at the Plasma-Membrane. *Protoplasma* **151**, 167-170.
- Reski, R.** (1998). Development, genetics and molecular biology of mosses. *Botanica Acta* **111**, 1-15.
- Ringli, C., Baumberger, N., Diet, A., Frey, B. and Keller, B.** (2002). ACTIN2 is essential for bulge site selection and tip growth during root hair development of Arabidopsis. *Plant Physiology* **129**, 1464-1472.
- Robinson, R. C., Turbedsky, K., Kaiser, D. A., Marchand, J. B., Higgs, H. N., Choe, S. and Pollard, T. D.** (2001). Crystal structure of Arp2/3 complex. *Science* **294**, 1679-1684.
- Sagot, I., Rodal, A. A., Moseley, J., Goode, B. L. and Pellman, D.** (2002). An actin nucleation mechanism mediated by Bni1 and profilin. *Nature Cell Biology* **4**, 626-631.

- Sakakibara, K., Nishiyama, T., Sumikawa, N., Kofuji, R., Murata, T. and Hasebe, M.** (2003). Involvement of auxin and a homeodomain-leucine zipper I gene in rhizoid development of the moss *Physcomitrella patens*. *Development* **130**, 4835-4846.
- Sambrook, J., Fritsch, E. F. and Maniatis, T.** (1989). *Molecular Cloning: A Laboratory Manual*: Cold Spring Harbor, New York, NY: Cold Spring Harbor Press.
- Sawa, M., Suetsugu, S., Sugimoto, A., Miki, H., Yamamoto, M. and Takenawa, T.** (2003). Essential role of the C-elegans Arp2/3 complex in cell migration during ventral enclosure. *Journal of Cell Science* **116**, 1505-1518.
- Schaefer, D. G.** (2001). Gene targeting in *Physcomitrella patens*. *Current Opinion in Plant Biology* **4**, 143-150.
- Schaefer, D. G.** (2002). A new moss genetics: Targeted mutagenesis in *Physcomitrella patens*. *Annual Review of Plant Biology* **53**, 477-501.
- Schaefer, D. G. and Zryd, J. P.** (1997). Efficient gene targeting in the moss *Physcomitrella patens*. *Plant Journal* **11**, 1195-1206.
- Schnepf, E.** (1986). Cellular Polarity. *Annual Review of Plant Physiology and Plant Molecular Biology* **37**, 23-47.
- Schnepf, E., Deichgraber, G. and Bopp, M.** (1986). Growth, Cell-Wall Formation and Differentiation in the Protonema of the Moss, *Funaria-Hygrometrica* - Effects of Plasmolysis on the Developmental Program and Its Expression. *Protoplasma* **133**, 50-65.
- Schoffl, F., Rieping, M., Baumann, G., Bevan, M. and Angermuller, S.** (1989). The Function of Plant Heat-Shock Promoter Elements in the Regulated Expression of Chimaeric Genes in Transgenic Tobacco. *Molecular & General Genetics* **217**, 246-253.
- Schumaker, K. S. and Dietrich, M. A.** (1997). Programmed changes in form during moss development. *Plant Cell* **9**, 1099-1107.
- Sheahan, M. B., Staiger, C. J., Rose, R. J. and McCurdy, D. W.** (2004). A Green Fluorescent Protein Fusion to Actin-Binding Domain 2 of Arabidopsis Fimbrin Highlights New Features of a Dynamic Actin Cytoskeleton in Live Plant Cells. *Plant Physiol.* **136**, 3968-3978.
- Smith, L. G.** (2003). Cytoskeletal control of plant cell shape: getting the fine points. *Current Opinion in Plant Biology* **6**, 63-73.
- Sonobe, S. and Shibaoka, H.** (1989). Cortical Fine Actin-Filaments in Higher-Plant Cells Visualized by Rhodamine-Phalloidin after Pretreatment with M- Maleimidobenzoyl N-Hydroxysuccinimide Ester. *Protoplasma* **148**, 80-86.
- Straub, F. B.** (1942). Actin. *Stud. Inst. Med. Chem. Univ. Szeged* **2**, 3-15.
- Sunilkumar, G., Mohr, L., Lopata-Finch, E., Emani, C. and Rathore, K. S.** (2002). Developmental and tissue-specific expression of CaMV 35S promoter in cotton as revealed by GFP. *Plant Molecular Biology* **50**, 463-474.
- Thompson, R. F. and Langford, G. M.** (2002). Myosin superfamily evolutionary history. *Anatomical Record* **268**, 276-289.
- Traas, J. A., Doonan, J. H., Rawlins, D. J., Shaw, P. J., Watts, J. and Lloyd, C. W.** (1987). An Actin Network Is Present in the Cytoplasm Throughout the Cell-Cycle of Carrot Cells and Associates with the Dividing Nucleus. *Journal of Cell Biology* **105**, 387-395.
- Tsien, R. Y.** (1998). The green fluorescent protein. *Annual Review of Biochemistry* **67**, 509-544.
- Uemura, T., Yoshimura, S. H., Takeyasu, K. and Sato, M. H.** (2002). Vacuolar membrane dynamics revealed by GFP-AtVam3 fusion protein. *Genes to Cells* **7**, 743-753.
- Virag, A. and Griffiths, A. J. F.** (2004). A mutation in the *Neurospora crassa* actin gene results in multiple defects in tip growth and branching. *Fungal Genetics and Biology* **41**, 213-225.

- Walker, L. M. and Sack, F. D.** (1995). Microfilament distribution in protonemata of the moss *Ceratodon*. *Protoplasma* **189**, 229-237.
- Wasteneys, G. O. and Galway, M. E.** (2003). REMODELING THE CYTOSKELETON FOR GROWTH AND FORM: An Overview with Some New Views. *Annu. Rev. Plant Biol.* **54**, 691-722.
- Wasteneys, G. O., WillingaleTheune, J. and Menzel, D.** (1997). Freeze shattering: a simple and effective method for permeabilizing higher plant cell walls. *Journal of Microscopy-Oxford* **188**, 51-61.
- Weaver, A. M., Young, M. E., Lee, W. L. and Cooper, J. A.** (2003). Integration of signals to the Arp2/3 complex. *Current Opinion in Cell Biology* **15**, 23-30.
- Welch, M. D., DePace, A. H., Verma, S., Iwamatsu, A. and Mitchison, T. J.** (1997). The human Arp2/3 complex is composed of evolutionarily conserved subunits and is localized to cellular regions of dynamic actin filament assembly. *Journal of Cell Biology* **138**, 375-384.
- Welch, M. D. and Mullins, R. D.** (2002). CELLULAR CONTROL OF ACTIN NUCLEATION. *Annual Review of Cell and Developmental Biology* **18**, 247-288.
- Welch, M. D., Rosenblatt, J., Skoble, J., Portnoy, D. A. and Mitchison, T. J.** (1998). Interaction of human Arp2/3 complex and the *Listeria monocytogenes* ActA protein in actin filament nucleation. *Science* **281**, 105-108.
- Wernicke, W. and Jung, G.** (1992). Role of Cytoskeleton in Cell Shaping of Developing Mesophyll of Wheat (*Triticum-Aestivum* L). *European Journal of Cell Biology* **57**, 88-94.
- Westphal, M., Jungbluth, A., Heidecker, M., Muhlbauer, B., Heizer, C., Schwartz, J. M., Marriott, G. and Gerisch, G.** (1997). Microfilament dynamics during cell movement and chemotaxis monitored using a GFP-actin fusion protein. *Current Biology* **7**, 176-183.
- Winter, D., Podtelejnikov, A. V., Mann, M. and Li, R.** (1997). The complex containing actin-related proteins Arp2 and Arp3 is required for the motility and integrity of yeast actin patches. *Current Biology* **7**, 519-529.
- Winter, D. C., Choe, E. Y. and Li, R.** (1999). Genetic dissection of the budding yeast Arp2/3 complex: A comparison of the in vivo and structural roles of individual subunits. *PNAS* **96**, 7288-7293.
- Yang, N. S. and Christou, P.** (1990). Cell Type Specific Expression of a Camv 35s-Gus Gene in Transgenic Soybean Plants. *Developmental Genetics* **11**, 289-293.
- Yumura, S. and Fukui, Y.** (1998). Spatiotemporal dynamics of actin concentration during cytokinesis and locomotion in *Dictyostelium*. *Journal of Cell Science* **111**, 2097-2108.
- Zhou, X., Chandrasekharan, M. B. and Hall, T. C.** (2004). High rooting frequency and functional analysis of GUS and GFP expression in transgenic *Medicago truncatula* A17. *New Phytologist* **162**, 813-822.
- Zuo, J. R., Niu, Q. W. and Chua, N. H.** (2000). An estrogen receptor-based transactivator XVE mediates highly inducible gene expression in transgenic plants. *Plant Journal* **24**, 265-273.

This document was created with Win2PDF available at <http://www.daneprairie.com>.
The unregistered version of Win2PDF is for evaluation or non-commercial use only.